CONTENTS—Proceedings Vol. 48, 1952

From September 1951 JOURNAL

48-1 **Earthquake Resistant Design Considerations** 1
By R. R. MARTEL

48-2 **Comprehensive Numerical Method for the Analysis of Earthquake Resistant Structures** 5
By CHARLES S. WHITNEY, BOYD G. ANDERSON and MARIO G. SALVADORI
Discussion (Part 2, December 1952 JOURNAL) 28-1

48-3 **Multistory Buildings Designed to Resist Earthquakes** 29
By JOHN J. GOULD
Discussion (Part 2, December 1952 JOURNAL) 36-1

48-4 **Lightweight Concrete for Lower Construction Costs** 37
By J. A. MURLIN
Discussion (Part 2, December 1952 JOURNAL) 44-1

48-5 **Designing for Continuity in Prestressed Concrete Structures** 45
By ALFRED L. PARME and GEORGE H. PARIS
Discussion (Part 2, December 1952 JOURNAL) 64-1

48-6 **Pumice—Lightweight Aggregate** 65
By LESLIE I. NEHER

48-7 **Hydration Products Formed in Cement Pastes at 25 to 175 C** 77
By GEORGE L. KALOUSEK and MILTON ADAMS

Letters from Readers 93

LR 48-1 **Leveling Screws Simplify Setting Columns Bases** 93
LR 48-2 **Factors Influencing Concrete Strength** 94
LR 48-3 **Alkali-Aggregate Expansion Corrected with Portland-Slag Cement** 95
LR 48-4 **Rational Use of ACI Building Code for Economical Structures** 96
LR 48-5 **Water Solubility of Alkalies in Portland Cement** 97
LR 48-6 **Spacing Beam Stirrups** 98
LR 48-7 **Metal Versus Paper Molds for Test Cylinders** 98
LR 48-8 **Skepticism Regarding the Plastic Theory of Design** 99
LR 48-9 **Hooked Ends on Reinforcing Still Desirable** 103

Current Reviews 105

From October 1951 JOURNAL

48-8 **Advances in Precast Floor Systems** 113
By F. N. MENEFEE
Discussion (Part 2, December 1952 JOURNAL) 124-1

48-9 **Manufacture and Use of Machine-Made Precast Structural Elements** 125
By A. G. STREBLOW

48-10 **Tilt-Up Construction in Western United States** 133
By F. THOMAS COLLINS
Discussion (Part 2, December 1952 JOURNAL) 144-1

48-11 **Diagonal Tension in Reinforced Concrete Beams** 145
By ARTHUR P. CLARK
Discussion (Part 2, December 1952 JOURNAL) 156-1

48-12 **Coral and Salt Water as Concrete Materials** 157
By JOHN G. DEMPSEY
Discussion (Part 2, December 1952 JOURNAL) 168-1

48-13 **Load Carrying Capacity of Dowels at Transverse Pavement Joints** 169
By HENRI MARCUS
Discussion (Part 2, December 1952 JOURNAL) 184-1

Letters from Readers 185
LR 48-10 **Cracks in Tunnel Lining** 185
LR 48-11 **Reinforcing—What Is It?** 186
LR 48-12 **Determination of Fixed-End Moments in Beams with Irregular Loading Without Use of Formulas from Handbooks** 186
LR 48-13 **Masonry Walls in Cold Climates** 188

Current Reviews 189

From November 1951 JOURNAL

48-14 **Tilt-Up Construction Costs** 197
By F. THOMAS COLLINS and EARL BENNETSEN

48-15 **Effect of Temperature and Surface Area of the Cement on Air Entrainment** 205
By E. W. SCRIPTURE, JR., S. W. BENEDICT and F. J. LITWINOWICZ

48-16 **Foundation for a Large Turbogenerator** 213
By PAUL ROGERS
Discussion (Part 2, December 1952 JOURNAL) 224-1

48-17 **Measurement of the Distribution of Tensile and Bond Stresses Along Reinforcing Bars** 225
By R. M. MAINS
Discussion (Part 2, December 1952 JOURNAL) 252-1

48-18 **Insulation for Protection of New Concrete in Winter** 253
By L. H. TUTHILL, R. E. GLOVER, C. H. SPENCER and W. B. BIERCE
Addendum (Part 2, December 1952 JOURNAL) 272-1

Letters from Readers 273
LR 48-14 **Free Span Construction of Prestressed Concrete Bridges** 273
LR 48-15 **Comparative Tests of Preformed Expansion Joint Fillers for Concrete Pavements** 275

Current Reviews 277

From December 1951 JOURNAL

48-19 **Lateral Force Distribution in a Concrete Building Story** 281
By T. Y. LIN

48-20 **Air Entrainment and Resistance to Freezing and Thawing** 297
By E. W. SCRIPTURE, JR., S. W. BENEDICT and F. J. LITWINOWICZ
Discussion (Part 2, December 1952 JOURNAL) 308-1

48-21 **Streamlined Vacuum Concrete Buntons for Mine Shafts** 309
By PETER J. DOANIDES

48-22 **Simple Concrete Shell Structures** 321
By FELIX CANDELA
Discussion (Part 2, December 1952 JOURNAL) 332-1

48-23 **Concrete Footings for Walls and Columns** 333
By PAUL JAKOWLEW-HERBACZEWSKI

Letters from Readers 353
LR 48-16 **Kelly Ball vs. Slump Cone—Comparative Tests of Samples Taken at Travis Air Base** 353
LR 48-17 **Anchor Bolts for Setting Column Bases** 356

Current Reviews 357

From January 1952 JOURNAL

48-24 **Field Experiences in Building Multiple Story Reinforced Concrete Tanks** 365
By E. J. CRITZAS

48-25 **Conservation of Steel by Design** 373
By O. W. IRWIN
Discussion (Part 2, December 1952 JOURNAL) 380-1

48-26 **Automatic Jacks Speed Sliding-Form Construction** 381
By DAVID F. STOUT and ROBERT E. WILDE

48-27 **Shrinkage and Curing in Concrete Masonry Units** 393
By HARRY W. EASTERLY, JR.
Discussion (Part 2, December 1952 JOURNAL) 404-1

48-28 **Equivalent Load Method for Analyzing Prestressed Concrete Structures** 405
By ROBERT B. B. MOORMAN

48-29 **Why Small Jobs Frequently Get Poor Concrete** 417
By A. W. BRUST

Letters from Readers 425
LR 48-10 **Cracks in Tunnel Lining** 425
LR 48-12 **Determination of Fixed-End Moments in Beams with Irregular Loading Without Use of Formulas from Handbooks** 425
LR 48-18 **Cement Factor Determination** 428

Current Reviews 429

From February 1952 JOURNAL

48-30 **Analysis of Skewed Rigid Frames and Arches** 437
By JAMES P. MICHALOS
Discussion (Part 2, December 1952 JOURNAL) 456-1

48-31 **Use of Chicago Fly Ash in Reducing Cement-Aggregate Reaction** 457
By C. H. SCHOLER and G. M. SMITH

48-32 **Direct Design of Rectangular Columns with Bending About an Axis of Symmetry** 465
By HENRY J. COWAN

48-33 **Thermal Expansion of Aggregates and Concrete Durability** 485
By EDWIN J. CALLAN
Discussion (Part 2, December 1952 JOURNAL) 504-1

48-34 **Relative Economy of Prestressed and Conventional Reinforced Concrete Reservoirs** 505
By G. C. ERNST, C. O. BRUNKEN and A. R. RIVELAND

Letters from Readers 513
LR 48-19 **Additional Information on Inhibiting Alkali-Aggregate Expansion** 513
LR 48-20 **Water Content in Pumice Concrete** 514
LR 48-21 **Vibration of Pavement Concrete** 514
LR 48-22 **Skew Bending in Reinforced Concrete Computed by Plasticity** 516
LR 48-23 **Castle Bridge Across River Severn** 519

Current Reviews 521

From March 1952 JOURNAL

48-35 **New Techniques in the Study of Setting and Hardening of Hydraulic Materials** ... 525
By J. CALLEJA
Discussion (Part 2, December 1952 JOURNAL) 536-1

48-36 **Calcium Chloride in Concrete** 537
By J. J. SHIDELER
Discussion (Part 2, December 1952 JOURNAL) 560-1

48-37 **Reinforcing Steel in Concrete and the Concept of Safety** 561
By K. Hajnal-Konyi
Discussion (Part 2, December 1952 Journal) 580-1

48-38 **Applications of Vacuum Concrete** 581
By K. P. Billner

Letters from Readers 593
LR 48-24 Why Classify Old-Style Deformed Bars as Plain Bars in the 1951 Building Code? 593
LR 48-25 Grout Mix Computation Charts 597

Current Reviews 601

From April 1952 JOURNAL

48-39 **Exciting Adventures** 609
By H. F. Thomson

48-40 **Wave Velocity in Concrete** 613
By Johannes Andersen and Poul Nerenst
Discussion (Part 2, December 1952 Journal) 636-1

48-41 **Slip-Forms for Concrete Canal Lining** 637
By T. V. D. Woodford
Discussion (Part 2, December 1952 Journal) 644-1

48-42 **Short Cuts in the Design of Continuous Structures** 645
By I. E. Morris

48-43 **Illinois Experimental Continuously Reinforced Concrete Pavement after Four Years** .. 653
By J. D. Lindsay and H. W. Russell

48-44 **Effects of Temperature Changes on Concrete as Influenced by Aggregates** 661
By Stanton Walker, D. L. Bloem and W. G. Mullen

48-45 **Bond Properties of Welded Wire Fabric** 681
By Arthur R. Anderson

Current Reviews 693

From May 1952 JOURNAL

48-46 **Curing of Concrete**

Introduction 701
By A. G. Timms

Current Practices for Curing Concrete Pavements 705
By D. L. Robinson

Curing Structural Concrete 711
By H. J. Gilkey

Curing of Mass Concrete 716
By Roy W. Carlson and W. R. Johnson

Curing Concrete in Canal Lining 718
By H. C. Vollmer

General Review of Curing Methods 721
By G. E. Burnett
Discussion (Part 2, December 1952 Journal) 724-1

48-47 **Durability**

Railway Concrete 725
By C. B. PORTER

Railway Concrete Deterioration 731
By R. W. GILMORE

Concrete Pavements Can Be Durable 735
By F. H. JACKSON

Durable Concrete in Hydraulic Structures 740
By LEWIS H. TUTHILL

Durability of Hydraulic Structures 748
By BYRAM W. STEELE
Discussion (Part 2, December 1952 JOURNAL) 752-1

48-48 **Electric Heating of Concrete in Winter Construction** 753
By CHUZO ITAKURA

48-49 **Field Problems in Constructing a Prestressed Concrete Bridge** 769
By CLAIR L. JOHNSON

48-50 **Economy and Concrete Beams** 773
By HERBERT A. SAWYER, JR.

Letters from Readers 785
LR 48-26 Computation of Air in Air-Entraining Concrete by the Gravimetric Method 785
LR 48-27 Fire Resistance of Prestressed Concrete 786
LR 48-29 Frame Constants for Nonprismatic Members 788

Current Reviews 793

From June 1952 JOURNAL

48-51 **Introduction to Ultimate Load Design** 797
By LEO H. CORNING

48-52 **Why Design by the Ultimate Strength Theories?** 801
By BOYD G. ANDERSON
Discussion (June 1952 JOURNAL) 806

48-53 **Fundamental Concepts in Ultimate Load Design of Reinforced Concrete Members** 809
By EIVIND HOGNESTAD
Discussion (June 1952 JOURNAL) 828

48-54 **Review of Research on Ultimate Strength of Reinforced Concrete Members** 833
By C. P. SIESS
Discussion (June 1952 JOURNAL) 859
Discussion (Part 2, December 1952 JOURNAL) 864-1

48-55 **Practical Design at Ultimate Loads** 865
By R. C. REESE
Discussion (June 1952 JOURNAL) 878
Discussion (Part 2, December 1952 JOURNAL) 880-1

48-56 **Load Factors in Ultimate Design of Reinforced Concrete** 881
By T. Y. LIN
Discussion (June 1952 JOURNAL) 898

Letters from Readers 901
LR 48-28 Measuring Air in Hardened Concrete 901
LR 48-30 Why Not a Particular Type Cement for Each General Type Aggregate 903
LR 48-31 Why Complicate R/C Design? 904

Current Reviews 905

From Part 2 December 1952 JOURNAL

Index to Proceedings..... 913
Index to Current Reviews..... 922

Current ACI Standards

(As of December, 1952)

Listed below are ACI standards in effect at the time the closing portions of *Proceedings* V. 48 are published in the ACI JOURNAL, Part 2 December 1952:

Manual of Standard Practice for Detailing Reinforced Concrete Structures (ACI 315-51)

Not adaptable to Journal presentation, this is a separate publication of large format bound to lie flat. It presents typical engineering and placing drawings with discussion calling attention to important considerations in designing practice. 55 pages, $3.00; to ACI Members $1.75.

Building Code Requirements for Reinforced Concrete (ACI 318-51)

ACI JOURNAL, Apr. 1951, *Proc.* V. 47, pp. 589-652. In separate covers $0.50; to ACI Members $0.40.

Specifications for Concrete Pavements and Bases (ACI 617-51)

ACI JOURNAL, May 1951, *Proc.* V. 47, pp. 721-744. In separate covers $0.50; to ACI Members $0.40.

Recommended Practice for the Application of Mortar by Pneumatic Pressure (ACI 805-51)

ACI JOURNAL, May 1951, *Proc.* V. 47, pp. 709-720. In separate covers $0.50; to ACI Members $0.40.

Recommended Practice for the Application of Portland Cement Paint to Concrete Surfaces (ACI 616-49)

ACI JOURNAL, Sept. 1949, *Proc.* V. 46, pp. 1-16. In separate covers $0.50; to ACI Members $0.40.

Recommended Practice for Winter Concreting Methods (ACI 604-48)

ACI JOURNAL, Sept. 1948, *Proc.* V. 45, pp. 1-20. In separate covers $0.50; to ACI Members $0.40.

Minimum Standard Requirements for Precast Concrete Floor Units (ACI 711-46)

ACI JOURNAL, Oct. 1946, *Proc.* V. 43, pp. 133-148. In separate covers $0.50; to ACI Members $0.40.

Recommended Practice for the Construction of Concrete Farm Silos (ACI 714-46)

ACI JOURNAL, Oct. 1946, *Proc.* V. 43, pp. 149-164. In separate covers $0.50; to ACI Members $0.40.

Recommended Practice for the Design of Concrete Mixes (ACI 613-44)

ACI JOURNAL, June 1945, *Proc.* V. 41, pp. 651-672. In separate covers $0.50; to ACI Members $0.40. Also available in a Spanish edition: "Normas Practicas Recomendadas Por el ACI Para Proyectar Mezclas de Hormigon (ACI 613-44)." In separate covers $0.50.

Specification for Cast Stone (ACI 704-44)

ACI JOURNAL, June 1945, *Proc.* V. 41, pp. 701-704. In separate prints $0.35.

Recommended Practice for the Use of Metal Supports for Reinforcement (ACI 319-42)

ACI JOURNAL, June 1945, *Proc.* V. 41, pp. 621-624. In separate prints $0.35.

Recommended Practice for Measuring, Mixing and Placing Concrete (ACI 614-42)

ACI JOURNAL, June 1945, *Proc.* V. 41, pp. 625-650. In separate covers $0.50; to ACI Members $0.40.

A brief introduction to a group of papers on earthquake resistant design and construction setting forth some basic considerations.

Earthquake Resistant Design Considerations*

By R. R. MARTEL†

SYNOPSIS

Basic behavior characteristics of earthquakes, their effects on structures and considerations for further study of design criteria.

From observations of earthquake damage, some general rules of thumb for building earthquake resistant structures can be drawn. While helpful, these rough rules are not entirely satisfactory for design—they are not quantitative.

Buildings vary widely in plan, materials of construction, height, wall openings and partitions, quality of workmanship and foundation conditions. There are so many variables that damage data can be interpreted convincingly in different ways. The damage can often be attributed to varying combinations of forces. Moreover, there is no assurance that damage in a given area will be of the same detailed character for earthquakes originating on a different fault, or on the same fault at a different time.

For instance, in Long Beach, Calif., only a few of the ornamental cast stone light standards were damaged by the earthquake of Mar. 10, 1933, but 273 of these light standards were cracked by the relatively mild shock of Oct. 2, 1933. They were north of 27th Street and east of American Avenue. This damage would support the belief that resonance occurred and was confined to a restricted area which moved with greater velocity during the milder of the two earthquakes.

At the 79th Street School in Los Angeles, the older of the two buildings was damaged by the earthquake of March 10 to such an extent that it was vacated, the newer building, which was only slightly damaged, being used to house all the classes. The shock of October 2 caused considerable damage to the newer building (which had its axis at right angles to the other) and no additional damage to the older one. So all classes were then moved back to the older structure. It is apparent that the patterns of the two earthquakes were quite different.

*Presented at the ACI 47th Annual Convention, San Francisco, Calif., Feb. 20, 1951. Title No. 48-1 is a part of the copyrighted JOURNAL OF THE AMERICAN CONCRETE INSTITUTE, V. 23, No. 1, Sept. 1951, *Proceedings* V. 48. Separate prints are available at 35 cents each. **Discussion** (copies in **triplicate**) should reach the Institute not later than Jan. 1, 1952. Address 18263 W. McNichols Rd., Detroit 19, Mich.

†Professor of Structural Engineering, California Institute of Technology, Pasadena.

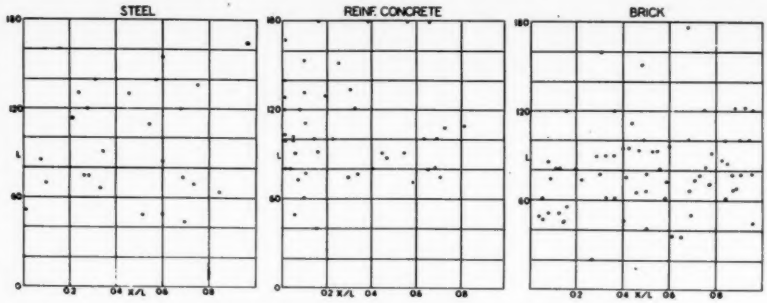

Fig. 1—Point of fracture of chimneys—Tokyo earthquake, 1923

Because they are relatively simple structures, it would seem that the point of fracture of chimneys of the same height and built of the same material would occur at about the same distance from the ground.

Mononobe made an extensive study of a large number of chimneys fractured in the Tokyo earthquake of 1923 (Fig. 1). L is the height of the chimneys and X the distance from the ground to the point of fracture.

It is difficult to detect any clear trends in these widely scattered points. Certainly there is nothing to substantiate the notion that fractures would occur at or near the center of percussion.

Now that we have seismometers, a more important use of damage data is to confirm or controvert the results of the present method of approach to the problem—the analytical.

To design with some degree of confidence, the engineer must know the forces acting on the structure. Starting with the forces he can then find the stresses and design members to resist the stresses. So the first step is to determine the forces. This is a job of working from the ground up, that is, beginning with the motion of the ground as recorded on seismometers.

The strong motion earthquake records taken by the U. S. Coast and Geodetic Survey give directly the acceleration of ground. This is a measure of the forces that would be exerted on a block or an approximation of the forces that would be exerted on a structure that deflects very little. This rough approximation can be reconciled with many cases of observed damage, but not with all. Like impact factors in bridges, this approximation produces tolerably satisfactory structures (as shown by the behavior of schools and elevated water tanks in the Imperial Valley earthquakes of 1940). But it may be too severe in some cases and not severe enough in others. When the deflections of the structure are taken into account, the problem becomes complex—appallingly so at first sight. It requires the analysis of a multimode damped system of vibration subjected to an irregular to and fro transient motion.

Studies by Biot and White show that the forces developed in the multimode system by any base motion can be obtained by superposition if we

know the response of simple single-degree of freedom systems or resonators having the same periods as those of a multimode system. A fairly good measure of the maximum forces in a complex building can be found from the maximum deflection of a resonator such as a single mass on a spring if its free period is the same as that of the first mode of the building.

The response of single-degree of freedom systems to an earthquake-like base motion can be found by (a) lengthy numerical step-by-step calculations, (b) a model on a shaking table the motion of which simulates that of the ground, (c) a torsion analyzer—a rather simple mechanical device which in effect is a special integrator, and (d) the analog computer.

Each one of a large series of resonators of varying periods can, in effect, be shaken by a motion simulating that of an earthquake and the responses of each one plotted. These responses give good indication of forces that would be developed in a whole series of buildings of the same periods as those of the resonators.

It should be stated that so far the resonators have not been damped, and hence they differ in this respect from most of the actual structures. The introduction of known damping in the models can be done rather easily on the analog computer and studies of its effect are in progress.

As might be expected, the resonator response curves for different earthquakes differ considerably. They nevertheless reveal a fairly well-defined general pattern with decreasing values of equivalent steady acceleration for increasing periods. This implies that the seismic coefficient in the code should be smaller for tall buildings than for short ones and is in accord with observed earthquake damage to actual structures.

This finding was an important reason for the revision of the Los Angeles Building Code a few years ago. Roughly the free period of buildings increases with the height. So for simplicity the seismic factor in both Los Angeles and San Francisco codes is expressed in terms of the number of stories in a building rather than its period.

Another important characteristic of all the resonator response curves is the striking variations in the equivalent accelerations for resonators that differ only slightly in period. This also is in accord with the observation that in some instances marked differences in damage occur to buildings that appear to be quite similar. It lends support to the hypothesis advanced by Housner that an earthquake is a series of random impulses—random in magnitude and random in time distribution.

Resonator response graphs have been made for many of the strong motion earthquakes for which USC & GS accelerograms are available. Fig. 2 and 3 show trends present in all graphs made. The small circles represent maximum acceleration (or horizontal shear in a simple one-story structure).

The straight lines connecting the circles are merely conveniences; there is no assurance that intermediate points would lie on the straight lines. The arrow on the acceleration ordinate is the maximum ground acceleration

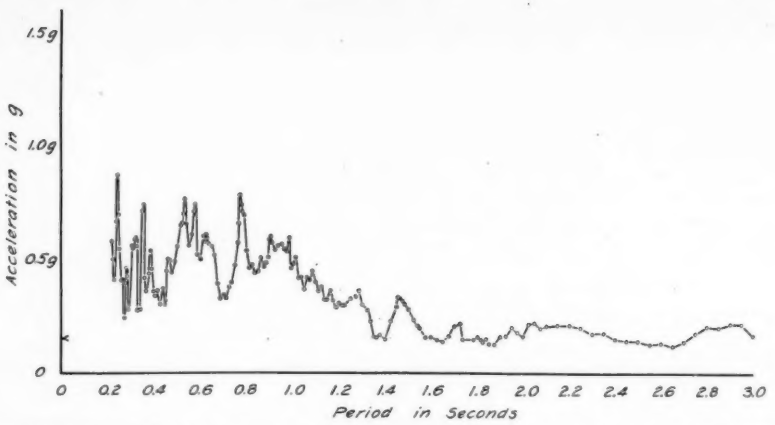

Fig. 2—Influence line for horizontal shear—resonator response vs period. March 10, 1933, earthquake, Vernon record, component—N 8° E

reported by the USC & GS. These graphs are for undamped systems; in most real structures the magnification would be reduced greatly by damping.

While the character of the effect of a few earthquakes on some simple structures has been defined within broad limits, many pertinent problems yet remain to be solved. In addition to the effect of damping, there is the influence of foundation conditions and the interaction of adjacent buildings through ground coupling. Only when we have answers to all these problems can we completely and satisfactorily reconcile observed damage and theory.

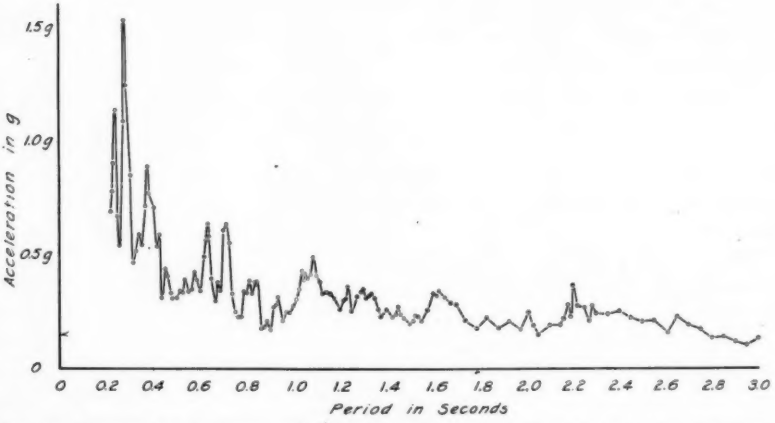

Fig. 3—Influence line for horizontal shear—resonator response vs period. March 10, 1933, earthquake, Vernon record, component—E 8° S

Comprehensive Numerical Method for the Analysis of Earthquake Resistant Structures*

By CHARLES S. WHITNEY†, BOYD G. ANDERSON‡ and MARIO G. SALVADORI§

SYNOPSIS

A new step-by-step method for the analysis of earthquake stresses in multi-story frame buildings is presented and compared with the rigorous solution of the same problem to evaluate its efficiency. The following essential factors influencing earthquake stresses are considered: (1) stiffness and internal damping of the resisting structure; (2) rocking of the foundation due to the yield of the ground and (3) period and amplitude of the earthquake components. It is shown how the method can be extended to buildings in which stresses beyond the elastic limit create plastic hinges. Estimates of time and labor required by the proposed method are presented.

INTRODUCTION

Although it long has been recognized that the design and analysis of structures subjected to blasts or earthquake forces are essentially applications of dynamics, the "practical" designer has continued to follow the procedures of building codes which assume the structure to be subjected to constant accelerations. Constant accelerations produce constant lateral inertia forces which are then specified as bearing some constant ratio to the total gravity load acting at any level. These ratios are usually based on arbitrary considerations determined from previous damage experience and, for further simplification, are made independent of the mass and stiffness of the structure, the elasticity of the foundation, and the characteristics of the "probable" earthquake.

If such lateral load ratios are specified to provide satisfactory survival of all structures, most buildings will be overdesigned and highly uneconomical. However, if economy is considered and the lateral force requirement reduced to provide for an average condition, the results cannot guarantee stability for the entire range of structures.

The availability of electrical calculators and the popularity of numerical methods for the solution of engineering problems (due mainly to the work

*Presented at the ACI 47th annual convention, San Francisco, February 20, 1951. Title No. 48-2 is a part of the copyrighted JOURNAL OF THE AMERICAN CONCRETE INSTITUTE, V. 21, No. 1, Sept. 1951, *Proceedings* V. 48. Separate prints are available at 50 cents each. **Discussion** (copies in **triplicate**) should reach the Institute not later than Jan. 1, 1952. Address 18263 W. McNichols Rd., Detroit 19, Mich.

†Member American Concrete Institute, Partner, Ammann and Whitney, Consulting Engineers, New York.

‡Member American Concrete Institute, Associate partner, Ammann and Whitney, Consulting Engineers, New York.

§Consulting Engineer, Ammann and Whitney, and Assoc. Prof. of Civil Engineering, Columbia University.

of Hardy Cross and R. V. Southwell) have in recent years directed attention to the possibility of tackling in a rational way problems which could not be analyzed before.

Thus, to rectify errors inherent in the general application of present equivalent static load methods, other, more rational methods of analysis have been proposed, among them Biot's spectrum method[1] and Timoshenko's step-by-step method,[2] or those derived from the latter.[3]

From their experience with step-by-step methods for the solution of blast problems in structures, the authors have developed a new step-by-step procedure for the determination of shears due to earthquake oscillations in buildings. The method is based on the following usual assumptions.

1. The mass of each story is concentrated at the corresponding floor level.
2. Oscillations of the building are due to shear only, since it can be shown that deflections due to the direct stress in the columns are negligible for structures having a height-to-width ratio of five or less.[4]
3. Story shear is a function only of the elastic deflection between floors.*

In addition, the authors have included the effect of an elastic subsoil which allows the building to rock under the action of earthquake forces. The condition of a highly rigid foundation which forces the building to follow the ground displacements without relative rotation or translation is presented as a special case.

The inherent accuracy of the proposed method is much higher than the accuracy of other methods available heretofore for the numerical solution of dynamic problems. Hence, it either allows the use of larger intervals for a given accuracy, with a consequent reduction in the volume of computation, or it greatly enhances the accuracy of a solution for a given time interval.

The work reported is exploratory in character and presents the results of the application of the method to two specific five-story buildings. It may be extended to buildings of any number of stories.

The results obtained by the approximate method are compared with the results of the rigorous solution of the same problem and indicate the accuracy and efficiency of the proposed procedure.

Finally, the methods described are general and hence applicable to loadings other than sinusoidal, to structures other than those assumed, and to many other problems of dynamic structural analysis.

ESSENTIAL EARTHQUAKE FACTORS

The following factors have been taken into account: earthquake displacements as functions of time, structural characteristics of the building and the interaction between the ground and the foundation.

Earthquake displacements

Although seismology has been in existence for almost two centuries, it is only in the last 20 years that accurate "strong motion" accelerograms and

*This assumption would be completely fulfilled in a structure with pin connections where the lateral resistance is supplied by diagonal bracing or in a continuous frame whose girders are of infinite stiffness. For other conditions the analysis must consider the redistribution of moments due to rotation of the joints.

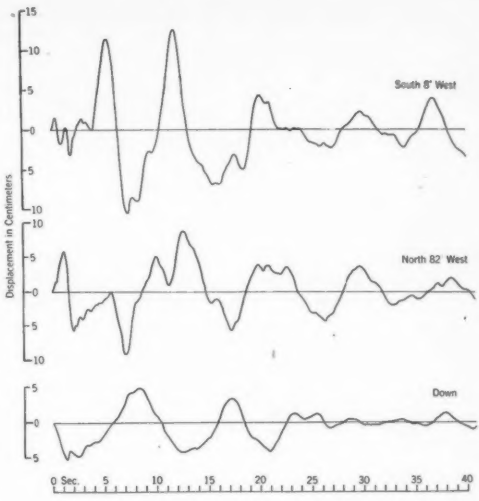

Fig. 1—Computed displacement components, Vernon Accelerogram, Long Beach earthquake, Mar. 10, 1933 (Prepared by U.S. Coast and Geodetic Survey)

reliable time-displacement curves have become generally available.[5] The method proposed can be applied to any such records. However, to be able to compare the results obtained by the proposed approximate method with the results given by a rigorous solution of the same problem, assumed sine displacement pulses have been used in connection with the two buildings analyzed. It may be well to notice that due to the unpredictability of earthquakes, sine curves of proper amplitudes and periods will often suffice for the analysis of a structure.[6]

Usual earthquake records give two horizontal components and one vertical component of the displacement. The two horizontal components are resolved and combined into two components parallel to the axes of the building, and a separate analysis is made along each axis of the structure. The influence of the vertical component on the horizontal shears is negligible.

The two structures considered have been subjected to the following analytical pulses:

1. A half-sine pulse of 0.6 sec duration (the duration of the shortest loop of substantial amplitude in the N-S horizontal displacement component, Vernon record, Long Beach earthquake, Mar. 10, 1933, Fig. 1).
2. A half-sine pulse of long duration (5 times as long as the pulse in (1) and corresponding to the duration of the loop of largest amplitude in the above record.
3. A half-sine pulse of very short duration (half the duration of the pulse in (1)).
4. A combination of 2 and 3 half-sine pulses of the same duration as in (1).

All pulses have an amplitude of one inch.

Structural characteristics

Two buildings with the same story heights and the same masses but with different stiffnesses (spring constants) have been considered. The stiffer building is indicated as Structure No. 1; the more flexible as Structure No. 2. Table 1 contains the physical properties of the two structures per foot of length and Fig. 2 represents an idealized picture of these buildings. Their width is 60 ft.

TABLE I—CHARACTERISTICS OF BUILDING TYPES

Floor No., i	Height, l_i, in.	Mass, M_i, lb-sec^2 per in.	Spring Constants, K_i	
			Bldg. No. 1, lb per in.	Bldg. No. 2, lb per in.
5	144.0	11.65	6840	3420
4	144.0	15.53	7980	3990
3	144.0	15.53	9120	4560
2	144.0	15.53	10260	5130
1	168.0	15.53	11400	5700
0	—	62.08	—	—

Ground-foundation interaction

Two assumptions are made: (1) The ground is perfectly rigid ($E = \infty$), in which case the building cannot rock on its foundations; (2) The ground has a Young's modulus, $E = 10{,}000$ psi, a Poisson's ratio, $\mu = 1/3$ (see ref. 1, p. 380) and reacts with a moment $B = \frac{\pi}{4} \frac{E_s}{1-\mu^2}\left(\frac{b}{2}\right) = 1.145 \times 10^9$ in.-lb per unit length per radian of rotation of the foundation but carries the foundation horizontally without relative translation.

RESULTS OF THE ANALYSIS

The results of the analysis, obtained by the procedures described later are presented graphically in this section.

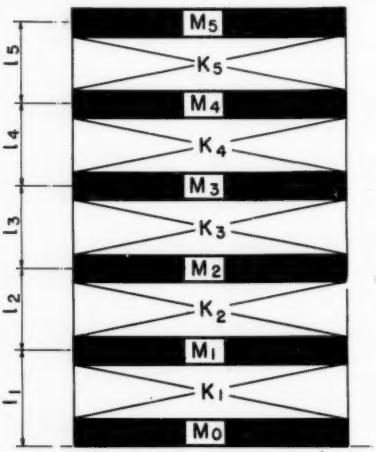

Fig. 2—Idealized building

Profiles

The computed values of displacement have been plotted for each floor level at time intervals of 0.05 sec to provide profiles of the face of the building.

Fig. 3 contains the profiles of Building No. 1 acted on by a half-sine pulse foundation displacement with a duration of 0.6 sec and an amplitude of 1 in. The fundamental period of Building No. 1 is 0.83 sec and the foundation is considered to be rigid.

The conditions of Fig. 4 are similar to those of Fig. 3 except that the duration of the displacement pulse has been reduced to 0.3 sec or approximately 1/3 the fundamental period of

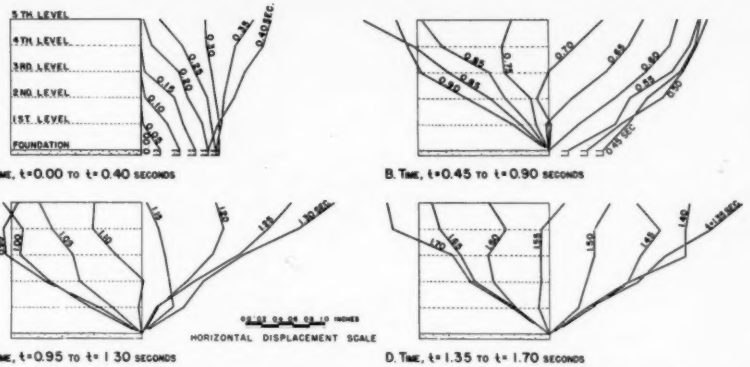

Fig. 3—Displacement profiles of Building No. 1 due to a single half-sine pulse ($T_0/2$ = 0.6 sec) of foundation translation

the building. This change in the duration of the foundation displacement produces a change in the characteristic shape of the building profiles. Where the pulse has a duration larger than half the fundamental period of the building the general shape of the profiles is concave upward. When the duration of the pulse is smaller than half the period of the building the general shape of the profiles becomes convex upward.

Fig. 5 shows the effect of the 0.6 sec half-sine pulse on Building No. 2. Since the fundamental period of Building No. 2 is 1.18 sec, the building is almost in "resonance" with the applied pulse. The characteristic shape of these profiles is intermediate between the shapes of Fig. 3 and 4 and approaches a straight line.

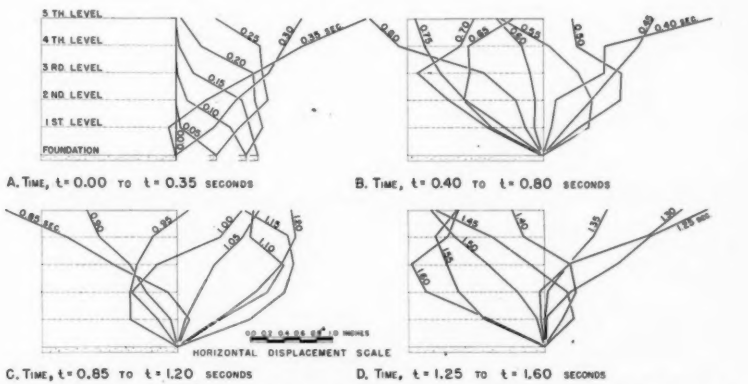
5TH LEVEL
4TH LEVEL
3RD LEVEL
2ND LEVEL
1ST LEVEL
FOUNDATION
A. TIME, t= 0.00 TO t= 0.35 SECONDS
B. TIME, t= 0.40 TO t= 0.80 SECONDS
C. TIME, t= 0.85 TO t= 1.20 SECONDS
D. TIME, t= 1.25 TO t= 1.60 SECONDS
HORIZONTAL DISPLACEMENT SCALE

Fig. 4—Displacement profiles of Building No. 1 due to a single half-sine pulse ($T_0/2$ = 0.3 sec) of foundation translation

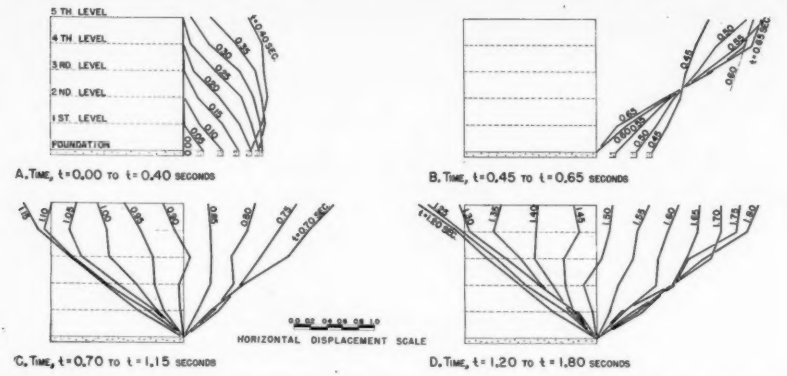

Fig. 5—Displacement profiles of Building No. 2 due to a single half-sine pulse ($T_0/2$ = 0.6 sec) of foundation translation

Displacements and shears

Fig. 6 presents the time-displacement curves for each of the 5 levels of Building No. 1, acted on by a half-sine pulse with an amplitude of 1 in. and a duration of 0.6 sec.

Fig. 7 gives the shears in each story corresponding to the above displacement. The story is designated by the same number designating the floor above it.

Influence of stiffness and rocking

Fig. 8 presents the effect on the displacements at the first floor level of varying the building or foundation stiffness. Buildings No. 1 and No. 2 have been considered to be identical in every respect except stiffness. The stiffness of No. 2 is half that of No. 1. The horizontal ground motion is as shown in the figure.

Fig. 9 shows the first story shears corresponding to the displacements of Fig. 8. The effect of reducing the building stiffness is seen to result in substantial reductions in shear although the total displacements are almost equal for the two buildings. This is true de-

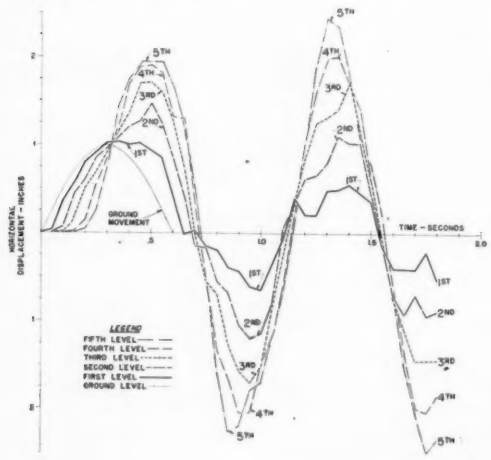

Fig. 6—Displacement curves of Building No. 1 due to a single half-sine pulse ($T_0/2$ = 0.6 sec) of foundation translation

spite the fact that the pulse is in "resonance" with the more flexible structure.

Fig. 9 also shows that in this case the maximum shears with and without rocking are approximately equal. However, it should be noted that the inclusion of the foundation elasticity has increased the natural period of the building so as to make it equal to the "period" of the applied displacement pulse. Hence the effect of rocking was somewhat hidden due to the approach to "resonance." On this basis, it may be inferred that in general rocking will reduce the value of the shears.

Influence of pulse duration

Fig. 10 contains the displacements at the first floor level of Building No. 1 due to three half-sine pulses having durations of 3, 0.6 and 0.3 sec and amplitudes of 1 in. The foundation has been assumed rigid.

Fig. 11 presents the shears in the first story corresponding to the displacemets in Fig. 10. It is apparent that the shears caused by the long half-sine pulse (duration 3 sec, T_o = 6 sec) are much smaller, but it should be remembered that the long half-sine pulses appearing in earthquake displacement

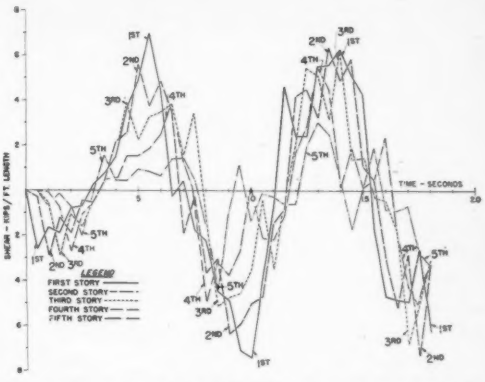

Fig. 7—Shear curves of Building No. 1 due to a single half-sine pulse ($T_o/2$ = 0.6 sec) of foundation translation

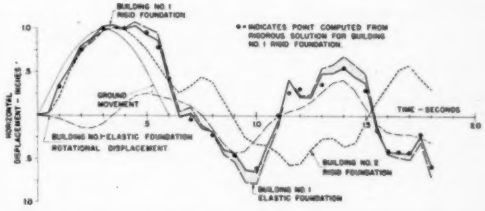
BUILDING NO. 1 RIGID FOUNDATION
** INDICATES POINT COMPUTED FROM RIGOROUS SOLUTION FOR BUILDING NO. 1 RIGID FOUNDATION
GROUND MOVEMENT
TIME - SECONDS
BUILDING NO. 1 ELASTIC FOUNDATION ROTATIONAL DISPLACEMENT
BUILDING NO. 2 RIGID FOUNDATION
BUILDING NO. 1 ELASTIC FOUNDATION

Fig. 8—Buildings No. 1 and 2—Comparison of first level displacements due to a single half-sine pulse ($T_o/2$ = 0.6 sec) of foundation translation

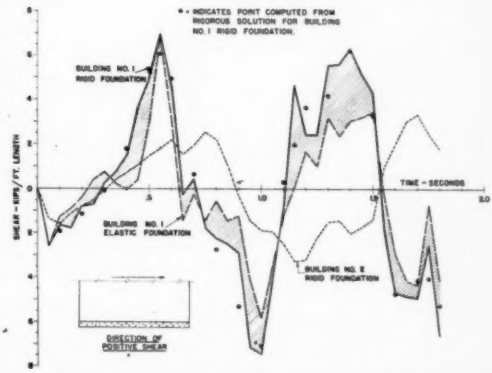
** INDICATES POINT COMPUTED FROM RIGOROUS SOLUTION FOR BUILDING NO. 1 RIGID FOUNDATION.
BUILDING NO. 1 RIGID FOUNDATION
TIME - SECONDS
BUILDING NO. 1 ELASTIC FOUNDATION
BUILDING NO. 2 RIGID FOUNDATION
DIRECTION OF POSITIVE SHEAR

Fig. 9—Buildings 1 and 2—Comparison of first story shears due to a single half-sine pulse ($T_o/2$ = 0.6 sec) of foundation translation

AMERICAN CONCRETE INSTITUTE LIBRARY

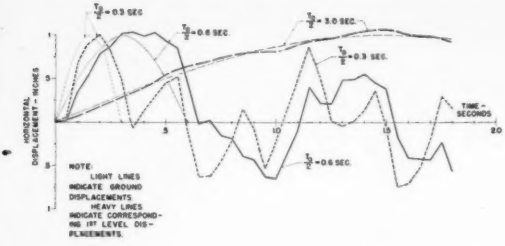
T/2 = 0.3 SEC.
T/2 = 0.6 SEC.
T/2 = 3.0 SEC.
T/2 = 0.3 SEC.
T/2 = 0.6 SEC.
HORIZONTAL DISPLACEMENT - INCHES
TIME - SECONDS
NOTE:
LIGHT LINES INDICATE GROUND DISPLACEMENTS
HEAVY LINES INDICATE CORRESPONDING 1ST LEVEL DISPLACEMENTS.

Fig. 10—Building No. 1—Comparison of first level displacements due to single half-sine foundation translation pulses of different period

curves have usually a much larger amplitude than the short pulses. In the actual earthquake considered in this study (see Fig. 1), the long pulses have an amplitude roughly 7 times the amplitude of the short pulses. Therefore the short pulse curve might well be compared with the dotted curve whose ordinates equal 7 times the dashed ordinates which represent the effect of the long pulse. It is thus seen that the influence of a short pulse of small amplitude may be greater than the influence of a long pulse of large amplitude.

Influence of a combination of half-sine pulses

Fig. 12 contains the displacements at the first floor level of Building No. 1 for the various foundation displacements shown (half-sine pulse, A; full sine pulse, B; and one and a half sine pulses, C).

Fig. 13 presents the shears corresponding to the displacements of Fig. 12.

Although this method could be applied to the total displacement curve of an actual earthquake it would seem more advantageous to analyze the displacement curve harmonically and to consider only those harmonic components whose periods are near one of the periods of the structure or whose amplitudes are very large. It can be shown that the influence of other components is usually negligible in comparison with the "resonance" components.

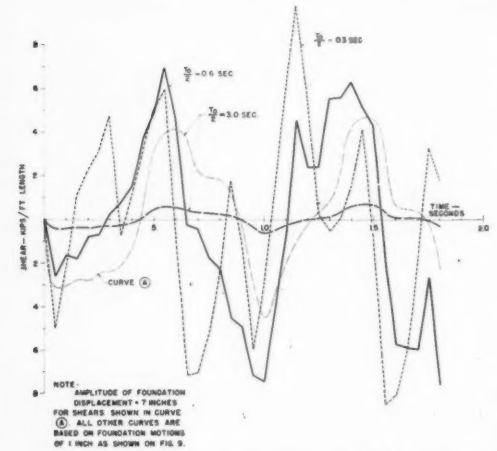
T/2 = 0.3 SEC
T/2 = 0.6 SEC
T/2 = 3.0 SEC.
SHEAR - KIPS/FT. LENGTH
TIME - SECONDS
CURVE (A)
NOTE:
AMPLITUDE OF FOUNDATION DISPLACEMENT = 7 INCHES FOR SHEARS SHOWN IN CURVE (A). ALL OTHER CURVES ARE BASED ON FOUNDATION MOTIONS OF 1 INCH AS SHOWN ON FIG. 9.

Fig. 11—Building No. 1—Comparison of first story shears due to single half-sine translation pulses of different period

Maximum shears

Fig. 14 presents a graphical comparison of the maximum shears developed in the frames of Buildings No. 1 and No. 2 for various foundation displacements. These shears have been computed from the results of the numerical procedure

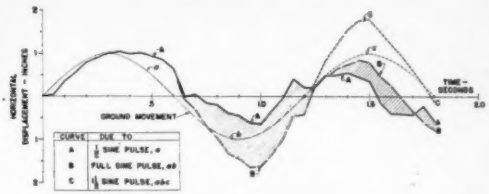

Fig. 12—Building No. 1—Comparison of first level displacements due to sinusoidal foundation translation pulses

applied to the given problems from time $t = 0$ to $t = 1.80$ sec. Shears corresponding to the typical code requirement that the design shears equal 1/10 the gravity loads have also been shown.

Maximum displacement profiles have been drawn by plotting the maximum values of relative elastic story translation consecutively from bottom to top of structure.

Other factors

A structure with 5 degrees of freedom can vibrate freely in only 5 specific configurations or modes, having specific frequencies. The various modes are influenced by damping in different ways. In general, the higher the frequency, the greater the influence of damping for the type of structure considered. It is perfectly feasible to introduce a damping term in the equations of motion of a structure and to solve them by the proposed step-by-step procedure, (See p. 20) but it may be noticed that even with a fairly high damping coefficient, the shears caused in the first few cycles will not be affected essentially by damping, since the amplitude of the first mode is reduced at most by 10 percent after a complete cycle.[6] Moreover the higher modes seldom contribute substantially to the shears, and hence the faster damping-out of the higher modes does not essentially change the picture, It seems therefore that damping may be ignored, in general, when the analysis can be confined to few vibrational cycles. Damping may be relied upon, however, to decrease the effect of resonance in the case of continued harmonic motion of the foundation for an interval of time which is long in com-

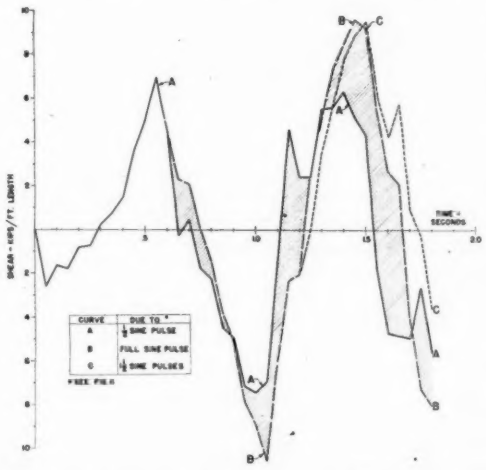

Fig. 13—Building No. 1—Comparison of first story shears due to sinusoidal foundation translation pulses

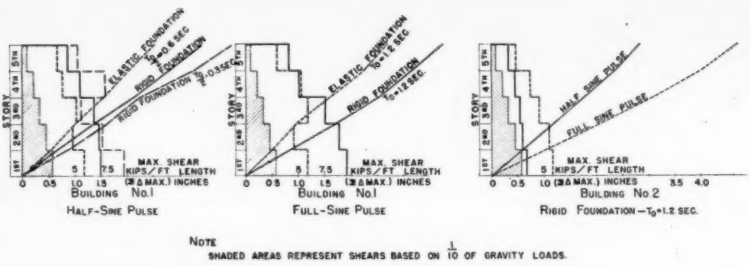

Fig. 14—Comparison of maximum shears in each story

parison with the period of the structure.

The influence of plastic hinges on the motion of the structure and on its shear has not been investigated numerically in this paper, but the proposed procedure has been adapted to take this influence into account as shown later. Plastic behavior of the soil may be taken into account similarly. The plastic behavior of the structure or of the soil effectively reduces the effect of resonance.

Summary

These investigations indicate the inadequacy of any method of earthquake design which does not consider the dynamic characteristics of the individual structure. The stresses produced in buildings have been shown to be functions of the mass and stiffness of the structure, and the stiffness of the foundation. Methods have also been presented to evaluate the influence of damping and plastic deformation.

On the basis of the results thus far obtained, the authors believe that further research along the lines here defined will lead to the development of better and more rational design procedures.

STEP-BY-STEP PROCEDURE

The step-by-step numerical procedure for the integration of the differential equations of motion used in obtaining the previous results was developed by Salvadori by extending a simple method devised by Fox[7] for one degree of freedom systems.

Differential equations of motion without damping and without rocking

Consider a building with N floors and indicate by M_i = the mass concentrated at the (i)th floor $(i = 0, 1, 2, \ldots, N)$

K_i = the spring constant under the (i)th floor, *i.e.*, the shear at the (i)th floor necessary to produce a unit displacement relative to the $(i\text{-}1)$th floor.

$x_i(t)$ = the absolute horizontal displacement of the (i)th floor at time t.

The fundamental equation of motion for the mass of the (i)th floor is obtained by noticing that the resultant force acting on the (i)th mass is the difference between the shears S_{i+1} and S_i above and below the (i)th floor and that, by Newton's second law this resultant must be equal to the mass, M_i, times its acceleration. Remembering the definition of K_i, the shears above and below, M_i, are (Fig. 15a, b):

$$S_{i+1} = K_{i+1}(x_{i+1} - x_i) \quad ; \quad S_i = -K_i(x_i - x_{i-1})$$

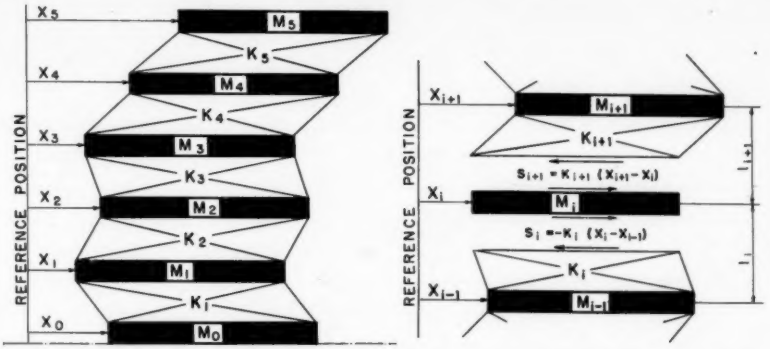

Fig. 15—Left—Distorted position of idealized building on a rigid foundation. Right—Typical force system for (*i*)th floor

Indicating by $\ddot{x}_i$ the second derivative of x_i with respect to time, *i.e.*, the acceleration of M_i, the equation of motion of M_i becomes

$$M_i\ddot{x}_i = K_{i+1}(x_{i+1} - x_i) - K_i(x_i - x_{i-1}) \quad \ldots\ldots (1)$$

Dividing Eq. (1) by M_i and letting

$$\frac{K_{i+1}}{M_i} = k_i'' \quad ; \quad \frac{K_{i+1} + K_i}{M_i} = k_i \quad ; \quad \frac{K_i}{M_i} = k_i' \quad \ldots\ldots (2)$$

Eq. (1) may be written

$$-k_i''x_{i+1} + \ddot{x}_i + k_ix_i - k_i'x_{i-1} = 0 \ (i = 1, 2, \ldots, N) \quad \ldots\ldots (3)$$

If we start counting time when the foundation begins to move under the action of the earthquake, each mass M_i starts moving from rest and hence

$$x_i(0) = 0 \quad ; \quad \dot{x}_i(0) = 0 \quad \ldots\ldots (4)$$

Eq. (3) form a system of N simultaneous, linear, second order differential equations with constant coefficients, which together with the $2N$ initial conditions (4) determine the N functions $x_i(t)$. The system is nonhomogeneous since the first equation ($i = 1$) contains the displacement of the ground floor $x_0(t)$, which is assumed known and identical with the earthquake displacement.

Equations of motion with damping

Experimental evidence on the type of damping occurring in buildings is relatively small and not too reliable. It is therefore permissible under the circumstances to select the type of damping most readily adaptable to the mathematical treatment. It is therefore assumed that the frictional resistance G_{i+1} developed by the (i)th story is proportional to the velocity of the (i+1)th floor relative to the (i)th floor. Indicating dx/dt by $\dot{x}$, the velocities of the (i+1)th and the (i)th floors are equal to $\dot{x}_{i+1}$ and $\dot{x}_i$. Hence, calling V_i the coefficient of viscous damping, (lb per ft per sec)

$$G_{i+1} = V_{i+1}(\dot{x}_{i+1} - \dot{x}_i) \quad ; \quad G_i = V_i(\dot{x}_i - \dot{x}_{i-1})$$

and the resultant frictional force on M_i equals

$$V_{i+1}(\dot{x}_{i+1} - \dot{x}_i) - V_i(\dot{x}_i - \dot{x}_{i-1})$$

Adding this force to the resultant, we obtain the following equations of motion:

$$M_i\ddot{x}_i = K_{i+1}(x_{i+1} - x_i) - K_i(x_i - x_{i-1}) + V_{i+1}(\dot{x}_{i+1} - \dot{x}_i) - V_i(\dot{x}_i - \dot{x}_{i-1}) \quad \ldots\ldots (5)$$

Dividing Eq. (5) by M_i and letting

$$\frac{V_{i+1}}{M_i} = v_i^{''} \quad ; \quad \frac{V_{i+1} + V_i}{M_i} = v_i \quad ; \quad \frac{V_{i-1}}{M_i} = v_i^{'} \quad ;$$

these equations may be written as

$$-v_i^{''}\dot{x}_{i+1} - k_i^{''}x_{i+1} + \ddot{x}_i + v_i\dot{x}_i + k_i x_i - v_i^{'}\dot{x}_{i+1} - k_i^{'}x_{i+1} = 0 \quad \ldots\ldots (6)$$

The N Eq. (6) with the $2N$ initial conditions (4) determine the N displacements x_i (t).

Equations of motion with rocking

When the foundation is free to rock on an elastic ground (Fig. 16) let us call

θ = the rocking angle in radians at time t
x_i = the absolute total displacement of the (i)th floor
l_i = the distance between M_i and M_{i-1}
L_i = the distance between M_i and the bottom of the foundation
y_i = $x_i - L_i\theta - x_o$, the elastic shear displacement of M_i, *i.e.*, the difference between the total displacement $x_i - x_o$ relative to the foundation and the rotational displacement $L_i\theta$
B = the elastic stiffness coefficient for rocking motion (resisting moment per unit rotation)
I_i = the polar moment of inertia of M_i around the centroidal axis of the building perpendicular to the plane of motion.

Assuming small oscillations, the equations of motion in translation are obtained from Eq. (1) by substituting y_i for x_i:

$$M_i\ddot{x}_i = K_{i+1}(y_{i+1} - y_i) - K_i(y_i - y_{i-1}) \quad \ldots\ldots (7)$$

Dividing by M_i and substituting $y_i = x_i - L_i\theta - x_o$ and

$$g_i = k_i^{''}l_{i+1} - k_i^{'}l_i, \quad \ldots\ldots (8)$$

Eq. (7) may be rewritten as

$$-k_i^{'}x_{i+1} + \ddot{x}_i + k_i x_i - k_i^{'}x_{i-1} + g_i\theta = 0 \quad \ldots\ldots (9)$$

The equation of motion in rotation requires the equilibrium of the moments due to the inertia forces and the external moment at the base of the structure. In the present case the moment of the inertia forces of M_i about a centroidal axis 0 of the base perpendicular to the plane of the motion consists of two parts: the moment L_i $(-M_i\ddot{x}_i)$ of the translational inertia forces and the moment $-I_i\ddot{\theta}$ of the translational inertia forces. The elastic moment at the base is $-B\theta$. Hence the equation of motion in rotation becomes:

$$\sum_{i=1}^{N} L_i M_i\ddot{x}_i + \left[\sum_{i=0}^{N} I_i\right]\ddot{\theta} + B\theta = 0 \quad \ldots\ldots (10)$$

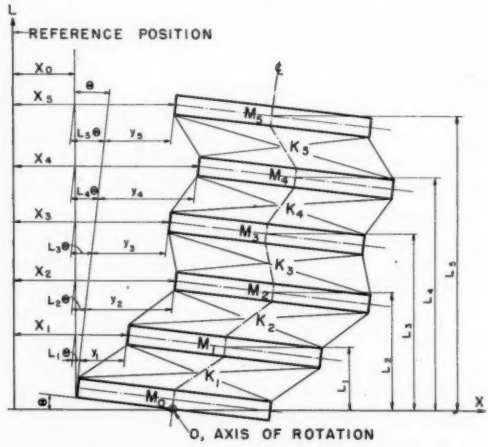

Fig. 16—Distorted position of idealized building on an elastic foundation

The initial conditions of rest require that

$$x_i(0) = 0 \quad ; \quad \dot{x}_i(0) = 0 \quad ; \quad \theta(0) = 0 \quad ; \quad \dot{\theta}(0) = 0 \quad \ldots\ldots (11)$$

The N Eq. (9) and Eq. (10) with the $(2N + 2)$ initial condi-

tions (11) define the N + 1 functions x_i and θ.

Rigorous solution

The differential systems set up in the three previous sections may be solved rigorously by any of the classical methods for the integration of differential equations. The Laplace transform method seems ideally suited to this purpose due to the rest initial conditions.[8] It was used in the rigorous solution of the equations without rocking [Eq. (3)] for the 5-story Building No. 1, whose characteristics appear in Table 1, acted upon by half and complete sine pulses of periods of 1.2 and 6 sec.

The rigorous solution of these systems becomes more and more laborious as the number of levels increases and hence it is advisable to resort to approximate methods of solution as soon as N exceeds 4 or 5.

Step-by-step integration of the rigid foundation problem

For this step-by-step procedure the values of the functions x_i are obtained at evenly spaced time intervals of duration h seconds, by first substituting for the second derivative the first two terms of their central difference expansions,[9]

$$\frac{d^2y}{dx^2} = \frac{1}{h^2}\left(\delta^2 - \frac{\delta^4}{12}\right) y \qquad (12)$$

and by operating then with $\left(1 + \frac{\delta^2}{12}\right)$ on each term of the equation, where δ^2 and δ^4 are the second and fourth central differences of y

$$\delta^2 y(t) = y(t+h) - 2y(t) + y(t-h)$$
$$\delta^4 y(t) = y(t+2h) - 4y(t+h) + 6y(t) - 4y(t-h) + y(t-2h)$$

Letting $t = nh$ and $x_i(nh) = x_i^n$ (13)

and dropping sixth difference terms, each second derivative is substituted by

$$\ddot{x}(nh) \doteq \frac{1}{h^2}\left(\delta^2 - \frac{\delta^4}{12}\right)\left(1 + \frac{\delta^2}{12}\right) x_i(nh)$$
$$\doteq \frac{1}{h^2}\,\delta^2\, x_i(nh)$$
$$= \frac{1}{h^2}\left[x_i^{n+1} - 2x_i^n + x_i^{n-1}\right] \qquad (14)$$

and each term involving an x_i is substituted by

$$\left(1 + \frac{\delta^2}{12}\right) x_i = \frac{1}{12}\left(x_i^{n+1} + 10\,x_i^n + x_i^{n-1}\right) = \frac{1}{12}\,Z\left(x_i^n\right) \qquad (15)$$

where the symbol Z in front of a function x_i^n : $Z\left(x_i^n\right)$ stands for the linear combination of values of x_i at the three instants $t = (n-1)h$, $t = nh$ and $t = (n+1)h$:

$$Z\left(x_i^n\right) = x_i^{n+1} + 10x_i^n + x_i^{n-1} \qquad (16)$$

By means of Eq. (14) and (16); Eq. (3) give

$$\frac{\delta^2}{h^2}\,x_i^n - \frac{1}{12}\,Z\left[k_i^*\,x_{i+1} - k_i x_i + k_i' x_{i-1}\right] = 0 \qquad (17)$$

Letting $a_i = \dfrac{k_i^*}{\frac{12}{h^2} + k_i}$; $b_i = \dfrac{k_i'}{\frac{12}{h^2} + k_i}$; $d_i = \dfrac{\frac{24}{h^2} - 10k_i}{\frac{12}{h^2} + k_i}$;

$$c_i = 10a_i \quad ; \quad e_i = 10b_i \qquad (18)$$

these equations become the set of N linear *algebraic* equations in the N unknowns x_i^{n+1}

$$-a_i x_{i+1}^{n+1} + x_i^{n+1} - b_i x_{i-1}^{n+1} = F_i^{n+1} \quad \ldots\ldots (19)$$

where

$$F_i^{n+1} = a_i x_{i+1}^{n-1} - x_i^{n-1} + b_i x_i^{n-1} + c_i x_{i+1}^{n} + d_i x_i^{n} + e_i x_{i-1}^{n} \quad \ldots\ldots (20)$$

These equations can be solved starting at $n = 1$ if the values of x_i at $n = 0$ and $n = 1$ (x_i^0 and x_i^1) are known. In this case x_i^1 is not known and the solution is started by assuming that x_i is zero at $t = 0$ and at a time $t = -h$, *i.e.*, by applying Eq. (19) at $n = 0$ and taking $x_i^0 = x_i^{-1} = 0$.* A Taylor series solution should not be used to start the step-by-step integration in the case of actual earthquake analyses because of uncertainties in the values of $\dot{x}_i(0) = 0$, $\ddot{x}_i(0) = 0$, etc. The simplified procedure used in this paper does not introduce important errors, as shown by the rigorous solutions, although the error due to backward differences is much larger than the error due to the Fox method.

When N is large, Eq. (19) may be solved by relaxation, trial and error, or successive approximations. Because each equation contains only 3 unknowns, any method of successive approximations will converge rapidly. In the problems solved here it was found convenient to solve the system (19) literally (by forward and backward substitution), thus obtaining explicit expressions for the x_i^{n+1} in terms of the preceding values of the x_i. It was found that the evaluation of x_i^n with 6 significant figures for the 5 floors took approximately 10 minutes, after the computations had been standardized. The numerical work was performed on a standard automatic desk type electric calculator. Appendix I (Case 1) contains a sample computation of the x_i for Structure No. 1.

Step-by-step procedure applied to the rocking problem

The transformation of the differential Eq. (9) and (10) into a set of simultaneous algebraic equations is done by means of the operators (14) and (15), as was done in the previous section. Eq. (9) become

$$\frac{1}{h^2}\,\delta^2 x_i + \frac{1}{12} Z \left[-k_i'' x_{i+1} + k_i x_i + k_i' x_{i-1} + g_i \theta \right] = 0 \quad \ldots\ldots (21)$$

Before transforming Eq. (10) it is convenient to eliminate from it the term $\sum_{i=1}^{N} L_i M_i \ddot{x}_i$. This is done by multiplying each Eq. (9) by $L_i M_i$ and adding:

$$\sum_{i=1}^{N} L_i M_i \ddot{x}_i = \sum_{i=1}^{N} L_i M_i \left[k_i'' x_{i+1} - k_i x_i + k_i' x_{i-1} - g_i \theta \right]$$

Introducing this value in Eq. (10), this becomes

$$\sum_{i=1}^{N} L_i M_i \left[k_i'' x_{i+1} - k_i x_i + k_i' x_{i-1} - g_i \theta \right] + \left[\sum_{i=0}^{N} I_i \right] \theta + B\theta = 0 \quad \ldots\ldots (22)$$

Letting:

$$\sum_{i=1}^{N} L_i M_i g_i = C \quad ; \quad \sum_{i=0}^{N} I_i = D$$

$$\frac{L_i M_i k_i''}{D} = \alpha_i'' \quad ; \quad \frac{L_i M_i k_i}{D} = \alpha_i \quad ; \quad \frac{L_i M_i k_i'}{D} = \alpha_i' \quad \ldots\ldots (23)$$

*This is equivalent to approximating $x_i(0)$ by backward differences.

Eq. (22) may be written as

$$\ddot{\theta} + \frac{B-C}{D}\,\theta + \sum_{i=1}^{N}\left[\alpha_i''x_{i+1} - \alpha_i x_i + \alpha_i' x_{i-1}\right] = 0 \quad \ldots\ldots (24)$$

and by means of Eq. (14) and (15) reduces to

$$\frac{1}{h^2}\,\delta^2\theta^n + \frac{1}{12}\,Z\left\{\left(\frac{B-C}{D}\right)\theta^n + \sum_{i=1}^{N}\left[\alpha_i''\,x_{i+1}^n - \alpha_i\,x_i^n + \alpha_i'\,x_{i-1}^n\right]\right\} = 0 \quad (25)$$

To solve the system of $N+1$ Eq. (21) and (25), we write Eq. (21) explicitly:

$$-a_i x_{i+1}^{n+1} + x_i^{n+1} - b_i x_{i-1}^{n+1} = F_i^{n+1} - r_i\,Z\theta^n \quad \ldots\ldots (26)$$

where $r_i = \dfrac{g_i}{\dfrac{12}{h^2} + k_i}$

and solve them first for $r_i = 0$. The values $x_{i,s}$ thus obtained are identical with the x_i without rocking. We then solve Eq. (26) for $F_i^n = 0$ and $Z\theta^n = -1$, calling the roots $x_{i,r}$. The roots of (26) are then given by

$$x_i^n = x_{i,s}^n - Z\theta^n\,x_{i,r} \quad \ldots\ldots (27)$$

Further, the third term in Eq. (25) may be rewritten, substituting expressions (27) for x_i^n:

$$Z\left\{\sum_{i=1}^{N}\left[\alpha_i''x_{i+1}^n - \alpha_i x_i^n + \alpha_i' x_{i-1}^n\right]\right\} = \sum_{i=1}^{N}\left[\alpha_i''x_{i+1,s}^{n+1} - \alpha_i x_{i,s}^{n+1} + \alpha_i' x_{i-1,s}^{n+1}\right] +$$

$$10\sum_{i=1}^{N}\left[\alpha_i''x_{i+1}^n - \alpha_i x_i^n + \alpha_i' x_{i-1}^n\right] + \sum_{i=1}^{N}\left[\alpha_i''x_{i+1}^{n-1} - \alpha_i x_i^{n-1} + \alpha_i' x_{i-1}^{n-1}\right] -$$

$$\sum_{i=1}^{N}\left[\alpha_i''x_{i+1,r} - \alpha_i x_{i,r} + \alpha_i' x_{i-1,r}\right] Z(\theta^n) \equiv U^n - QZ(\theta^n) \quad \ldots\ldots (28)$$

By means of Eq. (28), Eq. (25) becomes

$$\frac{1}{h^2}\,\delta^2\theta^n + \frac{1}{12}\left[\frac{(B-C)}{D} - Q\right]Z\theta^n + \frac{1}{12}\,P^n = 0 \quad \ldots\ldots (29)$$

which solved for θ^{n+1} gives

$$\theta^{n+1} = W\theta^n - \theta^{n-1} + P^n \quad \ldots\ldots (30)$$

where

$$W = \frac{\dfrac{24}{h^2} - 10E}{\dfrac{12}{h^2} + E} \quad ; \quad P^n = \frac{-U^n}{\dfrac{12}{h^2} + E} \quad ; \quad Q = \sum_{i=1}^{N}\left[\alpha_i''x_{i+1,r} - \alpha_i x_{i,r} + \alpha_i' x_{i-1,r}\right]$$

$$E = \frac{B-C}{D} - Q \quad \ldots\ldots (31)$$

Solving Eq. (30) for θ^{n+1}, evaluating $Z\theta^n$ and substituting in Eq. (27) we obtain the values of x_i^n.

The solution is started at $n = 0$ assuming again θ^{-1} and x_i^{-1} to be zero.

The evaluation of the x_i^n with 6 significant figures for the 5-story Structure No. 1 was found to take approximately 20 minutes, after the $x_{i,s}$ (displacements without rocking) had been obtained. Appendix I (Case 2) contains a sample computation of the x_i for Structure No. 1.

Step-by-step solution of the damping equations

Because Eq. (6) contains terms involving the first derivatives of x_i, the operators (14) and (15) are not applicable. However, Eq. (6) may also be transformed into a system of algebraic equations by substitution of central averaged differences for the derivatives:

$$\frac{-v_i''}{h}\mu\delta x_{i+1}^n - k_i'' x_{i+1}^n + \frac{1}{h^2}\delta^2 x_i^n + \frac{v_i}{h}\mu\delta x_i^n + k_i x_i^n - \frac{v_i'}{h}\mu\delta x_{i-1}^n - k_i' x_{i-1}^n = 0 \quad \ldots\ldots (32)$$

By letting

$$\frac{v_i''}{2h} = \gamma_i'' \quad ; \quad \frac{v_i}{2h} = \gamma_i \quad ; \quad \frac{v_i'}{2h} = \gamma_i' \quad \ldots\ldots (33)$$

these equations become

$$\gamma_i'' x_{i+1}^{n+1} + \left[\frac{1}{h^2} + \gamma_i\right] x_i^{n+1} - \gamma_i' x_{i-1}^{n+1} =$$

$$k_i'' x_{i+1}^n + \left[\frac{2}{h^2} - k_i\right] x_i^n + k_i' x_{i-1}^n - \gamma_i'' x_{i+1}^{n-1} + \left[\gamma_i - \frac{1}{h^2}\right] x_i^{n-1} - \gamma_i' x_{i-1}^{n-1} \equiv E_i^n \quad \ldots\ldots (34)$$

Eq. (34) may be solved step-by-step starting with $n = 0$ and assuming x_i^0 and x_i^{-1} to be zero.

Superposition of solutions

Due to the linearity of the differential equations in the elastic range, the displacements due to the sum of two or more earthquake curves are the sum of the displacements due to each curve. Thus to obtain the free vibrations of a structure after a half-sine pulse of duration $\frac{T_0}{2}$, we may solve the equations for 2 identical sine earthquake displacements of period T_0 with a time lag of $\frac{T_0}{2}$, and superimpose the solutions. The superposition of the displacements may be expressed analytically as follows:

$$x_{i,\ half\ sine\ pulse}(t) = x_i(t) + x_i\left(t - \frac{T_0}{2}\right) \qquad \left(t > \frac{T_0}{2}\right) \quad \ldots\ldots (35)$$

Similarly, to obtain the free vibrations due to a complete sine pulse of period T_0, we superimpose

$$x_{i,\ sine\ pulse}(t) = x_i(t) - x_i(t - T_0) \qquad (t > T_0) \quad \ldots\ldots (36)$$

The same superposition holds for the shears. Thus it is possible to approximate an earthquake graph by superposition of half-sine pulses and to obtain the corresponding shears.

Development of plastic hinges

Plastic hinges develop between the (i)th and the $(i+1)$th floor level whenever the forces $K_{i+1}(x_{i+1} - x_i)$ exceed the elastic limit. Assuming an elastic-plastic behavior of a structure as given in Fig. 17 and calling $S_{yp\ (i+1)}$ the value of the shear corresponding to the elastic limit, this value must be substituted for the elastic shear in Eq. (1) as soon as $K_{i+1}\ (x_{i+1} - x_i) > S_{yp\ (i+1)}$. Thus Eq. (1) are substituted by

$$M_i\ddot{x}_i = S_{yp(i+1)} - K_i(x_i - x_{i+1}) \quad \ldots\ldots (37)$$

If, moreover, the shear between the (i)th and the $(i-1)$th floor

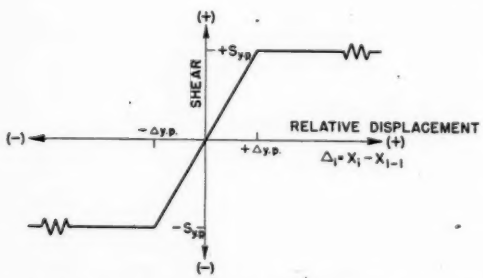

Fig. 17—Idealized curve of resistance vs displacement

also exceeds the elastic limit $S_{yp(i)}$ Eq. (1) reduce to

$$M_i\ddot{x}_i = S_{yp(i+1)} - S_{yp(i)} \quad \ldots\ldots (38)$$

which is valid for

$$K_{i+1}(x_{i+1} - x_i) > S_{yp(i+1)}$$
$$K_i(x_i - x_{i-1}) > S_{yp(i)} \quad \ldots\ldots (39)$$

The step-by-step equations corresponding to (37) are

$$x_i^{n+1} - a_i x_{i-1}^{n+1} = s_{i+1} - w_i\left(10x_i^n + x_i^{n-1} - 10x_{i-1}^n - x_{i-1}^{n-1}\right) \quad \ldots\ldots (40)$$

Where $$w_i = \frac{k_i' h^2}{12 + k_i' h^2}$$

$$s_{i+1} = \frac{12\, S_{yp(i+1)}\, h^2}{(12 + k_i' h^2) M_i} \quad \ldots\ldots (41)$$

The step-by-step integration of Eq. (38) reduces to

$$x_i^{n+1} = h^2(s_{i+1} - s_i) + 2x_i^n - x_i^{n-1} \quad \ldots\ldots (42)$$

Eq. (40) or (42) must be used *as soon as* the first, or both, equations (39) become valid. They must be used until a reversal of stress takes place, that is, *until the relative velocities* $\dot{q}_i'' = \dot{x}_{i+1} - \dot{x}_i$ and $\dot{q}_i' = \dot{x}_i - \dot{x}_{i-1}$ change sign.

For this purpose these velocities must be evaluated as soon as Eq. (39) become valid and at each step from then on. As soon as $\dot{q}_i''$ and/or $\dot{q}_i'$ change sign, one must revert to Eq. (40) or (19).

Accuracy and labor

Step-by-step processes are justified when (1) rigorous solutions are unobtainable; (2) they entail a saving of labor; and (3) they can be obtained by unskilled computers.

The numerical experiments performed indicate that the step-by-step procedure advanced becomes practical for the analysis of structures more than 5 or 6 stories high, and decidedly advantageous when the influence of damping or rocking must be taken into account. Its use should be preferable to a rigorous solution when plastic hinges develop.

The procedure does not entail mathematical difficulties and is a purely arithmetical method requiring an ordinary electric calculator. The procedure is also ideally suited for use with an I.B.M. punch card machine for a thorough analysis with a small time interval.

Any step-by-step method entails an accumulation of errors. In this connection it must be noticed that the other procedures available to date[2,3] contain an error of the order of h^3 or h^4 at each step. The present method has an error of the order of h^6 for all cases which ignore damping and of the order of h^3 for those cases where damping is taken into account. Inasmuch as it was proved that the influence of damping is usually not appreciable, it may be reasserted that the proposed method has a smaller error and hence either allows the use of a larger time interval, h, or reduces considerably the accumulation of errors with the use of a given time interval. A comparison of the results obtained step-by-step with the results of the rigorous solution for the shears and displacements of Building No. 1 subjected to a half-sine pulse of ground displacement has been shown in Fig. 8 and 9. Even after as many as 36 steps covering a total time equal to 1½ times the fundamental period of the structure, the absolute magnitude of the accumulated errors has remained within practical limits.

ACKNOWLEDGMENTS

The authors acknowledge the extensive contributions of Edward Cohen, designing engineer, Ammann and Whitney, in the development of the methods of analysis and in the organization and application of the numerical procedures presented.

They also thank Frank Neuman, U. S. Coast and Geodetic Survey, for making available information on basic data regarding strong motion records.

BIBLIOGRAPHY

1. Biot, M. A., "Analytical and Experimental Methods in Engineering Seismology," *Trans.*, ASCE, V. 100, 1943, p. 365.

2. Timoshenko, S., *Vibration Problems in Engineering*, D. Van Nostrand Co., New York, N. Y., 1937, p. 126.

3. Newmark, N. M., *"Dynamic Behavior of Structures,"* presented at ASCE Annual Meeting, Chicago, Ill., Oct. 1950.

4. Spurr, H. V., *Wind Bracing*, McGraw Hill Book Co., New York, 1930, p. 117, Fig. 31.

5. U. S. Department of Commerce, Coast & Geodetic Survey, *Earthquake Investigations in California 1934-1935*, Special Publication No. 201, and other publications of the same Department.

6. Ockleston, A. J., "The Effect of Earthquakes on Framed Buildings," *Journal*, Institution of Civil Engineers, No. 5, Mar. 1941, p. 41.

7. Fox, L. and Goodwin, E. T., "Some New Methods for the Numerical Integration of Ordinary Differential Equations," *Proc.*, Cambridge Phy. Soc., V. 45, Pt. 3, p. 373.

8. Gardner, M. F. and Barnes, J. L., *Transients in Linear Systems*, John Wiley & Sons, New York, 1942, Chap. VII.

9. Salvadori, M. G., "The Numerical Solution of Buckling Problems by Finite Differences," *Proc.*, ASCE, Dec. 1949.

APPENDIX I—METHODS OF COMPUTATION

Case 1—Rigid Foundation

The finite difference equations (19)

$$-a_i x_{i+1}^{n+1} + x_i^{n+1} - b_i x_{i-1}^{n+1} = F_i^{n+1}$$

$$F_i^{n+1} = a_i x_{i+1}^{n-1} - x_i^{n-1} + b_i x_{i-1}^{n-1} + c_i x_{i+1}^{n} + d_i x_i^{n} + e_i x_{i-1}^{n}$$

applied to a five story structure become

$$\text{(A1)} \quad -a_1 x_2^{n+1} + x_1^{n+1} = b_1 x_0^{n+1} + F_1^{n+1}$$

$$\text{(A2)} \quad -a_2 x_3^{n+1} + x_2^{n+1} - b_2 x_1^{n+1} = F_2^{n+1}$$

$$\text{(A3)} \quad -a_3 x_4^{n+1} + x_3^{n+1} - b_3 x_2^{n+1} = F_3^{n+1}$$

$$\text{(A4)} \quad -a_4 x_5^{n+1} + x_4^{n+1} - b_4 x_3^{n+1} = F_4^{n+1}$$

$$\text{(A5)} \quad x_5^{n+1} - b_5 x_4^{n+1} = F_5^{n+1}$$

A simultaneous solution of Eq. (A1) to (A5) yields the following

$$\text{(A6)} \quad x_2^{n+1} = a_1 x_2^{n+1} + A_1$$

$$\text{(A7)} \quad x_3^{n+1} = \lambda_2 x_3^{n+1} + A_2$$

$$\text{(A8)} \quad x_3^{n+1} = \frac{A_3}{p_3}$$

$$\text{(A9)} \quad x_4^{n+1} = \lambda_4 x_3^{n+1} + A_4$$

$$\text{(A10)} \quad x_5^{n+1} = b_5 x_4^{n+1} + A_5$$

where

$$A_1 = b_1 x_0^{n+1} + F_1^{n+1}$$

$$A_2 = A_1 j_2 + f_2 F_2^{n+1}$$

$$A_3 = F_3^{n+1} + a_3 A_4 + b_3 A_2$$

$$A_4 = A_5 j_4 + f_4 F_4^{n+1}, \qquad A_5 = F_5^{n+1}$$

$$f_2 = \frac{1}{1 - a_1 b_2}$$

$$f_4 = \frac{1}{1 - a_4 b_5}$$

$$j_2 = \frac{b_2}{1 - a_1 b_2}$$

$$j_4 = \frac{a_4}{1 - a_4 b_5}$$

$$\lambda_2 = \frac{a_2}{1 - a_1 b_2}$$

$$\lambda_4 = \frac{b_4}{1 - a_4 b_5}$$

$$p_3 = 1 - \frac{a_3 b_4}{1 - a_4 b_5} - \frac{b_3 a_2}{1 - a_1 b_2}$$

$$F_1^{n+1} = a_1 x_2^{n-1} - x_1^{n-1} + b_1 x_0^{n-1} + c_1 x_2^n + d_1 x_1^n + e_1 x_0^n$$
$$F_2^{n+1} = a_2 x_3^{n-1} - x_2^{n-1} + b_2 x_1^{n-1} + c_2 x_3^n + d_2 x_2^n + e_2 x_1^n$$
$$F_3^{n+1} = a_3 x_4^{n-1} - x_3^{n-1} + b_3 x_2^{n-1} + c_3 x_4^n + d_3 x_3^n + e_3 x_2^n$$
$$F_4^{n+1} = a_4 x_5^{n-1} - x_4^{n-1} + b_4 x_3^{n-1} + c_4 x_5^n + d_4 x_4^n + e_4 x_3^n$$
$$F_5^{n+1} = \quad - x_5^{n-1} - b_5 x_4^{n-1} \quad + d_5 x_5^n + e_5 x_4^n$$

The elastic constants a_i, b_i, c_i, d_i, e_i, f_i, g_i, λ_i, p_i may be computed independently once and for all. The dynamic constants F_i^{n+1} are a function of the displacements x_1^n and x_i^{n-1} and must therefore be computed for each time interval.

To obtain the displacements x_i^{n+1} the following procedure may be used:

1. Compute F_1^{n+1}, add $b_1 x_0^{n+1}$ and record as A_1^{n+1}
2. Compute $f_2 F_2^{n+1}$, add $j_2 A_1$ and record as A_2^{n+1}
3. Compute F_5^{n+1}, and record as A_5^{n+1}
4. Compute $f_4 F_4^{n+1}$ add $j_4 A_5$ and record as A_4^{n+1}
5. Compute F_3^{n+1}, add $a_3 A_4$, $b_3 A_2$ divide by p_3 and record as x_3^{n+1} (Eq. A8)
6. Solve Eq. A7 for x_2^{n+1}
7. Solve Eq. A6 for x_1^{n+1}
8. Solve Eq. A9 for x_4^{n+1}
9. Solve Eq. A10 for x_5^{n+1}
10. Proceed to the next time interval.

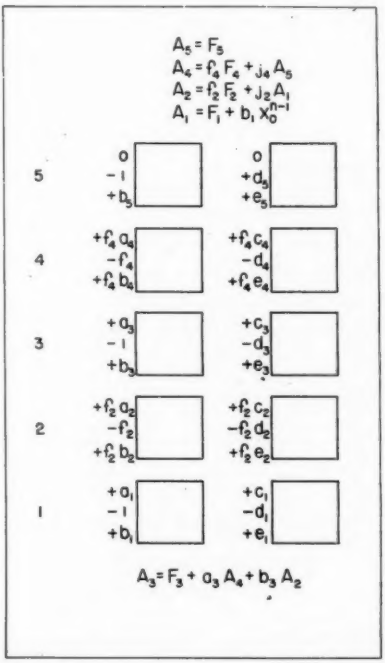

Fig. 18—Computing frame for use with Table 2

These computations may be tabulated as in Table 2. If an automatic desk type calculator is used, it is necessary to record only the five values of x_i^{n+1} and the auxiliary values of A_1, A_2, A_4 and A_5 in each step.

The work of calculation may be speeded by the use of a computing frame as shown in Fig. 18. The frame is placed on Table 2 so that the values of x^{n-1} and x^n appear in the open blocks. If the frame is moved vertically so that the center of the i-th box is opposite the i-th floor displacement, it can be seen that the successive multiplication and algebraic addition of the products of the constants on the frame and the opposite values of x to their right will yield the values of $f_i F_i^{n+1}$. The additional computations indicated on the frame give the values of A_i^{n+1} which are recorded (except for A_3^{n+1}) in the lower half of Table 1 to the right of the frame. The values of x_i^{n+1} may now be computed and recorded in the upper half of the table to the right of the frame. The frame is then shifted one interval to the right and the operation repeated.

TABLE 2—METHOD OF RECORDING COMPUTATIONS OF BUILDING DISPLACEMENTS

Fl. \ t	0		(n−1)h		nh		(n+1)h	
l	X_l		X_l		X_l		X_l	
5	0		X_5^{n-1}		X_5^n		X_5^{n+1}	
4	0		X_4^{n-1}		X_4^n		X_4^{n+1}	
3	0		X_3^{n-1}		X_3^n		X_3^{n+1}	
2	0		X_2^{n-1}		X_2^n		X_2^{n+1}	
1	0		X_1^{n-1}		X_1^n		X_1^{n+1}	
0	0		X_0^{n-1}		X_0^n		X_0^{n+1}	
			A		A		A	
5			A_5^{n-1}		A_5^n		A_5^{n+1}	
4			A_4^{n-1}		A_4^n		A_4^{n+1}	
2			A_2^{n-1}		A_2^n		A_2^{n+1}	
1			A_1^{n-1}		A_1^n		A_1^{n+1}	

$X_5 = b_5 X_4 + A_5$
$X_4 = \lambda_4 X_3 + A_4$
$X_3 = A_3/p_3$
$X_2 = \lambda_2 X_3 + A_2$
$X_1 = a_1 X_2 + A_1$

The computations for the x_i shown in Fig. 3 and 6 are given in Tables 3 and 4 and Fig. 19. Table 3 gives the computation of the elastic constants for Building No. 1 with a time interval, h, equal to .05 sec. Table 4 and Fig. 19 are the same as Table 2 and Fig. 18 except that numerical values have been inserted.

Case 2—Elastic Foundation

The displacements computed on the basis of a rigid foundation may be corrected as follows to include the effect of elastic foundation rocking:

(27) $$x_i^{n+1} = x_{i,s}^{n+1} - Z\,[\theta^n]\,x_{i,r}$$

where $x_{i,s}^{n+1}$ are identical with the x_i^{n+1} computed for the condition of a rigid foundation and $x_{i,r}$ are the roots of Eq. (26) for the condition $x_0 = F_1^n = 0$ and $Z\,[\theta^n] = -1$, and are independent of time, *i.e.*

(A11) $$-a_i x_{i+1,r} + x_{i,r} - b_1 x_{i-1,r} = r_i$$

$$\text{where } r_i = \frac{g_i}{\frac{12}{h^2} + k_i}$$

For a five story structure Eq. (26) become

(A12) $$x_{1,r} - a_1 x_2 = r_1$$
(A13) $$x_{2,r} - a_2 x_3 - b_2 x_1 = r_2$$
(A14) $$x_{3,r} - a_3 x_4 - b_3 x_2 = r_3$$
(A15) $$x_{4,r} - a_4 x_5 - b_4 x_3 = r_4$$
(A16) $$x_{5,r} - b_5 x_4 = r_5$$

The simultaneous solution of equations A12 through A16 yields

$$x_{1,r} = R_1 + a_1 x_2$$
$$x_{2,r} = R_2 + \lambda_2 x_3$$
$$x_{3,r} = \frac{R_3}{p_3}$$
$$x_{4,r} = R_4 + \lambda_4 x_5$$
$$x_{5,r} = R_5 + b_5 x_4$$

where

$R_1 = r_1$
$R_2 = g_2R_1 + f_2r_2$
$R_3 = r_3 + a_3R_4 + b_3R_2$
$R_4 = g_4R_5 + f_4r_4$
$R_5 = r_5$

TABLE 3—ELASTIC CONSTANTS FOR BUILDING NO. 1, TIME INTERVAL, h = 0.05 SEC

	1	2	3	4	5	6	7	8	9
Fl. No.	K #/in	$(10^2)M$ #sec^2/in	$(10^2)k_i'$	$(10^2)k_i''$	$(10^2)k_i$	$(10^5)a_i$ $-(10^4)c_i$	$(10^5)b_i$ $-(10^4)e_i$	$(10^5)d_i$	$(10^4)f_i$
1	11 400	1554	73360	66 023	139383	10 660	11 844	-70 041	10 000
2	10260	1554	66 023	58 687	124 710	9 705	10918	-47 478	10 118
3	9120	1554	58 687	51 351	110 038	8 703	9946	-23 793	10 000
4	7980	1554	51 351	44 015	95 366	7 650	8925	+ 1 101	10 084
5	6840	1166	58 662	—	58 662	—	10 890	+69 316	10 000

	10	11	12	13	14	15	16	17
Fl. No.	$(10^5)f_i a_i$	$(10^5)f_i c_i$	$(10^5)f_i b_i$	$(10^5)f_i e_i$	$(10^5)f_i d_i$	$(10^5)j_i$	$(10^5)\lambda_i$	$(10^5)p_i$
1								
2	9819	98 193	11 047	110 470	-48 037	11 047	9819	
3								98240
4	7714	77 143	9 000	90 000	+ 1 110	7714	9 000	
5								

TABLE 4—NUMERICAL VALUES SUBSTITUTED FOR SYMBOLS OF TABLE 2, RIGID FOUNDATION

Fl. \ t	0	.35	.40	.45
(l)	X_l	X_l	X_l	X_l
5	0	1.443 65	1.764 90	1.964 20
4	0	1.215 48	1.694 80	1.895 64
3	0	1.146 49	1.374 98	1.704 39
2	0	1.074 18	1.204 73	1.278 68
1	0	1.032 91	.997 24	1.027 48
0	0	.965 53	.866 03	.707 11
	A_l	A_l	A_l	A_l
5		1.311 28	1.580 34	1.757 76
4		1.112 30	1.571 05	1.742 24
2		.961 61	1.350 78	1.111 33
1		.918 40	.868 82	.891 17

$X_5 = 0.108\,94\ X_4 + A_5$
$X_4 = 0.090\,00\ X_3 + A_4$
$X_3 = A_3/0.982\,40$
$X_2 = 0.098\,19\ X_3 + A_2$
$X_1 = 0.106\,60\ X_2 + A_1$

AMERICAN CONCRETE INSTITUTE LIBRARY

To complete the solution of Eq. (27) the value of $Z[\theta^n] = \theta^{n+1} + 10\theta^n + \theta^{n-1}$ must be determined, where the rotations θ^n and θ^{n-1} are known and the unknown rotation θ^{n+1} is defined as follows:

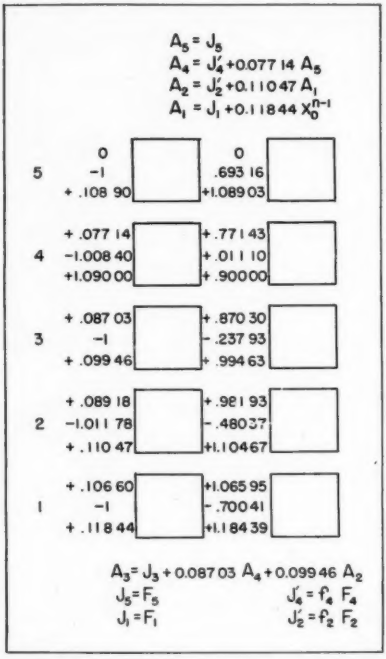

$$\theta^{n+1} = W\theta^n - \theta^{n-1} + P^n \text{ with}$$

$$W = \frac{\frac{24}{h_2} - 10E}{\frac{12}{h^2} + E}$$

$$P^n = \sum_{i=1}^{N} \left[\beta_i'' x_{i+1,s}^{n+1} - \beta_i x_{i,s}^{n+1} + \beta_i' x_{i-1,s}^{n+1}\right] + \sum_{i=1}^{N} \left[\beta_i'' x_{i+1}^{n-1} - \beta_i x_i^{n-1} + \beta_i' x_{i-1}^{n-1}\right] + 10 \sum_{i=1}^{N} \left[\beta_i'' x_{i+1}^{n} - \beta_i x_i^{n} + \beta_i' x_{i-1}^{n}\right]$$

$$E = \frac{B - C}{D} \doteq Q$$

B = elastic stiffness of foundation in rocking

$$C = \sum_{i=1}^{N} L_i M_i g_i \quad ; \quad D = \sum_{i=0}^{N} I_i$$

$$Q = \sum_{i=1}^{N} \left[\alpha_i'' x_{i+1,r} - \alpha_i x_{i,r} + \alpha_i' x_{i-1,r}\right]$$

Fig. 19—Computing frame with numerical values substituted for symbols in Fig. 18 to be used with Table 4

TABLE 5—ELASTIC CONSTANTS FOR ROCKING FOR BUILDING NO. 1, TIME INTERVAL, h, EQUALS 0.05 SEC

	1	2	3	4	5	6	7	8	9
Fl. No.	(10) g_i	$(10^5)r_i$	$(10^5)R_i$	$(10^5)x_{i,r}$	L_i	$(10^6)\alpha_i''$	$(10^6)\alpha_i$	$(10^6)\alpha_i'$	$(10^5)Q_i$
1	-281 699	-454 806	-454 806	- 481 435	168	293 598	619 818	326 220	+ 225 061
2	-105 637	-174 690	-226 989	- 249 302	312	484 670	1029 923	545 254	- 117 836
3	-105 637	-179 034	-228 251	-232 340	456	619 818	1328 182	708 364	- 71 551
4	105 637	-183 599	-306 111	-327 022	600	699 043	1514 594	815 551	- 815 319
5	-844 734	-1568 207	-1568 207	-1603 820	744	——	866 813	866 813	+1106 746

	10	11	12
Fl. No.	$(10^{-9})\beta''$	$(10^{-9})\beta$	$(10^{-9})\beta'$
1	56 818	63 131	119 948
2	93 794	105 519	199 313
3	119 948	137 084	257 032
4	135 280	157 827	293 107
5	——	167 747	167 747

$B = 114\,511 \times 10^2$
$C = -103\,093 \times 10^8$
$D = 587\,088 \times 10^{-1}$
$Q = 327\,597 \times 10^5$
$\varepsilon = 193\,522 \times 10^{-9}$
$W = 114\,686 \times 10^{-5}$

$$\alpha_i'' = \frac{L_i M_i k_i''}{D} \quad ; \quad \alpha_i' = \frac{L_i M_i k_i'}{D} \quad ; \quad \alpha_i = \frac{L_i M_i k_i}{D} \quad ; \quad g_i = k_i'' l_{i+1} - k_i' l_i$$

$$\beta_i'' = \epsilon\, \alpha_i'' \quad ; \quad \beta_i' = \epsilon\, \alpha_i' \quad ; \quad \beta_i = \epsilon\, \alpha_i \quad ; \quad \epsilon = \frac{1}{\frac{12}{k^2} + E}$$

All the factors above except P are independent of time. P, however, is a function of the $x_{i,s}^{n+1}$ and x_i^n; and x_i^{n-1} must therefore be computed for each time interval.

$$P^n = \begin{bmatrix} \beta_1'' x_{2,s}^{n+1} - \beta_1 x_{1,s}^{n+1} + \beta_1' x_0^{n+1} \\ + \beta_2'' x_{3,s}^{n+1} - \beta_2 x_{2,s}^{n+1} + \beta_2' x_{1,s}^{n+1} \\ + \beta_3'' x_{4,s}^{n+1} - \beta_3 x_{3,s}^{n+1} + \beta_3' x_{2,s}^{n+1} \\ + \beta_4'' x_{5,s}^{n+1} - \beta_4 x_{4,s}^{n+1} + \beta_4' x_{3,s}^{n+1} \\ - \beta_5 x_{5,s}^{n+1} + \beta_5' x_{4,s}^{n+1} \end{bmatrix} + \begin{bmatrix} \beta_1'' x_2^{n-1} - \beta_1 x_1^{n-1} - \beta_1' x_0 \\ + \beta_2'' x_3^{n-1} - \beta_2 x_2^{n-1} - \beta_2' x_1^{n-1} \\ + \beta_3'' x_4^{n-1} - \beta_3 x_3^{n-1} - \beta_3' x_2^{n-1} \\ + \beta_4'' x_5^{n-1} - \beta_4 x_4^{n-1} - \beta_4' x_3^{n-1} \\ - \beta_5 x_5^{n-1} - \beta_5' x_4^{n-1} \end{bmatrix}$$

$$+10 \begin{bmatrix} \beta_1'' x_2^n - \beta_1 x_1^n \\ + \beta_2'' x_3^n - \beta_2 x_2^n + \beta_2' x_1^n \\ + \beta_3'' x_4^n - \beta_3 x_3^n + \beta_3' x_2^n \\ + \beta_4'' x_5^n - \beta_4 x_4^n + \beta_4' x_3^n \\ - \beta_5 x_5^n + \beta_5' x_4^n \end{bmatrix}$$

The procedure of computation is as follows:

1. Compute P^n as given above
2. Subtract θ^{n-1} and add $W\theta^{n+1}$
3. Record θ^{n+1}
4. Compute $Z[\theta^n] = \theta^{n+1} + 10\,\theta^n + \theta^{n-1}$ and multiply $Z[\theta^n]$ times $x_{i,r}$ to get the rocking correction.
5. Subtract this correction algebraically from $x_{i,s}^{n+1}$ to obtain the true x_i^{n+1}.

When using an automatic desk calculator which can multiply accumulatively and negatively only the value of θ^{n+1} and x_i^{n+1} need be recorded.

For the computation of P^n a computing frame such as shown in Fig. 20 is helpful in systematizing the work. Fig. 21 is similar to Fig. 20 except that numerical values have been substituted for the symbols β_i. All computations are performed using the same table (Table 2) as for the rigid foundation solution.

The computation of the elastic constants for rocking for Building No. 1 are given in Table 5. Table 6 gives the solution with rocking corresponding to Table 4 for the condition of a rigid foundation. x_i and $\bar{x}_i$ are substituted in Table 6 for $x_{i,s}$ and x_i respectively to avoid conflict in notation.

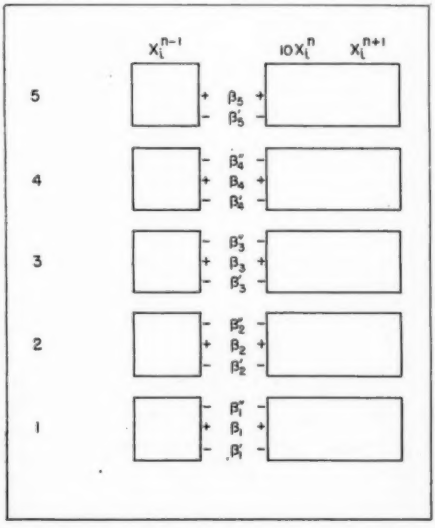

Fig. 20—Computing frame for use in computing P^n

TABLE 6—NUMERICAL VALUES FOR ROCKING ON AN ELASTIC FOUNDATION

Fl. \ t	0	.35		.40		.45	
	X_i	X_i	$\overline{X}_i$	X_i	$\overline{X}_i$	X_i	$\overline{X}_i$
5		1.443 65	1.340 85	1.764 90	1.781 21	1.964 20	2.123 33
4		1.215 48	1.194 52	1.694 80	1.698 13	1.895 64	1.928 09
3		1.146 49	1.131 60	1.374 98	1.377 34	1.704 39	1.727 44
2		1.074 18	1.058 17	1.204 73	1.207 27	1.278 68	1.303 47
1		1.032 91	1.002 05	.997 24	1.002 14	1.027 48	1.075 25
0		.965 93	.965 93	.866 03	.866 03	.707 11	.707 11
	A_i	A_i	$(10^8)\theta_i$	A_i	$(10^8)\theta_i$	A_i	$(10^8)\theta_i$
5	0	1.311 28	7 326	1.580 34	84 676	1.757 76	138 147
4	0	1.112 30		1.571 05		1.742 24	
2	0	.961 61		1.350 78		1.111 33	
1	0	.918 41		.868 82		.891 17	

$X_5 = 0.108\,94\ X_4 + A_5$
$X_4 = 0.090\,00\ X_3 + A_4$
$X_3 = A_3/0.982\,40$
$X_2 = 0.098\,19\ X_3 + A_2$
$X_1 = 0\,106\,60\ X_2 + A_1$

$\theta^{n+1} = W\theta^n - \theta^{n-1} + P^n$
$Z(\theta^n) = \theta^{n+1} + 10\theta^n + \theta^{n-1}$
$\overline{X}_i = X_i - Z(\theta^n)\,X_{i,r}$

$X_{5,r} = -16.038\,20$
$X_{4,r} = -3.270\,22$
$X_{3,r} = -2.323\,40$
$X_{2,r} = -2.498\,02$
$X_{1,r} = -4.814\,35$

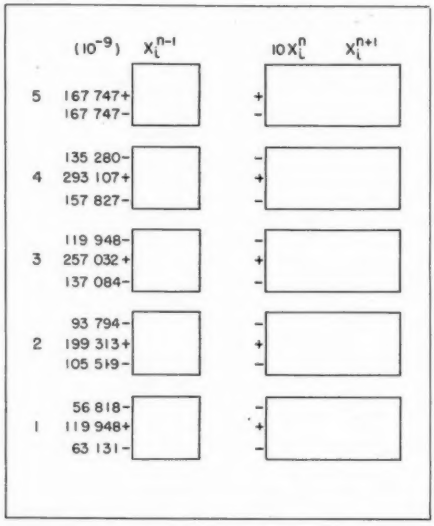

Fig. 21—Computing frame with numerical values substituted for symbols β_i in Fig. 20 for use with Table 6.

Discussion of a paper by Charles S. Whitney, Boyd G. Anderson and Mario G. Salvadori:

Comprehensive Numerical Method for the Analysis of Earthquake Resistant Structures*

By S. K. GHASWALA and AUTHORS

By S. K. GHASWALA†

The paper is a notable piece of work in the analytical field of engineering seismology and represents an advance over the conventional methods of approach. Design of structures to resist seismic forces or other ground vibrations was until recently relegated to the domain of statics and inaccurate and uneconomical methods adopted in analyzing their effects. It is only in the last three decades, and especially after the great Japanese Kwanto earthquake which rocked and severely damaged Tokyo and Yokohoma in September, 1923, that engineers and physicists were roused from their slumber and forced to investigate these problems more thoroughly. This period, as shown by the writer elsewhere,[1] formed the fifth and most modern phase of development in engineering seismology. It resulted in establishment of the world renowned Earthquake Research Institute at Tokyo Imperial University, source of some of the most monumental and authoritative works in the field.

Since then the true effect of earthquakes on structures has been revealed more and more clearly, and the criterion of seismic design correctly recognized as a transient dynamic vibration phenomena. These studies led to two schools of thought, one holding to the principle of rigidity combined with strength as the essential factor, while the other held to a highly flexible type of construction since it was believed that in practice sufficient strength and rigidity were difficult to attain economically. These have been modified at present in light of extensive theoretical and practical work done by Jacobsen, Ruge and others in the United States; Velezuela in Chile; and Imamura, Sezawa, Kanai and others in Japan.

The correct perspective of structural design was brought out when the data furnished by accelerograms, especially of strong motion waves, was used in conjunction with existing seismological knowledge. According to this concept, the structure is visualized as floating on a medium in which highly irregular waves are propagating with attributes of distributed elasticity and damping effects, so that like a ship in the ocean, its motion is de-

*ACI Journal, Sept. 1951, *Proc.* V. 48, p. 5. Disc. 48-2 is a part of copyrighted Journal of the American Concrete Institute, V. 24, No. 4, Dec. 1952, Part 2, *Proceedings* V. 48.

†Consulting Engineer, Bombay, India.

pendent upon its own rigidity, mass and size relative to the waves and is not completely synchronous with the motion of the surrounding fluid. Further, an important effect on resonance phenomena is produced by internal friction and yield point in the surrounding soil, while the final effects of reflected, refracted, and diffracted waves on an agglomeration of buildings are considerably modified by the individual structures themselves.

In developing the numerical step-by-step method, the authors have considered most of the above concepts, and thereby given an analytical solution which is believed to be more accurate than evolved hitherto. The effects of plasticity of the structure and of the soil remain to be fully evaluated.

The writer believes that these rigorous methods of analysis, in spite of their high accuracy are far too involved and of limited significance to structural engineers, especially those unfamiliar with electric computing devices or IBM punch card machines which form essential tools for the solution of differential equations encountered in such numerical analyses.

Since the presentation of this paper, an important publication has been released by the American Society of Civil Engineers, through a joint committee of the San Francisco, Calif., section.[2] This paper, which contains an exhaustive bibliography outlines an approach to seismic forces which although not quite new in its basic concept, has been extended to a rational dynamic method for establishing the requisite design forces on a structure. It involves the determination of total lateral force or base shear transmitted into the structure from the ground, and the distribution of that shear as equivalent forces applied to that structure. Transformed into the form of building codes, this method gives, within limits of practical feasibility, the most accurate and easy solution for the seismic design of structures attempted up to now. It is worth detailed scrutiny and comparison with the paper under discussion.

In conclusion, the writer states that without in any way belittling the high merits of this paper, the more rigorous and complicated procedures given here need encouragement and considerable experimental support to guide the formulation of less rigorous but more practical methods of analysis.

REFERENCES

1. Ghaswala, S. K., "Developments in Engineering Seismology," *Civil Engineering* (London), Dec. 1947, p. 522, and Jan. 1948, p. 37.

2. Anderson, A. W., and others, "Lateral Forces of Earthquake and Wind," *Proceedings*, ASCE, Separate No. 66, V. 77, Apr. 1951, 38 pp., and Discussion No. D-66, V. 78, May 1952, 26 pp.

AUTHORS' CLOSURE

The authors wish to thank Mr. Ghaswala for his discussion. While the method might be used directly for the design of larger and more important structures, they agree that it is too involved to be readily used for the design of ordinary structures.

The method is expected to be of more use, however, as a research tool which can be used to evaluate the effect of building flexibility, rocking or yield of the supporting foundations, damping in the members and other effects pertinent to obtaining safe construction at minimum costs.

While the effect of plasticity was not included in the representative examples, the plastic action of the members and supporting soil can be considered by minor modifications of the step-by-step procedures. Such procedures accounting for strain in the plastic range have been used in evaluating the blast resisting capacity of structures. The equations during the time of plastic action are simplified as the resistances become constant or near constant values at strains exceeding the yield strength of the materials.

Such conflict as was quoted by Mr. Ghaswala between the schools of thought on "flexible" construction contrasted by "rigid" construction might be resolved if comparisons in damage and construction economies are made possible by adequate analytical tools.

Preliminary studies indicate that a detailed analysis of the action of a few selected buildings can be plotted to give useful design data for a large range of typical constructions.

No attempts were made in the paper to answer the detailed questions posed by the action of seismic forces on structures though examples were given to show application of the method to typical problems. Similar and more extended investigations could be conducted on other problems and general conclusions could be drawn from such detailed studies.

Title No. 48-3

Multistory Buildings Designed to Resist Earthquakes*

By JOHN J. GOULD†

SYNOPSIS

Earthquake resistant provisions of the San Francisco building code were met by the exclusive use of reinforced concrete in the construction of eleven 13-story apartment buildings. The X-shaped apartments have flat-slab floors with wide flat beams over corridors. Exterior walls are of the bearing-wall type without columns. Many interior partitions are of reinforced concrete to resist vertical as well as horizontal loads. An advantage of the interior bearing wall system is that lateral bracing for earthquake resistance is increased at little extra cost.

It was estimated that the extra cost of earthquake resistance was only 1 to 2 percent of the total, as compared with otherwise sound minimum construction, due to the structural system chosen.

INTRODUCTION

California engineers have been aware since 1906 of the necessity of designing structures to resist earthquakes. Following the Long Beach earthquake in 1933, state laws were passed making mandatory the design of almost all buildings with a minimum amount of earthquake resistance. Various building codes have since been adopted, each more stringent than the previous. The 1947 San Francisco code is far more restrictive than elsewhere, particularly with regard to tall buildings. Since many buildings have successfully withstood major Pacific Coast earthquakes, although designed with little or no special earthquake resistance, the San Francisco requirements appear to be overly conservative. For the buildings described in this paper, earthquake loads to be resisted were 75 percent higher than those required under the Los Angeles building code.

To illustrate further the wide discrepancy between earthquake experience and building code requirements, consider the case of the 12-story Flood Building in San Francisco. This steel frame and brick wall building withstood the 1906 earthquake with but minor damage, yet an analysis of the structure shows it would resist horizontally less than 0.75 percent of the vertical loads based on the present code. The same building would now have to be designed against earthquake loads nine times as great. This and other comparisons seem to show the futility of great refinements and ultra conservatism in earthquake designs.

*Presented at the ACI 47th Annual Convention, San Francisco, Calif., Feb. 20, 1951. Title No. 48-3 is a part of the copyrighted JOURNAL OF THE AMERICAN CONCRETE INSTITUTE, V. 23, No. 1, Sept. 1951, *Proceedings* V. 48. Separate prints are available at 35 cents each. **Discussion** (copies in **triplicate**) should reach the Institute not later than Jan. 1, 1952. Address 18263 W. McNichols Rd., Detroit 19, Mich.

†Member American Concrete Institute, Consulting Engineer, San Francisco, Calif.

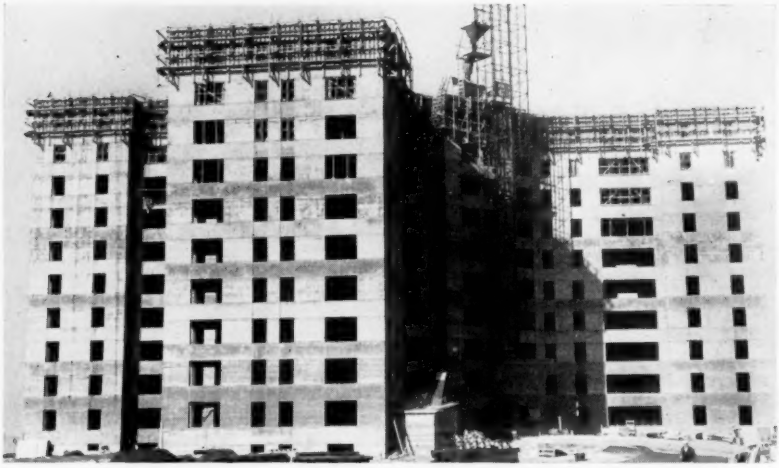

Fig. 1—Exterior of 13-story apartment tower building under construction

Based upon observation of damage in Long Beach, it appears that the choice of sound materials, the use of honest workmanship coupled with simple, honest design and competent supervision should be the guiding factors in building structures to resist earthquakes.

STRUCTURAL DESIGN

In the structural design of eleven 13-story apartment buildings built at Parkmerced for about 30 million dollars, the provisions of the new San Francisco code were met by the exclusive use of reinforced concrete (Fig. 1). Floors were slab type with wide flat beams over corridors. Exterior walls were of the bearing-wall type without columns. Many interior partitions commonly built of plaster or other materials were built of reinforced concrete to resist vertical as well as horizontal loads. These provisions resulted in extremely economical structures. It is estimated that the extra cost of the heavy earthquake resistance was only 1 to 2 percent of the total cost as compared with otherwise sound minimum construction.

The owners of the project, Metropolitan Life Insurance Co., desired a permanent investment with a sound long-term income. To meet this need, the architect developed an X-shaped plan, with a central area housing elevators and stairs and using a minimum of corridors. Story height is 9 ft with over-all building height 135 ft. The typical floor has 12 apartments on 15,000 sq ft, giving a total of 152 apartments in each building.

The structure was designed for a 40 psf live load plus a 20 psf partition load. Building laws require a minimum wind load of 15 psf from ground level to 60 ft above ground, and 20 psf above that. Earthquake forces vary from

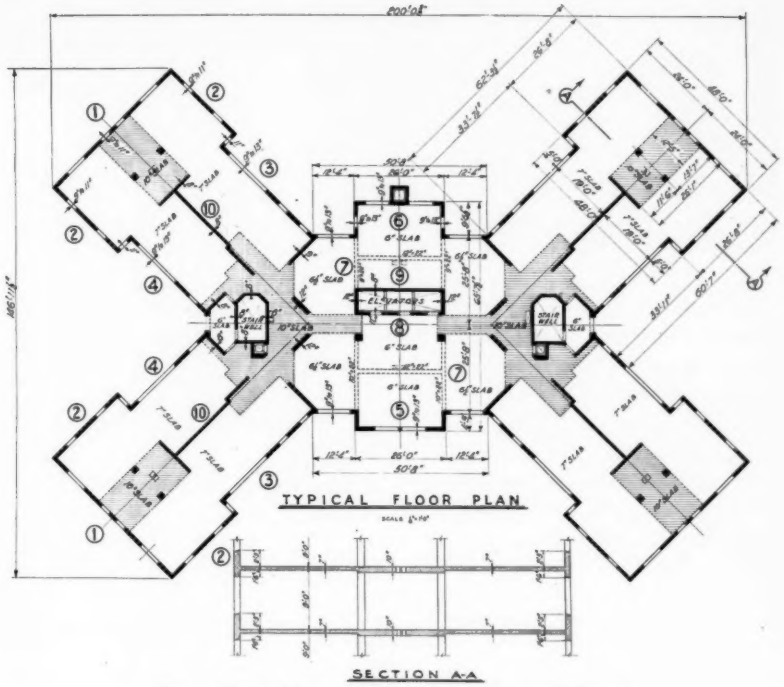

Fig. 2—Typical floor plan of 13-story tower apartment unit

8 percent of the design column loads at the roof to 5.3 percent of the column loads in the first story, to be applied horizontally in any direction. The design column loads represent all of the dead loads plus 60 percent of the live loads.

The general framing layout is shown in Fig. 2. The slabs from interior wall "10" to exterior walls "3" and "4" are 7 in. thick on an 18-ft span. Although a 5-in. slab would have been adequate for strength, the thicker slab was chosen on the basis of deflections—especially those due to plastic flow of the concrete—and the necessity of reducing deflections to minimize cracking of interior partitions. Little difference was found between the cost of a 7-in. and a 5-in. slab because less reinforcing steel was necessary with the thicker slab. By using a 7-in. slab, it is estimated that elastic deflections will be held to about 0.07 in. for dead loads plus live loads. Considering plastic flow, the deflection should be about 0.40 in. or 1/500 of the span over a period of 10 years, after which they should be practically stable.

In the areas between walls "1" and "10" and in the corridors near the intersections of the wings, the slab is thickened to 10 in. At the elevators near the center of the building, it was necessary to use 25-ft span beams.

Fig. 3—Interior view of typical floor of apartment building showing flat-slab construction, exterior and interior concrete bearing walls

Deflections of these beams were analyzed, and considerable redistribution of slab steel was found advisable since deflections of the slab supports showed a marked change in the bending moments and shears as compared to an analysis based on unyielding supports.

Bottoms of the slabs and shallow beams were painted, giving the rooms 8 ft-4 in. and the corridors 8 ft-2 in. ceiling heights. The well balanced concrete mix and excellent workmanship make it practically impossible to tell that the ceilings are not plastered.

Exterior bearing walls have no columns and in general vary from 13 in. thick at first floor to 9 in. minimum thickness in the upper stories. In any wall the pilasters between windows and the spandrels have the same thickness in any story, thereby simplifying formwork. This condition is also believed to reduce cracks in concrete often found at points of abrupt changes in section. Interior concrete bearing walls, generally 8 in. thick, were used around stairs, incinerators, elevators and as a dividing wall between apartments in the wings of the buildings. By using reinforced concrete for these elements, a number of beams and columns as well as plaster partitions were eliminated (Fig. 3) and it is in this regard that the structural design differs from usual practice on the West Coast.

Under conservative earthquake provisions a prime advantage of the interior bearing wall system is that for lateral bracing the resistance of the building is increased at little extra cost. For example, at the first floor, interior walls "10" carry at least 20 percent of the lateral load. A secondary advantage of this system is that there are no breaks around columns or beams in the various rooms, resulting in better appearance and more usable floor area. Furthermore, interior bearing walls provide greater rigidity against vertical load deflections and provide greater safety from fragments.

Lateral earthquake loads as determined by the building code amounted to a horizontal force of 2370 kips at the base. This corresponds to a wind load of 91 psf on the maximum exposure, and 131 psf on the minimum exposure. Structurally, this and other provisions equal or exceed the September, 1950, recommendations of the Atomic Energy Commission for construction resistant to atomic bomb blasts. Some Japanese reinforced concrete buildings designed

to resist earthquakes, located as close as 700 ft of ground zero of atomic bomb blasts, suffered but minor structural damage.

To comply with the code, lateral loads on the Parkmerced buildings were distributed according to relative rigidities of the various resisting elements, assuming floor diaphragms to be rigid. In determining the rigidities of various walls, the shear distortion from floor to floor, the amount of distortion from bending of the wall as a whole, and the yielding of the foundation were analyzed. The last two factors, usually not considered in low buildings, were important here because of the large difference in the depth and shape of the resisting elements. For example, wall "2-3" is 62 ft long with other walls corresponding to flanges connected to it, giving a large moment resistance. Wall "10" is only 30 ft long, has small flanges and is a 135 ft high cantilever. Its shear resistance is high, but its resistance due to moment distortion and foundation yielding is low for the higher stories.

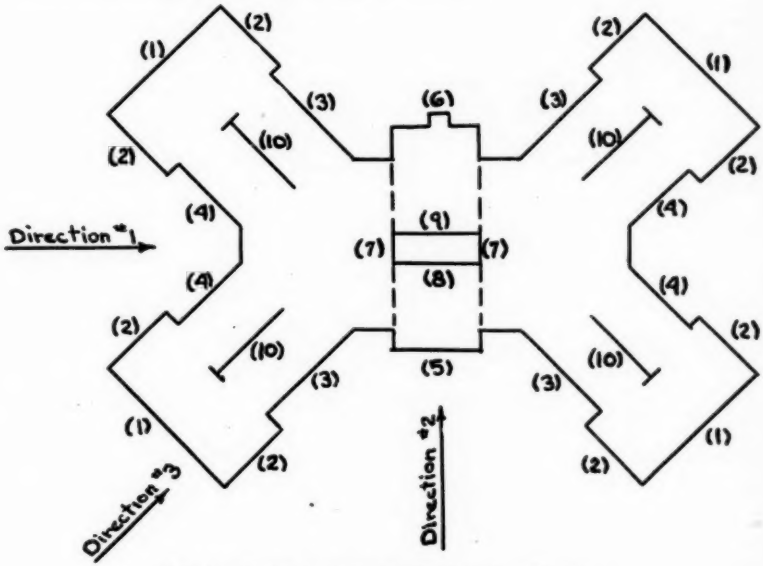

Fig. 4—Bracing elements effective in various directions

	Direction 1	Direction 2	Direction 3
Exterior walls	4 walls (1) @ 45° 8 walls (2) @ 45° 4 walls (3) @ 45° 4 walls (4) @ 45° 1 wall (5) @ 0° 1 wall (6) @ 0°	4 walls (1) @ 45° 8 walls (2) @ 45° 4 walls (3) @ 45° 4 walls (4) @ 45°	1 wall (5) @ 45° 1 wall (6) @ 45° 2 walls (1) @ 0° 4 walls (2) @ 0° 2 walls (3) @ 0° 2 walls (4) @ 0°
Interior walls	1 wall (8) @ 0° 1 wall (9) @ 0° 4 walls (10) @ 45°	2 walls (7) @ 0° 4 walls (10) @ 45°	2 walls (10) @ 0° 2 walls (7) @ 45° 1 wall (8) @ 45° 1 wall (9) @ 45°

TABLE 1—SHEAR DISTRIBUTION TO WALL ELEMENTS BASED ON RIGIDITIES INCLUDING MOMENT AND FOUNDATION DEFLECTIONS*

Floor	Total load on bldg.	Wall 1		Wall 2—3		Wall 2—4		Wall 5		Wall 6		Wall 7		Wall 8		Wall 9		Wall 10	
	Shear, kips	Max. % stress	Shear, kips	Max. % stress	Shear, kips	Max. % stress	Shear, kips	Max. % stress	Shear, kips	Max. % stress	Shear, kips	Max. % stress	Shear, kips	Max. % stress	Shear, kips	Max. % stress	Shear, kips	Max. % stress	Shear, kips
R-13	220.8	.1011	22.10	.1985	43.80	.1326	29.30	.020	4.32	.020	4.32	.0366	8.09	.016	3.54	.017	3.76	.0311	6.87
13-12	447.0	.1005	44.80	.1977	88.40	.1332	59.60	.023	10.30	.020	8.94	.0365	16.30	.015	6.71	.017	7.60	.0317	14.20
12-11	655.0	.1012	66.20	.1965	128.50	.1326	86.90	.020	13.10	.022	14.40	.0364	23.80	.016	10.50	.018	11.80	.0324	21.20
11-10	846.0	.1012	85.50	.1959	165.80	.1325	112.10	.021	17.80	.022	18.60	.0361	30.60	.017	14.40	.018	15.20	.0332	28.10
10-9	1040.0	.1005	104.10	.1946	202.20	.1328	138.00	.021	21.90	.024	25.00	.0359	37.40	.017	17.70	.019	19.80	.0341	35.50
9-8	1200.0	.0998	119.90	.1947	232.80	.1321	158.90	.021	25.20	.024	28.80	.0354	42.50	.017	20.40	.020	24.00	.0354	42.50
8-7	1370.0	.1004	137.20	.1905	261.00	.1326	181.50	.021	28.80	.025	34.30	.0353	48.40	.019	26.00	.023	31.50	.0368	50.40
7-6	1530.0	.1001	153.10	.1890	289.00	.1321	202.20	.021	32.10	.027	41.30	.0350	53.50	.018	27.60	.022	33.60	.0389	59.50
6-5	1670.0	.0994	166.00	.1854	309.90	.1338	223.50	.021	35.10	.028	46.80	.0343	57.30	.019	31.80	.023	38.40	.0415	69.30
5-4	1810.0	.0995	180.00	.1805	326.80	.1335	241.80	.021	38.00	.030	54.30	.0337	61.00	.021	38.00	.025	45.20	.0455	82.40
4-3	1970.0	.0898	177.00	.1837	362.00	.1335	263.00	.020	39.40	.033	65.00	.0329	64.90	.022	43.30	.028	55.20	.0512	100.80
3-2	2080.0	.0938	195.00	.1695	352.20	.1316	273.80	.019	39.50	.034	70.80	.0317	66.00	.031	64.50	.033	68.70	.0594	123.60
2-1	2230.0	.0902	201.00	.1607	358.00	.1300	290.00	.019	42.40	.035	78.10	.0300	67.00	.027	60.20	.041	91.50	.0731	163.00
1-B	2370.0	.0823	195.00	.1422	337.80	.1207	286.00	.016	38.00	.034	80.60	.0279	66.20	.030	71.20	.062	147.00	.1043	247.20

*Maximum stresses are based upon worst condition of direction of load as indicated by Fig. 4.

Because of the complex orientation of the walls, the building was analyzed for lateral forces in three major directions as shown in Fig. 4. It can be shown that two identical wall elements placed at 0° and 45° respectively to a load, have rigidities and stresses as follows. The wall at 0° is twice as rigid as the one at 45°. The wall at 0° has a unit stress 41 percent greater than the one at 45°. By finding the rigidities of the walls as previously mentioned, and summing up their resistances for each direction of load, the proportional resistance of each wall to the total load was determined, and hence the load on the wall.

Table 1 lists the total shear on the building at each of the floor levels, with the maximum proportion of load taken by each bracing wall for any of the three directions. As an example, each wall "10" in the lowest story resists 10 percent of the total load (two walls effective in any direction). In the upper stories, because of its shallow depth, each wall resists only 3 percent.

The stresses in the various floor diaphragms are determined from the wall loads. Each wall above the floor contributes a load to the diaphragm as determined from relative rigidities. The location of increments of load on the system from loads on that floor are determined from the location of basic vertical loads. These forces are resisted by the walls under the floor as determined by their rigidities. The algebraic summation of these loads and their lever arms determines shears and moments in the floor diaphragm. These forces were generally quite low and did not affect slab thicknesses, but caused special consideration for the reinforcing at the re-entrant corners where the wings join the main body of the structure and at floor openings.

Because of the arrangement of bracing elements, the resistance of wall "1" was checked against the local loads tributary to it, to insure a satisfactory torsional rigidity of the structure as a whole. It was found that in this particular case the loads normally assigned to wall "1" by its relative rigidity for translational forces were adequate to resist any torsional forces that might develop.

The structural design was adapted to meet mass production and mass building methods—speed, simplicity of formwork, ease of placing and maintaining reinforcement, and speed and ease of placing concrete.

All piers and spandrels with the reinforcement were detailed first at full scale so that positive assurance was obtained for the easy introduction of vibrators at all points. Concrete with a design strength of 3000 psi was used containing 6 sacks of cement and 3 lb of Plastiment admixture per cu yd. Slump was held at 4 to 6 in. maximum. Construction keys were carefully roughened and grouted. This is especially important in earthquake resistant design as experience has proved that many failures occur at these weakened planes in otherwise well built buildings.

Bent and top bars in slabs were generally made a minimum diameter of $\frac{5}{8}$ in. to assure their position during concreting. Slabs were not cambered.

None of the structural elements had special requirements as to mix, forms, or reinforcing steel (there was no welding or milling of bars) so that the utmost economy in concrete work was possible.

FINISHED STRUCTURE

Since construction of the buildings, several pertinent observations have been made.

1. The buildings were generally founded on sand, using spread footings with a bearing value of 8000 psf. No measurable settlement has been observed so far.
2. In three buildings, a number of small cracks were found in basement walls. Investigation indicated that in these particular locations, calcium chloride was used as an admixture.
3. Few cracks have been found in the supported floor slabs. As far as can be determined. there were fewer cracks where the slump was held to 4 in. than where a 6-in. slump was used, Temperature reinforcement in slabs was 0.2 percent. Of 3700 concrete cylinder tests made, the minimum 28-day strength was 3050 psi while the maximum was 5520 psi. These results refer to the 6-sack mix of the 70,000 cu yd of concrete furnished by the Pacific Coast Aggregate Co.
4. In general, exterior walls of the building above the first floor have unusually few cracks (all very small). This is attributed to excellent workmanship, low slump concrete, high percentage of reinforcing steel (resulting from design against earthquake forces), continuity of wall sections and reinforcing steel, and the admixture used.
5. The actual cost of constructing forms and placing concrete was about 25 percent less than the lowest previous estimates made. Some forms had as many as 13 reuses. These savings do not reflect further economies in plaster work by the elimination of columns, pilasters and interior plaster partitions replaced by concrete.

SUMMARY

The structures described, because of their simplicity and low cost, are believed to furnish some of the best available protection against fire, severe earthquakes, hurricanes and atomic blasts. During any of these disasters, buildings built throughout of monolithic reinforced concrete, reduce hazards from flying fragments to a minimum. The structures discussed possess 4 to 5 times the resistance to horizontal forces of buildings built under current Eastern practice—their costs however are similar.

Had Tokyo and Hiroshima been built of properly engineered reinforced concrete, destruction from earthquakes and the A-bomb would have been infinitely less. Casualties would have been sharply reduced. These long range objectives applicable to seismic regions and target areas in the United States seem to be within economic reach of the American building industry in the near future.

ORGANIZATION

The entire project was built for the Metropolitan Life Insurance Co. of New York by Starrett Brothers and Eken, Builders, New York City, with Dinwiddie Construction Co., San Francisco, as contractors for the form and concrete work. The Pittsburgh Testing Laboratory, San Francisco, designed concrete mixes and tested all of the structural materials. Leonard A. Schultze and Associates of New York were the architects; Thomsen and Wilson of San Francisco, associate architects. Detailed inspection of the work was done by the owners' engineers. L. T. Evans of Los Angeles was the foundation and soil engineer. The writer was the consulting structural engineer, with Henry J. Degenkolb as chief engineer and T. O. Treverton as chief draftsman.

Discussion of a paper by John J. Gould:

Multistory Buildings Designed to Resist Earthquakes*

By E. L. HOWARD and CLYDE HART†

Mr. Gould spoke about the concrete used as being of good quality and uniformity. This discussion concerns itself with some test results of specimens taken at the job site from the concrete as delivered.

The plant that batched the materials was on the job site. The operator concerned himself with only one mix at a time, thus he was able to maintain better control than would have been possible in a commercial ready-mixed concrete plant. All concrete was transit mixed in 5-cu yd mixer trucks. Layout and facilities of the batching plant allowed for plenty of storage space for the aggregates which were trucked 47 miles from the Centerville plant of Pacific Coast Aggregates, Inc. This material in storage gave maximum moisture control of the sand.

The Pittsburgh Testing Laboratory designed the concrete mixes and this report includes results of compression tests it made during the course of the job. The writers are indebted to Parker Robinson of Pittsburgh Testing Laboratory for his cooperation in providing this information. During the job his men and ours worked in close harmony and an ideal inspection, without "sloppy work" and loss of time, was the result.

Aggregates were tested at the gravel plant by the Pacific Coast Aggregates testing department and graded as shown in Table A. Pacific Coast Aggregates also made concrete cylinders for compression tests. Results of these tests are averaged and shown in Table B. Shown also in Table B are the several mixes designed by the Pittsburgh Testing Laboratory.

Concrete cylinders for testing were made from concrete obtained as the transit mixer truck discharged its load. After casting, the cylinders remained on the job, protected by moisture-proof boxes, until the following day. Specimens were then moist cured at 70 F until broken. Both laboratories use the 6 x 12-in. paraffined paper mold for casting test specimens. Consistency of the concrete on this job was measured by the Kelly consistency meter.‡ Slumps were taken during the first part of the job to find the relationship between the Kelly meter reading and slump, but the ease of operation of the meter soon caused the discard of the slump cone.

*ACI JOURNAL, Sept. 1951, *Proc.* V. 48, p. 29. Disc. 48-3 is a part of copyrighted JOURNAL OF THE AMERICAN CONCRETE INSTITUTE, V. 24, No. 4, Dec. 1952, Part 2, *Proceedings* V. 48.

†Pacific Coast Aggregates, Inc., San Francisco, Calif.

‡For description of meter see "Inspection of Ready-Mixed Concrete," by E. L. Howard, ACI JOURNAL, June 1950, *Proc.*, V. 46, pp. 777-784.

TABLE A—AVERAGE GRADINGS OF AGGREGATES—1547 SAMPLES

Sieve	Percent passing			
	Coarse gravel	Fine gravel	Coarse sand	Fine sand
1¼ in.	100			
1 in.	69	100		
¾ in.	4	89		
⅜ in.		28		
No. 4		2	95	
No. 8			75	
No. 16			58	
No. 30			36	99
No. 50			13	53
No. 100			2	1.8

TABLE B—CONCRETE MIX AND CYLINDER TEST DATA—PACIFIC COAST AGGREGATES TEST SPECIMENS

Mix No.	1806	1822	1883	1884	2004	2006	2007
1¼ x ¾-in. gravel, lb	884	910	....	....	....	....	935
¾ x ¼-in. gravel, lb	1103	1147	1775	1703	1783	1815	1175
Coarse sand, lb	998	1017	1238	1312	1373	1273	1040
Fine sand, lb	231	235	200	200	206	200	235
Cement, lb	611	564	564	611	470	564	564
Plastiment admix, lb	3¼	3	3	3¼	2½	3	3
Slump, in.	4	4½	4½	5	4	4	4¼
Kelly meter	2	2.3	2.3	2.5	2	2	2
Compressive strengths							
Avg. 28-day, psi	4621	4185	4350	4530	3255	4550	4317
Max. 28-day, psi	5490	5100	5040	5760	3880	5520	5290
Min. 28-day, psi	4100	3460	3875	3365	2840	3280	3050
No. cylinders	28	52	99	64	16	86	36
90 percent of avg.	4160	3770	3915	4080	2930	4095	3885
80 percent of avg.	3700	3550	3480	3625	2600	3640	3455
Percent less than 90	7	5.8	2	4.7	0.7	7	5.5
Percent less than 80	0	0	0	3.1	0	1.2	2.8

TABLE C—28-DAY CYLINDER TEST DATA—PITTSBURGH TESTING LABORATORY TEST SPECIMENS

PCA 1806*	PTL 271†
Highest break	5877 psi
Lowest break	3423 psi
Average	4308 psi
Percent cylinders under 90 percent of avg.	9.4
Percent cylinders under 80 percent of avg.	1.9
Total number of cylinders	53
PCA 1822*	**PTL 287†**
Highest break	6324 psi
Lowest break	3032 psi
Average	4381 psi
Percent cylinders under 90 percent of avg.	19.5
Percent cylinders under 80 percent of avg.	5.8
Total number of cylinders	361
PCA 1883*	**PTL 294A†**
Highest break	6417 psi
Lowest break	2641 psi
Average	4634 psi
Percent cylinders under 90 percent of avg.	12.5
Percent cylinders under 80 percent of avg.	1.7
Total number of cylinders	917
PCA 1884*	**PTL 270A†**
Highest break	6510 psi
Lowest break	2381 psi
Average	4614 psi
Percent cylinders under 90 percent of avg.	21
Percent cylinders under 80 percent of avg.	2.7
Total number of cylinders	2.9

*Pacific Coast Aggregates, Inc., mix number.
†Pittsburgh Testing Laboratory mix number.

Strengths of cylinders tested by the Pittsburgh Testing Laboratory have been averaged and are shown in Table C. The highest and lowest break for each mix is shown, as well as the percent of cylinders that broke below 90 percent average and 80 percent average. It can be readily seen that the concrete was of good quality and uniform throughout the job.

Material and labor shortages enhance interest in lightweight concrete construction

Lightweight Concrete For Lower Construction Costs*

By J. A. MURLIN†

SYNOPSIS

From accurate construction costs taken from the contractor's records on a cost plus fixed fee contract, it is demonstrated that the use of lightweight expanded shale concrete plus flat-plate design substantially reduced the cost of the structural frame of a two-story office building. Comparative figures are given for eight different types of construction in normal or lightweight concrete. The method of analysis used in designing the lightweight flat plate is discussed.

The mix design for the lightweight concrete is given and the plant set-up for the use of mixers in series is described. Results of laboratory tests of control cylinders are shown.

INTRODUCTION

Ever increasing costs of labor and materials—most especially labor—even before the present emergency, presented a tremendous challenge to the imagination and resourcefulness of architects and structural engineers. And now that we are faced with a "just-short-of-war" economy with its priorities, allocations, controls and shortages, it is even more challenging. If the structural engineer can devise a new type of structural framing requiring less skilled construction labor, or can use a new material requiring smaller quantities of such critical materials as reinforcing steel, then he has made a valuable contribution to the construction industry and also to the national economy.

A stimulation to the structural engineer's imagination is a lesson learned in the aircraft industry early in the development of the all-metal plane. Although high-strength steel alloys are far stronger per inch of thickness than alloys of aluminum, the strength-weight ratio was so much in favor of aluminum alloys their use was quickly found to be more efficient. For example an X-4130 steel has a yield point of 70,000 psi and weighs 490 lb per cu ft. Its strength-weight ratio is then 70,000/490 = 143. 24 ST aluminum has a yield point of 60,000 psi and weighs 173 lb per cu ft. Its strength weight ratio is 350, or an increase over that particular steel of 350/143 = 144 percent.

The same comparison is made for lightweight and hard rock concrete in Table 1.

*Presented at the ACI 47th annual convention, San Francisco, Calif., February 21, 1951. Title No. 48-4 is a part of copyrighted JOURNAL OF THE AMERICAN CONCRETE INSTITUTE, V. 22, No. 1, Sept. 1951, *Proceedings* V. 48. Separate prints are available at 35 cents each. **Discussion** (copies in **triplicate**) should reach the Institute not later than Jan. 1, 1952. Address 18263 W. McNichols Rd., Detroit 19, Mich.

†Member American Concrete Institute, Structural Engineer, George L. Dahl, Architects and Engineers, Dallas, Texas.

TABLE 1—STRENGTH-WEIGHT COMPARISON OF LIGHTWEIGHT AND HARD ROCK CONCRETE

No.	Material	Design strength, psi	Weight, lb per cu ft	Strength-weight ratio	Comparison, percent
1	2500 psi hard rock	1125	150	1125/150 = 7.5	
2	3000 psi hard rock	1350	150	1350/150 = 9	$\frac{(2)}{(1)} = \frac{9}{7.5} = 20$
3	4000 psi hard rock	1800	150	1800/150 = 12	$\frac{(3)}{(1)} = \frac{12}{7.5} = 60$
4	2500 psi lightweight	1125	85	1125/85 = 13.2	$\frac{(4)}{(1)} = \frac{13.2}{7.5} = 76$
5	3000 psi lightweight	1350	90	1350/90 = 15	$\frac{(5)}{(2)} = \frac{15}{9} = 67$
6	4000 psi lightweight	1800	95	1800/95 = 19	$\frac{(6)}{(3)} = \frac{19}{12} = 58$
					$\frac{(6)}{(2)} = \frac{19}{9} = 110$

COMPARATIVE STRENGTH AND COST

In Dallas, Texas, a two-story 192 x 120-ft office building was designed with columns on 24 ft centers each way. The economies of flat-plate design* having been amply demonstrated in a 3-story nurse's home with 17 x 15-ft bays, it was desired to use the same method of framing for this building. Table 2 gives comparative costs for two strengths of hard rock concrete and one lightweight concrete with the calculated dimensions of columns, thickness of slab and amount of steel required in each case to meet design requirements. For the lightweight construction, actual cost is given. Forming cost was computed at $.40 per sq ft, steel at $.10 per lb in place and hard rock concrete at $12.50 per cu yd of 3000-psi concrete in place.

TABLE 2—COMPARATIVE COSTS OF 24 x 24-FT BAY IN DIFFERENT MATERIALS

Item	3000 psi hard rock concrete, 20 x 20-in. columns, 11-in. slab, 4.15 lb steel per sq ft	4000 psi hard rock concrete, 19 x 19-in. columns, 9-in. slab, 5.96 lb steel per sq ft	4000 psi lightweight concrete, 16 x 16-in. columns, 8-in. slab, 3.82 lb steel per sq ft
Steel	2391 × 0.10 = 239.10	2859 × 0.10 = 285.90	2198 × 0.10 = 219.80
Concrete	19.6 × 12.50 = 245.00	16 x 13.10 = 209.00	14.2 × 14.50 = 206.90
Forms	576 × 0.40 = 230.00	576 × 0.35† = 202.00	576 × 0.28† = 161.00
Cost per bay	$714.10	$696.90	$586.80
Cost per sq ft	$1.24	$1.21	$1.02

†Forming cost computed in proportion to decrease in dead load.

In a multistory building reduction of structural dead load from 79,000 to 36,200 or 42,800 lb per bay for slabs (Fig. 1) and 4600 − 1810 or 2760 lb per column would have been significant—no attempt has been made to evaluate them in this case.

Fig. 2 illustrates the cleanliness of the design and the ease of installing air-

**Modern Developments in Reinforced Concrete*, No. 20, Portland Cement Assn., Chicago, Ill.

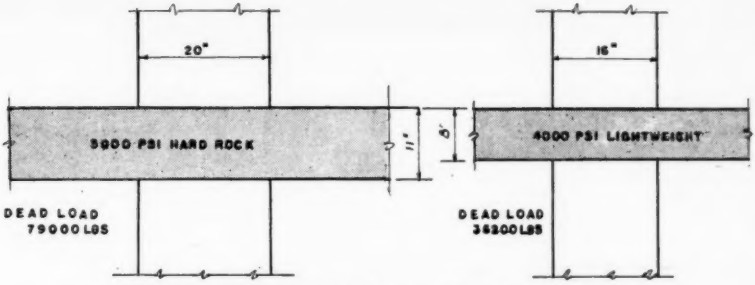

Fig. 1—Reduction of structural load through use of lightweight concrete

conditioning ducts and other mechanical services. Slabs were watched carefully for deflections—some deflection was observed, but most of it was attributable to settlement of forms during pouring. To prove that observation the slabs were load tested. When the 7-in. roof deck was placed, with shoring resting on the second floor slab and with no added support below, careful readings of slab deflections were made. No deflection over $\frac{1}{8}$ in. was observed. From Timoshenko's deflection formula*

$\Delta = \frac{0.063\ W\ d^4}{E\ t^3}$, E was calculated at 3,070,000. This, of course, was not a scientific determination of the elastic modulus. It is at best crude evidence that the slab is safe.

For design purposes it appears reasonable to assume that the elastic modulus will be about $\frac{3}{4}$ that of equivalent strength hard rock concrete. From the *Joint Committee Report*, Sec. 878, n for a 4000 psi hard rock concrete is assumed to be 8.

$$n = 8 - \frac{E_s}{E_c},\ E_c = 30{,}000{,}000/8 = 3{,}750{,}000$$

Hence for lightweight concrete $E_c = 3{,}750{,}000 \times 0.75 = 2{,}800{,}000$

*Timoshenko, S., *Theory of Plates and Shells*, McGraw-Hill Book Co., New York, p. 243.

Fig. 2—Uncluttered design makes installation of utilities easy

and $n = 30/2.8 = 10.7$ from which

$$k = \frac{1}{1 + \frac{f_s}{nf_c}} = \frac{1}{1 + \frac{20000}{10.7 \times 1800}} = \frac{1}{2.04} = 0.490$$

and $$j = 1 - \frac{0.490}{3} = 1 - 0.063 = 0.837$$

and $$A_s = 0.717 \times M/d$$

and $$K = \frac{f_c}{2} k j = 370$$

These then are the design constants for a 4000 psi lightweight concrete. It may well be decided during design to increase the thickness of a lightweight slab or the depth of a beam beyond that determined from the above constants for a balanced design. The additional saving in reinforcing steel usually will pay for the additional concrete. For example, a beam 20 in. wide is required to carry a moment of 900 ft-kips.

From the above, $d = \sqrt{\frac{900 \times 12{,}000}{20 \times 370}} = 1460 = 38$ in.

And $A_s = \frac{900}{38} \times 0.77 = 17$ sq in.

Suppose it is decided to increase the effective beam depth to 46 in.

now $p = \frac{17}{46 \times 20} = 0.0185$

$np = 10.7 \times 0.0185 = 0.198$

$2np = 0.396$

$(np)^2 = 0.039$

Then k = the new position of the neutral axis =

$$\sqrt{2np + (np)^2} - np =$$

$$\sqrt{0.396 + 0.039} - 0.198 = 0.66 - 0.198 = 0.462$$

then $j = 1 - \frac{0.462}{3} = 1 - 0.154 = 0.846$

and $A_s = \frac{M}{d} \times 0.709$

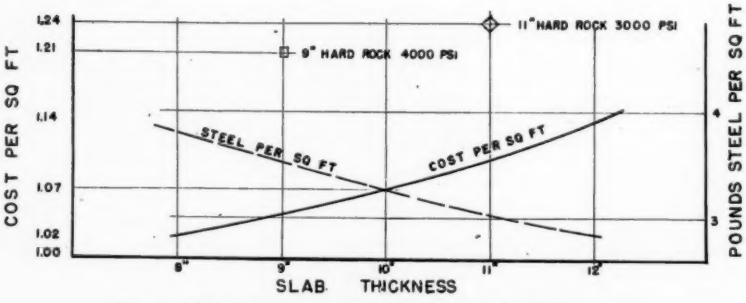

Fig. 3—Variation of cost and steel required with slab thickness

TABLE 3—COMPARISON OF TOTAL COST AND STEEL QUANTITIES REQUIRED FOR DIFFERENT TYPES OF CONSTRUCTION

	Type	Concrete		Total cost, dollars per sq ft	Percent of Item 1	Steel, lb per sq ft	Percent of Item 1
		Type	Strength, psi				
1	8-in. flat plate	Lightweight		1.02		3.81	
2	10-in. flat plate	Lightweight	3000	1.07	105	3.28	86
3	9-in. drop panel, 8 x 8 ft, 6½-in. slab	Hard rock	3000	1.07	105	4.00	105
4	10-in. flat plate	Lightweight	4000	1.08	106	3.28	86
5	12-in. flat plate	Lightweight	3000	1.14	112	2.85	75
6	9-in. flat plate	Hard rock	4000	1.21	118	4.96	130
7	11-in. flat plate	Hard rock	3000	1.24	121	4.15	109
8	72 x 18-in. flat beam with 6-in. one-way slab	Hard rock	3000	1.35	132	4.17	109

$$\text{hence } A_s = \frac{900 \times 0.709}{46} = 13.9 \text{ sq in.}$$

a saving of 3 sq in. of steel, which amounts to $1.08 per linear ft of beam. This procedure is recommended in any long-span structure. This same 24 x24-ft bay size was also calculated increasing lightweight slab thickness from 8 to 12 in. Fig. 3 shows the estimated cost and weight of steel required as the lightweight slab thickness is increased from 8 to 12 in. The designer may well decide to increase slab thickness to decrease the steel even though the total cost increases. Total cost still remains below that for an equivalent hard rock slab shown in the upper part of the figure.

To complete the cost comparison, estimates were made for the same building designed for eight different types of construction (Table 3).

MIXING AND FIELD CONTROL

While Kluge, Sparks and Tuma* suggest use of an air-entraining admixture to prevent bleeding and aid in workability, it has been expedient in this area to use a fine "blow sand." Fig. 4 shows excessive bleeding and resultant honeycombing at the base of a column due to a lack of fines in the mix. Fig. 5 shows the results of adding the proper proportion of fine sand to the mix. The proportion of blow sand, or air-entraining agent—or combination of both — should be determined by laboratory analysis of both the sand and the lightweight aggregate. Sieve analysis of blow sand used is given in Table 4.

TABLE 4—SIEVE ANALYSIS OF BLOW SAND†

Retained on	Percent
No. 4	0
No. 8	1
No. 16	4
No. 30	6
No. 50	50
No. 100	96

†Weight—88.3 lb per cu ft, dry and loose

*Kluge, Ralph W., Sparks, Morris M. and Tuma, Edward C., "Lightweight-Aggregate Concrete," ACI JOURNAL May, 1949, *Proceedings*, V. 45, pp. 625-642.

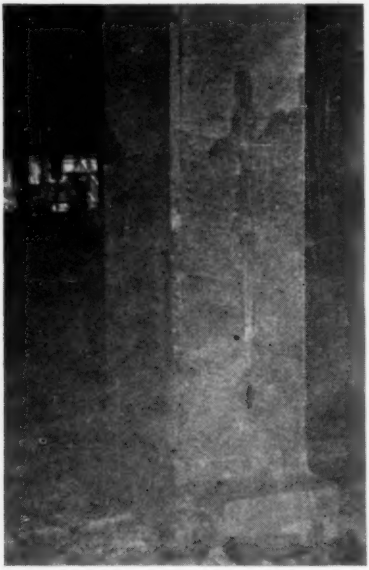

Fig. 4—Bleeding and honey combing due to lack of fines in mix

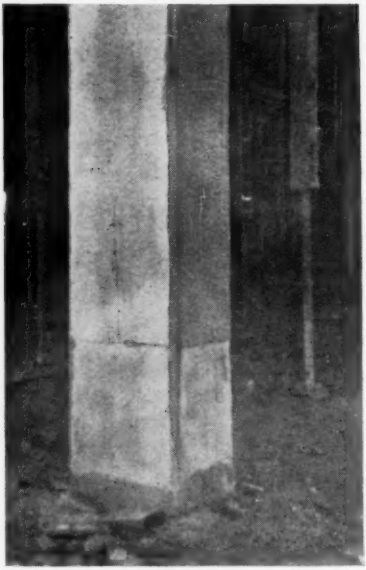

Fig. 5—Corrected condition after addition of blow sand

Generally it will be found necessary to have the lightweight aggregate furnished in two batches, fines to $\frac{3}{16}$-in., and $\frac{3}{16}$ in. to coarse. Most producers provide a maximum size of $\frac{3}{8}$ in. Some as large as $\frac{1}{2}$ in. However, if the producer has adequate screening and sizing equipment, and there is not too much segregation or loss of fines in shipment, the aggregate may be shipped as a "blend," *i.e.*, both fines and coarse in one batch. The specification used was:

> Lightweight aggregate shall be an expanded shale, weighing not more than 1300 lb nor less than 1150 lb, per cu yd on graded dry basis, and shall be so graded from coarse to fine to produce:
>
> | Total passing | Percent by weight |
> |---|---|
> | $\frac{3}{8}$-in. | 95-100 |
> | No. 4 | 85-95 |
> | No. 16 | 35-45 |
> | No. 50 | 15-25 |
> | No. 100 | 10-15 |

TABLE 5—APPROXIMATE MIX DESIGN PROPORTIONS

	Cement		Lightweight aggregate		Blow sand		Water		Total vol., cu ft
	lb	cu ft abs. vol.	lb	cu ft abs. vol.	lb	cu ft abs. vol.	gal.	cu ft abs. vol.	
6-sack	564	2.88	1610	18.10	400	2.48	50	3.47	26.93
7-sack	658	3.35	1550	17.40	420	2.60	53	3.67	27.02

The mix proportions (Table 5) are not accurate because on the job the water added at the mixer was reduced to about 6 gal. per sack total water. The water in the aggregate stock pile varied from 13 to 18 gal. per cu yd so the water added had to be watched carefully.

The slump cone test is a poor indicator of water content or of workability of lightweight concrete; the best guide is to keep the water as low as possible; if the concrete will come out of the mixer it will flow in the forms perfectly. The internal lubrication provided by the blow sand permits the wet concrete to be placed into any form; when the vibrator is applied the mass flows smoothly into place. And a monolithic finished slab is as easily trowelled as hard rock concrete. Shrinkage cracks were almost never seen, whether 1½-in. thick topping or 8 in. slabs. Slabs were cured by keeping them wet for three days.

On-the-site mixing is best accomplished by two ½-yd mixers feeding a 1-yd mixer or paver. Aggregate and sand are placed in the ½-yd mixers and water added and mixed for 2 minutes. The cement is placed in the skip of the large mixer before the wetted aggregate and sand is taken out of the two smaller mixers. In the large mixer the concrete is mixed 2 minutes more. With this set up a capacity of 24 cu yd per hour is feasible.

Fig. 6 shows the laboratory results from test cylinders representing concrete as placed. The two curves extending to 56 days are for the two-story office building—the shorter curve extending to 28 days is for another building still under construction. It illustrates the effect of more careful batching and water control. It is significant that this lightweight concrete seems to continue to pick up strength at a constant rate to at least 56 days, while the curve for hard rock concrete flattens out much earlier. This is explained

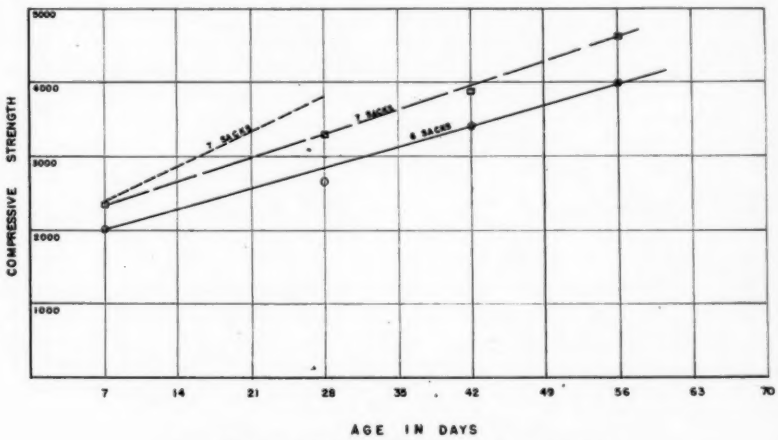

Fig. 6—Strengths of lightweight concrete test cylinders

by the comparatively large amount of water trapped in the pores or capillaries of the crushed lightweight aggregate. This water seems to slow completion of the hydration cycle but does not prevent the concrete from eventually attaining design strength. This may explain why the lightweight concrete had much less shrinkage cracking than an equivalent strength hard rock concrete.

CONCLUSION

Lightweight-aggregate concrete can contribute significantly to structural design, creating design possibilities not hitherto considered economical or practical. In multistory construction the large reduction of dead load will reduce the cost of the structure. If employed in designs where its properties may be used to full advantage, considerable saving in reinforcing steel is possible.

Discussion of a paper by J. A. Murlin:

Lightweight Concrete for Lower Construction Costs*

By JACOB FELD and AUTHOR

By JACOB FELD†

The writer has no argument with the statement that the flat plate form of floor construction is the most economical (except for heavy loads) but does not see where the paper has proved the further economy of lightweight aggregates in the concrete for such use. The economy of flat slab design for multistory residential and office use has been demonstrated by examples in many cities. For instance, two apartment buildings built in 1950-51, in Dallas and Ft. Worth, Texas, of flat plate designs resulted in 10 to 12 percent reduction in the cost of concrete frames as compared with ordinary beam and slab framing for the same architectural plans.

In designs of this type, the writer has found that concrete slab thickness is usually governed by the ACI Building Code's minimum empirical rules; the strength of the concrete mix by the necessary shear strength rather than compressive strength; and the reinforcing required, except over column areas, by the minimum required for shrinkage and temperature. A 1949-50 study of the possible use of lightweight concrete for the roof slabs of several apartment buildings to better control temperature gradients found a lack of reliable data on shear and bond strengths for concrete mixes with the lightweight materials available.

The comments included herewith are based on the experience with flat plate designs and construction of normal concrete mixes and the above mentioned study on lightweight concrete. Reference is made to articles in *Engineering News-Record,* May 4, 1950, pp. 34-35, and Aug. 16, 1951, pp. 35-36. The writer reported results of a full-scale load test on a flat plate floor in Washington, D. C., in *Engineering News-Record,* July 6, 1950, p. 47. A complete summary of design and details issued in various countries, as well as a report on loading and failure tests, appeared in *Annales de l'Institut Technique du Batiment,* Jan. 1951 (in French).

There are a number of questions which should be further investigated before acceptance of the author's cost analysis. Table 1 lists strength-weight ratios on the basis of compressive stress, which is no criterion in flat plate design. What will this table show if the shear strength is used as a basis of

*ACI Journal, Sept. 1951, *Proc.* V. 48, p. 37. Disc. 48-4 is a part of copyrighted Journal of the American Concrete Institute, V. 24, No. 4, Dec. 1952, Part 2, *Proceedings* V. 48.

†Consulting Engineer, New York, N. Y.

comparison? Table 2 evaluates costs of slab construction on the assumptions that all reinforcement (both heavy and lighter bar systems) cost the same per pound and that form cost is directly proportional to the weight of the concrete. Neither of these assumptions agree with the writer's experience.

If the data in Table 3 are accurate, then Fig. 1 shows a comparison of the most economical lightweight concrete design with the most expensive normal concrete design. Assuming that the 4000 psi lightweight concrete can be permitted a unit shear of 108 psi (computed for a total 60 psf superimposed load with 16 x 16-in. columns), the most economical normal concrete design is a 9½-in. slab of 4000 psi with 16 x 16-in. columns or 8½-in. slab with 18 x 18-in. columns. It is true that lightweight concrete requires sufficiently less reinforcing to compensate for the cost difference between normal and lightweight concrete. But more data are needed to prove that the shear strength can be obtained and that the ceiling surface for lightweight concrete is as acceptable as the ordinary concrete. Any special ceiling treatment will upset the entire comparison of cost.

AUTHOR'S CLOSURE

Not to take advantage of the reduction in forming costs for a lightweight flat plate is unfair, for one of the reasons why the flat plate design has proved its economy over beam-and-slab and other types of framing is because its form costs are so low. Obviously then, it will require fewer shores or jacks, less cross bracing, fewer purlins, and less labor to erect a slab form to carry 67 psf than a form to carry 112 psf.

The writer has re-calculated the cost of the following flat plate slabs using the same live load which Dr. Feld used in his calculations. In this tabulation, no form costs are considered except the difference in cost of forming the larger columns in each case. The unit cost for column forms is assumed at 50 cents per contact sq ft.

Flat plate—24 x 24 ft—60 psf live load

Slab	8-in. heavy, 4000 psi	8-in. lightweight, 4000 psi
Column	24 x 24 in.	16 x 16 in.
Column shear	101 psi	101 psi
Steel per bay	2446 lb	1809 lb
Steel per sq ft	4.25 lb	3.12 lb
Concrete cost @ $9.35 per cu yd	$147	@ $12.80 per cu yd $190
Steel cost @ $0.11 per lb	$270	..... $199
Difference in column forms	$13.50	
Cost of materials	$430.50	..... $389
Cost per sq ft	75 cents	..... 67½ cents
Slab	9-in. heavy, 4000 psi	9-in. lightweight, 4000 psi
Column	19 x 19 in.	14 x 14 in.
Column shear	103 psi	94 psi
Steel per bay	2291 lb	1721 lb
Steel per sq ft	3.98 lb	2.98 lb
Concrete cost @ $9.35 per cu yd	$159	@ $12.80 per cu yd $211
Steel cost @ $0.11 per lb	$252	..... $189

Difference in column forms	$8.50	
Cost of materials	$419.50	..... $400
Cost per sq ft	73 cents	..... 69½ cents
Slab	9½-in. heavy, 4000 psi	9½-in. lightweight, 4000 psi
Column	17 x 17 in.	16 x 16 in.
Column shear	104 psi	82 psi
Steel per bay	2272 lb	1637 lb
Steel per sq ft	3.94 lb	2.84 lb
Concrete cost @ $9.35 per cu yd	$165	@ $12.80 per cu yd $222
Steel cost @ $0.11 per lb	$250	..... $180
Difference in column forms	$1.50	
Cost of materials	$416.50	..... $402
Cost per sq ft	72.2 cents	..... 69.7 cents

In this tabulation the size of the columns were selected to keep the unit shear at or near $0.25\,f'_c$ because in each case less than 50 percent of the negative steel passes over the column. Neglecting cost of forms for the slabs, the lowest cost is for the 8-in. lightweight slab; the lowest cost heavy slab is the 9½-in. slab. The weight of the 8-in. lightweight slab is 60 psf, and 119 psf for the 9½-in. sand and gravel concrete slab—practically double the lightweight slab.

Notice also that a price differential of $3.45 per cu yd is used between the 5-sack heavy concrete and the 5-sack lightweight concrete. These are the current ready-mixed concrete prices in Dallas. About two years ago, no ready-mixed concrete plant would quote on lightweight concrete. Since that time every plant in the area has recognized the tremendous demand and will furnish ready-mixed lightweight concrete at or near the above price. However, to penalize lightweight concrete with such a high price differential is a bit rough. Actually those contractors who have had experience in handling, placing, and finishing concrete made with expanded clay and expanded shale aggregate in this area will credit the lightweight material with a saving of 50 cents to $1 per cu yd.

Because the lightweight concrete flat plate does make such a good looking ceiling, it has been used in several store buildings where the live load requirement is 100 psf and with larger column spacing. Accordingly, the following comparisons are made, again with no credit assumed for any saving in forming costs nor any credit for easier handling, placing, or finishing.

Flat plate—26 x 26 ft—100 psf live load

Slab		9½-in. lightweight, 4000 psi
Column size		22 x 22 in.
Column shear		105 psi
Steel per bay		2982 lb
Steel per sq ft		4.42 lb
Concrete cost		@ $12.80 per cu yd $270
Steel cost		@ $0.11 per lb $328
Cost of materials		..... $598
Cost per sq ft		..... 88.5 cents
Slab	10½-in. heavy, 4000 psi	10½-in. lightweight, 4000 psi
Column	26 x 26 in.	18 x 18 in.

Column shear	105 psi	104 psi
Steel per bay	3589 lb	2599 lb
Steel per sq ft	5.3 lb	3.84 lb
Concrete cost @ $9.35 per cu yd	$220	@ $12.80 per cu yd $290
Steel cost @ $0.11 per lb	$397	..... $285
Difference in column forms	$11.50	
Cost of materials	$628.50	..... $575
Cost per sq ft	93 cents	..... 85 cents
Slab	11½-in. heavy, 4000 psi	11½-in. lightweight, 4000 psi
Column	24 x 24 in.	18 x 18 in.
Column shear	101 psi	93 psi
Steel per bay	3356 lb	2597 lb
Steel per sq ft	4.95 lb	3.85 lb
Concrete cost @ $9.35 per cu yd	$237	@ $12.80 per cu yd $317
Steel cost @ $0.11 per lb	$369	..... $285
Difference in column forms	$10	
Cost of materials	$616	..... $602
Cost per sq ft	91.2 cents	..... 89 cents
Slab	12½-in. heavy, 4000 psi	12½-in. lightweight, 4000 psi
Column	20 x 20 in.	18 x 18 in.
Column shear	101 psi	83 psi
Steel per bay	3228 lb	2463 lb
Steel per sq ft	4.78 lb	3.65 lb
Concrete cost @ $9.35 per cu yd	$254	@ $12.80 per cu yd $345
Steel cost @ $0.11 per lb	$356	..... $271
Difference in column forms	$3.30	
Cost of materials	$613.30	..... $616
Cost per sq ft	91 cents	..... 91.2 cents

In making cost estimates of this kind it is obviously wrong to rest one's case upon the cost of one typical panel; only a fragmentary picture is obtained, and often a misleading one. The entire structure must be considered. For example, a two-story store building to be built in Alexandria, La., was designed as a monolithic lightweight expanded clay concrete structure using a flat plate with 100-lb live load with column centers at 25 x 26 ft. The flat ceilings were left exposed, eliminating the usual suspended ceiling, thus story height was reduced. A saving of about 10 cents per sq ft over sand-gravel concrete was demonstrated after absorbing the cost of the lightweight concrete. A lightweight aggregate producing plant is in Alexandria, and the cost differential for ready-mixed concrete is less than $3.00 per cu yd. After subsoil investigation it was found necessary to drive concrete piles to a depth of 65 ft. Had the building been built of heavy concrete this foundation piling would have cost $16,000 additional, or some 30 cents per sq ft. Thus, in this instance, the lightweight structural concrete is credited with a saving of more than 40 cents per sq ft. All cases are not quite so dramatic, but to a lesser degree the same principle does apply.

Nor are the savings to be found only in flat plate designs. This writer has used lightweight concrete in 80-ft rigid frames and almost every conceivable structural framework and in each case has been able to demonstrate substantial economies.

A design guide: method of analysis for continuous prestressed concrete members

Designing for Continuity in Prestressed Concrete Structures*

By ALFRED L. PARME† and GEORGE H. PARIS‡

SYNOPSIS

The design of simply supported prestressed members has been well established but the design of continuous prestressed concrete structures has received little attention because of difficulty in analyzing such members. A method of analysis is developed for continuous prestressed members that reduces the problem to the same simplicity of analysis by moment distribution as for ordinary continuous reinforced concrete members.

The method is relatively simple and does not involve abstract integrations of complicated expressions. The problem of design is simplified to the extent that a physical relationship can be seen between the profile of the curved wires and the forces they exert on the structure. Because the stresses produced by these forces can be readily determined, the method of analysis offers greater flexibility in the design of continuous prestressed structures.

The advantages of continuity in reinforced concrete are common knowledge. Engineers recognized these advantages for many years, but it was not until fast simple methods of analysis were developed that they commenced to take advantage of continuity. Even though the value of continuity is now well established for conventional reinforced concrete, little progress has been made in applying the principles to the design of prestressed concrete structures.

The chief advantage of continuity in reinforced concrete lies in the shallow section that can be used to carry a given load. Thus maximum clearance is provided and the dead load is reduced to a minimum, which is important in long spans. These same advantages should apply to continuous prestressed concrete. Furthermore, the number of end anchorages and prestressing operations required will be fewer than in a structure consisting of several simply supported prestressed concrete spans.

For simply supported prestressed concrete members the most economical design is generally one in which some of the prestressing steel is curved. Economy results from a better distribution of stresses throughout the member. The same principle applies to continuous prestressed concrete members

*Received by the Institute Jan. 29, 1951. Title No. 48-5 is a part of copyrighted JOURNAL OF THE AMERICAN CONCRETE INSTITUTE, V. 23, No. 1, Sept. 1951, *Proceedings* V. 48. Separate prints are available at 50 cents each. **Discussion** (copies in **triplicate**) should reach the Institute not later than Jan. 1, 1952. Address 18263 W. McNichols Rd., Detroit 19, Mich.

†Member American Concrete Institute, Structural and Railways Bureau, Portland Cement Assn., Chicago, Ill.
‡Structural and Railways Bureau, Portland Cement Assn., Chicago, Ill.

but it has been difficult to determine the stresses in the structure, created by the prestress force.

STRESS ANALYSIS

Stresses in a simply supported prestressed member can be analyzed by either of two methods. The first and general method is to consider the member subject to direct load and bending due to the eccentricity of the applied prestress force and to apply the familiar formula $P/A + My/I$ to obtain the stresses in any transverse section. From Fig. 1 we have the expression for stresses induced by the prestress force at any section

$$f_c = \frac{P_1 + P_2}{A} + \frac{(P_1e_1 + P_2e_2)y}{I} \quad \text{(1a)}$$

in which

P_1, P_2 = horizontal components of applied prestress forces
e_1, e_2 = eccentricity or distance from centroid of section to centroid of the respective steel and is considered positive when the moment created by the eccentricity causes compression at the top. Thus e is positive when it is above the centroid of the section
y = distance from centroidal axis to any fiber and is positive when it is measured upward
I = moment of inertia of section
A = area of section

It should be noted in this illustration that e_1 is a constant value while e_2 varies along the member. If the profile of the cable is made a second degree parabola, with the origin at midspan and at e_1, then

$$e_2 = e_1 + c\left(\frac{2x}{l}\right)^2 \quad \text{(1b)}$$

in which c is the maximum ordinate at $x = l/2$. Eq. (1a) then reduces to

$$f_c = \frac{P_1 + P_2}{A} + \frac{\left\{P_1e_1 + P_2\left[e_1 + c\left(\frac{2x}{l}\right)^2\right]\right\} y}{I} \quad \text{(1c)}$$

A second method of analyzing stresses produced by the prestress force is to consider the entire member as a free body and the prestress force as an external load. Thus in Fig. 1 the external loads acting on the member are the horizontal forces P_1 and P_2 and a vertical component equal to $P_2 \times$ tangent ϕ. However, since this vertical force acts at the support it can be neglected. In addition to these loads the curved cable exerts a continuous upward force on the concrete along the entire length of the member.

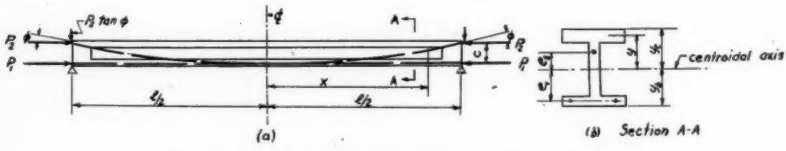

Fig. 1—Prestressed beam with curved and straight cables

Fig. 2—Portion of curved cable in a member

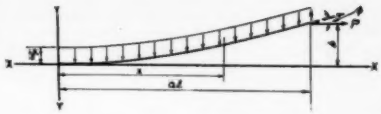

If friction between cable and concrete is neglected, the pressure exerted on the concrete is at all points normal to the plane of contact and tension in the cable is constant. The normal pressure exerted by the cable therefore is equal to the tension in the cable divided by the radius of curvature. This is the actual pressure exerted by the cable.

Most prestressed continuous beams are shallow, with depth to span ratio of about 1/30. Consequently the horizontal component of the tension in the cable is approximately equal to the tension in it. For a second degree parabola, with a ratio of rise to span length of 1/30, the maximum difference of the tension in the cable and its horizontal component is less than 1 percent. Therefore, the horizontal component may be assumed constant and the curved cable held in equilibrium by a uniform vertical load.

If Fig. 2 represents a portion of the curved cable in a member, then the uniform load w_p necessary to maintain equilibrium is

$$w_p\, a\, l = -P \tan \phi \qquad (2a)$$

where w_p is considered positive when it acts downward.

The expression for a second degree parabola is

$$y = b \left(\frac{x}{al}\right)^2 \qquad (2b)$$

Therefore

$$\tan \phi = \frac{dy}{dx} = \frac{2bx}{(al)^2} \qquad (2c)$$

and at $x = a$

$$\tan \phi = \frac{2b}{a\, l} \qquad (2d)$$

Therefore

$$w_p = -\frac{2Pb}{(a\, l)^2} \qquad (2e)$$

when $a = \frac{1}{2}$ and $b = c$, then

$$w_p = -\frac{8Pc}{l^2} \qquad (2f)$$

Since the concrete exerts this force on the cable, the cable exerts an equal but opposite force on the concrete. All of the forces induced by prestressing which act on the member are as shown in Fig. 3. The moment due to these forces about the centroidal axis at a section x distance from midspan is

$$M_p = P_1 e_1 + P_2 (c + e_1) + \frac{w_p\, l^2}{8}\left[1 - \left(\frac{2x}{l}\right)^2\right] \qquad (3a)$$

Substituting in Eq. (3a), the value of w_p as given by expression (2f)

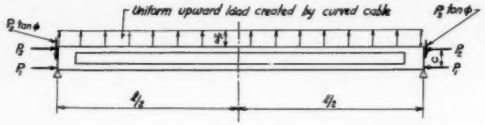

Fig. 3—Forces induced by prestressing

$$M_p = P_1 e_1 + P_2 (c + e_1) - P_2 c \left[1 - \left(\frac{2x}{l} \right)^2 \right] \quad \text{(3b)}$$

or

$$M_p = P_1 e_1 + P_2 \left[e_1 + c \left(\frac{2x}{l} \right)^2 \right] \quad \text{(3c)}$$

The stress at any point will be

$$f_c = \frac{P_1 + P_2}{A} + \frac{\left\{ P_1 e_1 + P_2 \left[e_1 + c \left(\frac{2x}{l} \right)^2 \right] \right\}}{I} y \quad \text{(3d)}$$

which is exactly the same as Eq. (1c). Thus it is proved by identity that the moment produced in a prestressed member by curved cables can be obtained by applying an external force on the member. The same method of analysis can be applied to members in which the profile of the cables is not parabolic. The only difference is that the external forces are no longer uniform, but vary with the profile of the cables. However, slight variations from the parabolic profile, such as a sinusoidal profile, do not affect greatly the magnitude or direction of the vertical forces.

The validity of this method of analysis applies equally well when the profile of the cables consists of two parabolic curves as shown in Fig. 4. This profile can be used in continuous structures and is generally preferable to the use of straight cables employed in members with variable depth. Since the profile shown in Fig. 4 must be a smooth, continuous curve, the tangents of the two parabolas at their common point must be equal; consequently by Eq. (2d)

$$\frac{2c_1}{a_1} = \frac{2c_2}{a_2} \quad \text{(4a)}$$

or

$$\frac{c_1}{c_2} = \frac{a_1}{a_2} \quad \text{(4b)}$$

with $c_1 = c - c_2$ and $a_1 = \frac{1}{2} - a_2$

then

$$c_1 = 2a_1 c \quad \text{(4c)}$$

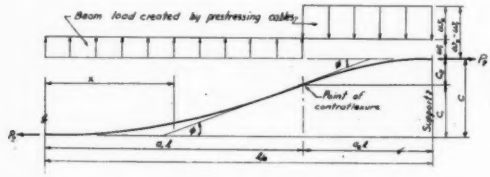

Fig. 4—Profile of cables which can be used in continuous structures

$$c_2 = 2a_2c \quad \text{(4d)}$$

By Eq. (2e), (4c) and (4d) we have

$$w_1 = -\frac{4P_2c}{a_1l^2} \quad \text{(5a)}$$

and

$$w_2 = \frac{4P_2c}{a_2l^2} \quad \text{(5b)}$$

Thus the two uniform loads on the member necessary to maintain the parabolic profile will be of different intensity. Dividing Eq. (5a) by (5b) we have as the ratio of the loads

$$\frac{w_1}{w_2} = -\frac{a_2}{a_1} \quad \text{(5c)}$$

$$w_2 = -\frac{w_1a_1}{a_2} \quad \text{(5d)}$$

Hence

$$w_2 - w_1 = -\frac{w_1}{2a_2} \quad \text{(5e)}$$

Substituting for w_1 its value as expressed in Eq. (5a), then

$$w_2 - w_1 = \frac{2P_2c}{a_1a_2l^2} \quad \text{(5f)}$$

Since the profile in Fig. 4 is composed of two different curves, it is not possible to express the moment produced by w_1 and w_2 as a continuous function of x. However, it will be shown that stresses produced at the center of the span by this procedure are equal to the stresses given by Eq. (1c). The moment at the center produced by the prestressing force is given by

$$M_p = P_1e_1 + P_2(c+e_1) + \frac{w_1l^2}{8} + \frac{(w_2-w_1)\,a_2^2l^2}{2} \quad \text{(6a)}$$

Substituting the values for w_1 and w_2-w_1 given by (5a) and (5f) and collecting common terms

$$M_p = P_1e_1 + P_2\,(c+e_1) - P_2\frac{c}{a_1}\left(\frac{1}{2} - a_2\right) \quad \text{(6b)}$$

$$M_p = P_1e_1 + P_2e_1 \quad \text{(6c)}$$

The stresses at the center will therefore be

$$f_c = \frac{P_1 + P_2}{A} + \frac{(P_2 + P_1)e_1y}{I} \quad \text{(6d)}$$

which is equal to the value given by Eq. (1c) at $x = 0$. The agreement obtained for values at midspan holds equally well at any other section along the member. Thus it is clearly established that the moment produced in a member by prestressing cables which follow a parabolic profile can be determined by means of uniform loads of proper magnitude and distribution. The important corollary follows that elastic behavior of a prestressed member with curved cables can likewise be established on the basis of external equivalent vertical loads.

DESIGN OF PRESTRESSED BEAMS

Two design examples illustrate the simplicity of this method of analysis and the reduction in depth made possible by continuity. One example compares the depth of section required for a fixed end member and a simply supported member. The other example develops a cross section for a continuous highway bridge and shows the shallow depth and small area of reinforcement required for an H20-S16 truck-train load. A method of determining the minimum theoretical depth is presented to compare the depth of a simply supported beam and a fixed end beam. This method is outlined in the example of the simply supported beam although it is not essential to the analysis of continuous structures.

In the first example a highway bridge with a 60-ft span and an over-all width of 28 ft is analyzed. The deck structure consists of a series of prestressed concrete girders with 24-in. flanges, placed side by side as shown in Fig. 5. A 6-in. slab is assumed cast on top of the girders which must be reinforced transversally to distribute wheel loads. This reinforcement can be either conventional reinforcement or prestressed cables. The following specifications are used in the design:

Load: H20-S16-44 American Assn. of State Highway Officials, Standard Specifications for Highway Bridges, 1949

Minimum concrete compressive strength at 28 days is 5000 psi

Maximum allowable concrete stress due to any combination of design loads and prestress is 2000 psi

No tensile concrete stress is allowed for any combination of design loads and prestress

Ultimate tensile strength of steel wire is 225,000 psi

Allowable initial steel stress is 150,000 psi

A reduction of 15 percent in the initial prestress force due to creep of concrete and steel is assumed

The ultimate carrying capacity of the beam is equal to or greater than 1.5 dead load plus 2.5 live load or 1.8 dead load plus 1.8 live load, whichever is more critical

Simple span

The maximum live load moment in one lane for a 60-ft span, given by AASHO Standard Specifications for Highway Bridges, 1949, is 806.5 ft-kips. The computed impact factor is 0.27. Hence, since there are 14 beams for two lanes, the live load moment designated as M_L per beam is

$$M_L = \frac{2 \times 806.5 \times 12{,}000 \times 1.27}{14} = 1{,}760{,}000 \text{ in.-lb}$$

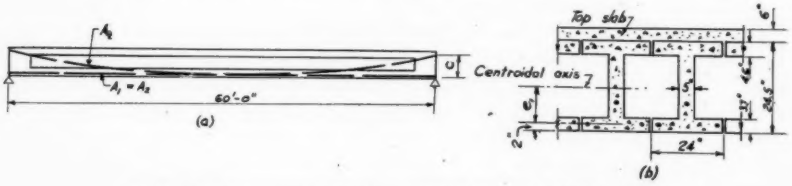

Fig. 5—Design example: simply supported deck of a highway bridge

The dead load moment for a 6-in. slab, per beam designated as M_{Ds} is

$$M_{Ds} = \frac{75 \times 2 \times 60^2 \times 12}{8} = 810{,}000 \text{ in.-lb}$$

The beam dead load will be assumed at 290 lb per ft. Therefore, the moment produced by this load which will be designated as M_{Db} is

$$M_{Db} = \frac{290 \times 60^2 \times 12}{8} = 1{,}570{,}000 \text{ in.-lb}$$

Total design load moment $M_L + M_{Ds} + M_{Db} = 4{,}140{,}000$ in.-lb. Selection of the proper outline of the beam involves the simultaneous satisfaction of a number of requirements. The major conditions which must be satisfied at any section are:

Top fibers

(1) Top fiber stress due to weight of prestressed beam and initial prestress force

$$f_c = \frac{P}{A} + \frac{(M_p + M_{Db})y_t}{I} \geqq 0 \leqq 2000 \text{ psi} \quad \text{(7a)}$$

(2) Top fiber stress due to total design loads and prestress force with the effect of creep included

$$f_c = 0.85\left(\frac{P}{A} + \frac{M_p y_t}{I}\right) + \frac{(M_L + M_{Ds} + M_{Db})y_t}{I} \geqq 0 \leqq 2000 \text{ psi} \quad \text{(7b)}$$

Bottom fibers

(3) Bottom fiber stress due to weight of prestressed beam and initial prestress force

$$f_c = \frac{P}{A} + \frac{(M_p + M_{Db})y_b}{I} \geqq 0 \leqq 2000 \text{ psi} \quad \text{(7c)}$$

(4) Bottom fiber stress due to total design loads and prestress force with the effect of creep included

$$f_c = 0.85\left(\frac{P}{A} + \frac{M_p y_b}{I}\right) + \frac{(M_L + M_{Ds} + M_{Db})y_b}{I} \geqq 0 \leqq 2000 \text{ psi} \quad \text{(7d)}$$

(5) The fifth condition is that the specified minimum concrete and steel strengths shall be equal to or more than the stresses produced by the dead load and live load times the appropriate load factor. This condition controls the minimum depth that can be used.

To determine dimensions of the beam necessary to fulfill all these conditions, it is appropriate to determine first the depth of beam which will satisfy the fifth condition. The ultimate load which can be sustained by a prestressed beam in which wires are bonded and fail by tension can be predicted by the same theory that applies to conventional reinforced concrete beams.*

Determination of ultimate load is based on Vernon P. Jensen's procedure.† For a rectangular section, the percentage of reinforcement, p_o, which gives a balanced design, *i.e.*, one in which failure occurs simultaneously by tension in the steel and compression in the concrete, is

$$p_o = \frac{f_c'}{2f_u} \times \frac{1 + \beta}{1 + \frac{(1 - \beta)f_u}{nf_c'}} \quad \text{(8a)}$$

in which

Design of Prestressed Concrete, Portland Cement Assn.
†*Ultimate Design of Reinforced Concrete*, Portland Cement Assn.

f_c' = cylinder strength of concrete
f_u = ultimate strength of steel
β = plasticity ratio given by

$$\beta = \frac{1}{1 + \left(\frac{f_c'}{4000}\right)^2} \quad \text{(8b)}$$

n = modular ratio given by

$$n = 5 + \frac{10{,}000}{f_c'} \quad \text{(8c)}$$

with $f_c' = 5000$ psi; $f_u = 225{,}000$ psi; $n = 7$ and $\beta = 0.39$ then $p_o = 0.00314$

The distance from the extreme compressive fiber to the neutral axis, $k_o d$, is obtained from the relationship that for balanced design

$$k_o = \frac{1}{1 + \frac{(1 - \beta) f_u}{n f_c'}} = 0.203 \quad \text{(8d)}$$

and since

$$j = 1 - \frac{1}{3}\left(1 + \frac{\beta^2}{1 + \beta}\right)k_o \quad \text{(8e)}$$

then substituting numerical values, we have $j = 0.926$.

The ultimate resisting moment is given by

$$bd^2 p_o j f_u = M \quad \text{(8)}$$

in which

b = width of beam
d = depth from compressive face of beam to centroid of steel

Equating ultimate resisting moment to ultimate load moment we have

$$bd^2 p_o j f_u = 1.5(810{,}000 + 1{,}570{,}000) + 2.5(1{,}760{,}000)$$

from which, with $b = 24$ in., $j = 0.926$, $f_u = 225{,}000$ psi, and $p_o = 0.00314$.

$$d = \sqrt{\frac{7{,}970{,}000}{0.926 \times 225{,}000 \times 24 \times 0.00314}} = 22.53 \text{ in.}$$

This is the minimum d that will satisfy the loading conditions. The distance from centroid of steel to extreme fiber depends upon code requirements for protection of reinforcement. A theoretical value of 2 in. is assumed. Therefore, the depth of beam is 24.53 in., say 24.50 in. The distance to the neutral axis is

$$22.53 \times k_o = 22.53 \times 0.203 = 4.59 \text{ in., say } 4.60 \text{ in.}$$

and the area of wire needed is

$$A_s = 22.53 \times 24 \times 0.00314 = 1.70 \text{ sq in.}$$

Although the preceding computations are based on a rectangular section, the values of d and A_s are applicable to any cross section as long as the top flange is 4.6 in. thick. In this example an I-beam is used. If the thickness of the web is now assumed at 5 in., the only unknown quantities to be determined are thickness of bottom flange and area of bottom steel which must exceed 1.70 sq in. It has been found that a variation in area of the bottom flange within a moderate range does not affect greatly the stresses produced by total design load and prestressing force. Hence, the final area of the bottom flange can be determined quickly by trial and error. A theoretical

thickness of bottom flange of 3.7 in. is assumed. With these dimensions: $A = 280$ sq in.; $I = 22{,}550$ in.^{4}; $y_t = +11.76$ in.; and $y_b = -12.74$ in.

To keep the lower fiber stress above zero, the area of steel is increased to 1.9 sq in. with $A_1 = 0.95$ sq in. and $A_2 = 0.95$ sq in. In actual practice, to conform to the allowable initial stress in the steel, the area of A_2 should be increased theoretically by 0.65 percent since the applied force is slightly greater than horizontal component P_2. The difference between applied force and its horizontal component is so small that this correction to the area will be neglected. Consequently, the horizontal component of the applied prestressing force is $1.9 \times 150{,}000 = 285{,}000$ lb. At the center of span the eccentricity is equal to -10.74 in. With these quantities the following values result:

$$\frac{P_1 + P_2}{A} = \frac{285{,}000}{280} = +1020 \text{ psi}$$

$$\frac{M_p y_t}{I} = \frac{285{,}000 \times (-)\,10.74 \times 11.76}{22{,}550} = -1600 \text{ psi}$$

$$\frac{M_p y_b}{I} = \frac{285{,}000 \times (-)\,10.74 \times (-)\,12.74}{22{,}550} = +1730 \text{ psi}$$

$$\frac{M_{Db} y_t}{I} = \frac{1{,}570{,}000 \times 11.76}{22{,}550} = +820 \text{ psi}$$

$$\frac{M_{Db} y_b}{I} = \frac{1{,}570{,}000 \times (-)\,12.74}{22{,}550} = -890 \text{ psi}$$

$$(M_L + M_{Db} + M_{Ds})\frac{y_t}{I} = \frac{4{,}140{,}000 \times 11.76}{22{,}550} = +2160 \text{ psi}$$

$$(M_L + M_{Db} + M_{Ds})\frac{y_b}{I} = \frac{4{,}140{,}000 \times (-)\,12.74}{22{,}550} = -2340 \text{ psi}$$

The stresses for the four conditions given by Eq. (7a-7d) are:

(1) $f_c = 1020 - 1600 + 820 = +240$ psi
(2) $f_c = 0.85\,(1020 - 1600) + 2160 = +1670$ psi
(3) $f_c = 1020 + 1730 - 890 = +1860$ psi
(4) $f_c = 0.85\,(1020 + 1730) - 2340 = 0$

The four design conditions at the center of the span are thus satisfied. With half the wires curved upward, and terminated the same distance above the centroidal axis as the straight wires terminate below it, the prestressing moment at the support is zero. Consequently the critical section occurs at midspan and the stresses at any other point are less critical.

Fixed end beam

To determine the theoretical reduction in depth obtained by fixity of ends, a fixed end beam subject to the same design conditions and loads will be analyzed. For a 60-ft span, the maximum negative moment produced by H20-S16-44 truck-train loading occurs when the heaviest axle load is placed 16.9 ft from the support. The maximum negative moment is $-915{,}000$ in.-lb. The maximum moment at midspan with the heaviest axle load placed at this point is 556,000 in.-lb. The maximum positive moment in the beam occurs a short distance from midspan, but for design purpose, the maximum

AMERICAN CONCRETE INSTITUTE LIBRARY

moment at midspan being almost equal to the maximum positive moment, the value at midspan will be used. If we assume that the prestressed girder weighs 221 lb per ft, the negative moments at the support due to the various loads are:

$$M_L = -915{,}000 \text{ in.-lb}$$
$$M_{Ds} = -540{,}000 \text{ in.-lb}$$
$$M_{Db} = -792{,}000 \text{ in.-lb}$$
$$M_L + M_{Ds} + M_{Db} = -2{,}250{,}000 \text{ in.-lb}$$

The positive moments at midspan are:

$$M_L = 556{,}000 \text{ in.-lb}$$
$$M_{Ds} = 270{,}000 \text{ in.-lb}$$
$$M_{Db} = 396{,}000 \text{ in.-lb}$$
$$M_L + M_{Ds} + M_{Db} = 1{,}223{,}000 \text{ in.-lb}$$

The ultimate moment at the support is

$$M = -1.5\,(543{,}000 + 792{,}000) - 2.5 \times 915{,}000 = -4{,}290{,}000 \text{ in.-lb}$$

The ultimate positive moment at midspan is

$$M = 1.5\,(270{,}000 + 396{,}000) + 2.5 \times 556{,}000 = 2{,}390{,}000 \text{ in.-lb}$$

Since the maximum moment occurs at the support, the minimum depth that can be used is determined by the ultimate resistance required at the support. Applying the same procedure used for the simple span example, we find

$$d = \sqrt{\frac{4{,}290{,}000}{0.926 \times 225{,}000 \times 24 \times 0.00314}} = 16.53 \text{ in.}$$

The area of steel required for this depth is

$$A_s = 0.00314 \times 24 \times 16.53 = 1.25 \text{ sq in.}$$

The thickness of the bottom flange is $16.53 \times 0.203 = 3.35$ in. The thickness of the top flange is chosen arbitrarily at 2.75 in., which is more than that required to satisfy the ultimate positive moment requirements. This assumes that prestressed wires will be placed in the web with a minimum protective coverage for the reinforcement of 2 in. With the web thickness again taken at 5 in., the properties of the section are: $A = 208$ sq in.; $I = 9606$ in.^{4}; $y_t = 9.58$ in.; and $y_b = -8.92$ in.

The fixed end moment due to the prestress force is determined by considering the external prestress force acting on the beam as shown in Fig. 6c. The uniform load w_p created by the curved cable is by Eq. (2f)

$$w_p = \frac{8P_2c}{l^2} \qquad (2f)$$

Hence the moment at support is

$$M^F = \frac{8P_2c}{12} \qquad (9a)$$

and the moment at midspan

$$M = \frac{8P_2c}{24} \qquad (9b)$$

It will be recognized immediately that the end moment of $\frac{8P_2c}{12}$ is just sufficient to resist the rotation of the beam at the support due to the load w_p. In

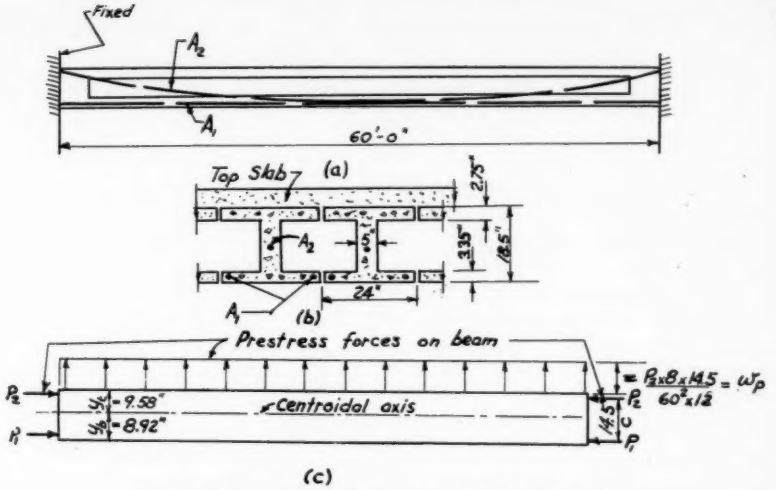

Fig. 6-—Design example: fixed-end deck of a highway bridge

other words, this moment is due to the curvature of the cable. In addition to this moment, end moments must be applied to resist the rotation due to eccentricity at the supports of the external forces P_1 and P_2, that is by the moment $(P_1e_2 + P_2e_2)$. In this case, since the moments at the two ends of the beam are the same, the restraining moment necessary to prevent rotation must be equal and opposite to $(P_1e_2 + P_2e_2)$. Hence, in the beam the restraining moment exerted by the support and the moment of the prestressed forces nullify each other and have no effect on the stresses.

If now we assume $A_2 = 1.25$ sq in. and $A_1 = 0.083$ sq in., then

$$P_2 = 1.25 \times 150{,}000 = 188{,}000 \text{ lb}$$
$$P_1 = 0.083 \times 150{,}000 = 12{,}500 \text{ lb}$$

Therefore, at the support by Eq. (9a), with $c = 14.5$ in., the prestressing moment is:

$$M_p^F = 188{,}000 \times 14.5 \times \frac{8}{12} = 1{,}820{,}000 \text{ in.-lb}$$

and at midspan by Eq. (9b)

$$M_p = \frac{-188{,}000 \times 14.5}{3} = -910{,}000 \text{ in.-lb}$$

The stresses produced at the support are:

$$\frac{P_1 + P_2}{A} = \frac{200{,}500}{208} = +960 \text{ psi}$$

$$\frac{M_{pyt}^F}{I} = \frac{1{,}820{,}000 \times 9.58}{9606} = +1810 \text{ psi}$$

$$\frac{M_{pyb}^F}{I} = \frac{1{,}820{,}000 \times (-)8.92}{9606} = -1690 \text{ psi}$$

$$\frac{M_{Db}y_t}{I} = \frac{-792{,}000 \times 9.58}{9606} = -790\text{psi}$$

$$\frac{M_{Db}y_b}{I} = \frac{-792{,}000 \times (-)8.92}{9606} = +730\text{ psi}$$

$$(M_L + M_{Ds} + M_{Db})\frac{y_t}{I} = \frac{-2{,}250{,}000 \times 9.58}{9660} = -2240\text{ psi}$$

$$(M_L + M_{Ds} + M_{Db})\frac{y_b}{I} = \frac{-2{,}250{,}000 \times (-)8.92}{9606} = +2090\text{ psi}$$

Consequently, the stresses for the four conditions at the support given by Eq. (7a-7d) are:

(1) $f_c = 960 + 1810 - 790 = +1980$ psi
(2) $f_c = 0.85\ (960 + 1810) - 2240 = +110$ psi
(3) $f_c = 960 - 1690 + 730 = 0$
(4) $f_c = 0.85\ (960 - 1690) + 2090 = +1470$ psi

At midspan

$$\frac{M_pY_t}{I} = \frac{-910{,}000 \times 9.58}{9606} = -905\text{ psi}$$

$$\frac{M_pY_b}{I} = \frac{-910{,}000 \times (-)\,8.92}{9606} = +840\text{ psi}$$

$$\frac{M_{Db}Y_t}{I} = \frac{396{,}000 \times 9.58}{9606} = +395\text{ psi}$$

$$\frac{M_{Db}Y_b}{I} = \frac{396{,}000 \times (-)8.92}{9606} = -370\text{ psi}$$

$$(M_L + M_{Db} + M_{Ds})\frac{Y_t}{I} = \frac{1{,}223{,}000 \times 9.58}{9606} = +1220\text{ psi}$$

$$(M_L + M_{Db} + M_{Ds})\frac{y_b}{I} = \frac{1{,}223{,}000 \times (-)\,8.92}{9606} = -1140\text{ psi}$$

Hence the stresses for the four conditions at midspan are:

(1) $f_c = 960 - 905 + 395 = 450$ psi
(2) $f_c = 0.85\ (960 - 905) + 1220 = 1270$ psi
(3) $f_c = 960 + 840 - 370 = 1430$ psi
(4) $f_c = 0.85\ (960 + 840) - 1140 = 390$ psi

It is evident from the above example that it is possible to satisfy design requirements at points of critical stresses in a fixed end prestressed member by curving the wires. Moreover, this can be achieved with a theoretical greater economy in materials than is possible in a simply supported beam. The savings in material are:

$$\text{Area of concrete} = \frac{280 - 208}{280} = 25\text{ percent}$$

$$\text{Depth of section} = \frac{24.5 - 18.5}{24.5} = 25\text{ percent}$$

$$\text{Area of steel} = \frac{1.90 - 1.33}{1.90} = 30\text{ percent}$$

The computed reduction in materials is based solely on theoretical stress requirements. It is quite possible that factors such as code requirements

regarding minimum coverage of reinforcement, maximum permissible deflection and construction requirements will minimize the savings.

Continuous beam

To demonstrate the facility of analyzing a continuous prestressed concrete structure by the procedure developed, and likewise to show possible economy, an analysis of one girder of a continuous three-span concrete bridge will be illustrated. Only essential details pertinent to the application of prestressing forces will be discussed. For other details, such as determination of influence lines and maximum moments, the methods employed are essentially those shown in *Continuous Concrete Bridges* and *Influence Lines Drawn as Deflection Curves* published by the Portland Cement Assn.

It is assumed that girders of constant cross section are spaced 7 ft on centers, and a 6-in. deck slab is cast on the girders after they are prestressed. In determining stresses in the girder, it has been assumed for simplicity that the 6-in. slab does not contribute to the strength of the girder. In reality the slab will act in unison with the girder. Consequently, stresses produced in the girder by truck-train loads will actually be smaller than those evaluated because of the larger effective moment of inertia.

In this example, 90-ft end spans with a 120-ft middle span have been assumed as shown in Fig. 7a. A truck-train loading plus impact based on the number of spans loaded as shown in Fig. 7a with the loads placed at critical points to produce the maximum moment is used. Since the girders are placed 7 ft on centers, seven-tenths of the truck loads shown in Fig. 7a, which are for a 10-ft lane, are used. The maximum positive and negative live load moments in ft-kips are recorded in Table 1. Rows 1 and 2 give the moments produced by the weight of girder assumed at 1 kip per ft and by the weight of slab taken at 0.525 kip per ft, respectively. Rows 5 and 6 represent summation of design load moments for maximum positive and maximum negative live load moments respectively.

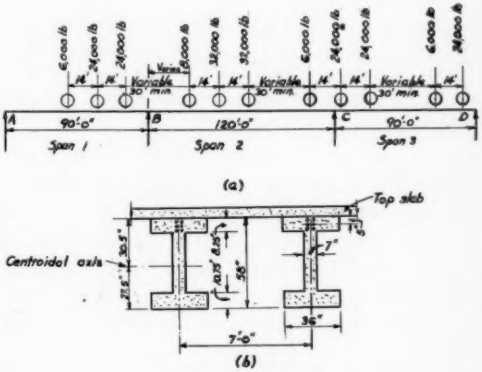

Fig. 7—Design example: continuous prestressed concrete bridge

TABLE 1—MOMENT IN FT-KIPS DUE TO VARIOUS LOADS AT TENTH POINTS

		1.0	1.1	.1.2	1.3	1.4	1.5	1.6	1.7	1.8	1.9	2.0	2.1	2.2	2.3	2.4	2.5
1	Girder	0	+ 250	+ 420	+ 510	+ 520	+ 440	+ 290	+ 60	− 260	− 660	−1140	− 490	+ 20	+ 380	+ 590	+ 660
2	Slab	0	+ 130	+ 220	+ 270	+ 270	+ 230	+ 150	+ 30	− 140	− 350	− 600	− 260	+ 10	+ 200	+ 310	+ 350
3	Maximum positive live load moment	0	+ 470	+ 760	+ 900	+ 940	+ 950	+ 860	+ 730	+ 510	+ 220	+ 130	+ 200	+ 540	+ 850	+1030	+1060
4	Maximum negative live load moment	0	− 80	− 150	− 230	− 300	− 380	− 460	− 530	− 600	− 790	−1150	− 550	− 360	− 290	− 270	− 270
5	Σ 1 + 2 + 3	0	+ 850	+1400	+1680	+1730	+1620	+1300	+ 820	+ 110	− 790	−1630	− 550	+ 570	+1430	+1930	+2070
6	Σ 1 + 2 + 4	0	+ 400	+ 490	+ 550	+ 490	+ 290	− 20	− 420	−1000	−1800	−2890	−1300	− 330	+ 290	+ 630	+ 710
7	Prestressing	0	− 610	−1080	−1410	−1600	−1650	−1410	− 740	+ 350	+1690	+2220	+1720	+ 400	− 670	−1340	−1530

As in the previous example, the minimum required depth of girder that will satisfy the ultimate stresses will be determined. The maximum moment occurs at the interior support. Hence, using values from Table 1 for the ultimate moment, we have

$$M = 1.5\ (-\ 600\ -\ 1140) + 2.5\ (-1150) = -\ 5490 \text{ ft-kips}$$

or

$$M = 1.8\ (-\ 600\ -\ 1140\ -\ 1150) = -\ 5200 \text{ ft-kips}$$

Now as previously indicated

$$p_o j f_u b d^2 = M$$

with

$$p_o = 0.00314$$
$$j = 0.926$$
$$f_u = 225{,}000 \text{ psi}$$
$$b = 36 \text{ in. (See Fig. 7b)}$$

therefore

$$d = \sqrt{\frac{5490 \times 12{,}000}{0.00314 \times 0.926 \times 225{,}000 \times 36}} = 52.9 \text{ in., say } 53 \text{ in.}$$

With 5 in. assumed as the distance from centroid of steel to concrete surface, the over-all depth, h, is 58 in. As before with $k_o = 0.203$, the thickness of the bottom flange is $0.203 \times 52.9 = 10.75$ in. The required area of steel is

$$A_s = 52.9 \times 36 \times 0.00314 = 5.98 \text{ sq in., say 6 sq in.}$$

The maximum positive moment which occurs at the center of the middle span is

$$M = 1.5\ (350 + 660) + 2.5\ (1060) = 4170 \text{ ft-kips}$$

Because this moment is smaller than the negative moment at the support, the top flange can be made shallower than the bottom flange. Taking moments at midspan about the steel, which is assumed 5 in. above the bottom fiber, by the theory of ultimate load design

$$36 f_c' \frac{(1+\beta)t}{2}\left[53 - \left(0.333 + \frac{\beta^2}{3\ (1+\beta)}\right)t\right] = 4170 \times 12{,}000$$

in which t is the thickness of top flange, with $\beta = 0.390$ and $f_c = 5000$ psi; then

$$36 \times 5000 \times 0.695t\ (53 - 0.369t) = 4170 \times 12{,}000$$

Solving the above equation, we have $t = 8.00$ in. The dimensions of the girder and the area of steel that satisfy ultimate load requirements have now been found. The profile of the wires is considered continuous and formed to parabolic curves with points of contraflexure at $0.15l$ from interior supports. The ends of the wires terminate at the centroid of the end section. It should be pointed out that although the cables are shown terminating at the centroid of the end section they can be spread out at this section. That is, some of the cables can terminate above and others below the centroid of the section. To satisfy requirements at points of maximum stress under design loads, the top flange was increased to 8.25 in. while the area of steel was increased to 6.25 sq in. The area, weight, distance from centroidal axis to extreme fibers, and moment of inertia of the section shown in Fig. 7b are, respectively: $A = 957$ sq in.; $I = 438{,}300$ in.^{4}; $w = 1$ kip per ft; $y_t = 30.48$ in.; and $y_b = 27.52$ in.

The moment induced by the prestress force will be solved by first deter-

mining the end moments created when the ends of each span are considered fixed. For span 1, the loading created by prestressing is indicated in Fig. 8a.

The fixed end moment coefficients for the various loads are taken from *Continuity in Concrete Building Frames*, Table 1, p. 10, published by the Portland Cement Assn.

$$M^F_{AB} = -\frac{11}{192}\,w_p l^2 - \frac{5}{192}\,w_1 l^2 - \frac{0.15^2\,(4 - 3 \times 0.15)}{12}\,(w_2 - w_1) l^2$$

$$M^F_{BA} = -\frac{5}{192}\,w_p l^2 - \frac{11}{192}\,w_1 l^2 - \frac{0.15^2\,(6 - 8 \times 0.15 + 3 \times 0.15^2)}{12}\,(w_2 - w_1) l^2$$

but it has been shown by Eq. (2f), (5a) and (5f) that

$$w_p = -8\frac{Pc'}{l^2}$$

$$w_1 = -\frac{4}{0.35}\,\frac{Pc}{l^2}$$

$$(w_2 - w_1) = \frac{2}{0.35 \times 0.015}\,\frac{Pc}{l^2}$$

Hence, with $c' = 1.88$ ft and $c = 4$ ft

$$M^F_{AB} = P\left[\frac{8 \times 1.88 \times 11}{192} + \frac{4 \times 4 \times 5}{0.35 \times 192} - \frac{2 \times 4 \times 0.15^2\,(4 - 3 \times 0.15)}{0.35 \times 12}\right]$$

$$M^F_{BA} = P\left[\frac{8 \times 1.88 \times 5}{192} + \frac{4 \times 4 \times 11}{0.35 \times 192} - \frac{2 \times 4 \times 0.15\,(6 - 8 \times 0.15 + 3 \times 0.15^2)}{0.35 \times 12}\right]$$

With $P = 6.25$ x $150 = 937.5$ kips, then $M^F_{AB} = 1778$ ft-kips and $M^F_{BA} = 1518$ ft-kips.

The joint at A is free to rotate. Consequently, if this joint is allowed to rotate, the moment produced at B by the vertical loads induced by prestressing is

$$M^F_{BA} = 1518 + 0.5 \times 1778 = 2407.0 \text{ ft-kips}$$

The prestressing thrust at B can be converted, as shown by the dash lines in Fig. 8a, into a moment and a thrust applied at the centroidal axis. Since joint A is free to rotate, it is apparent that to prevent rotation at B of beam AB by this prestressing moment, an equal though opposite moment must be exerted. These end moments can be neglected since they nullify each other.

For span BC, the loads produced by the curvature of cables are shown in Fig. 8b. The fixed end moments due to these loads are

$$M^F_{BC} = M^F_{CB} = -\frac{w_1 l^2}{12} - \frac{2(w_2 - w_1)\,a_2\,(3a_2 - 2a_2^2)l^2}{12} \qquad \text{(10a)}$$

but

$$w_1 = -\frac{4Pc}{a_1 l^2}$$

$$w_2 - w_1 = \frac{2Pc}{a_1 a_2 l^2}$$

Hence

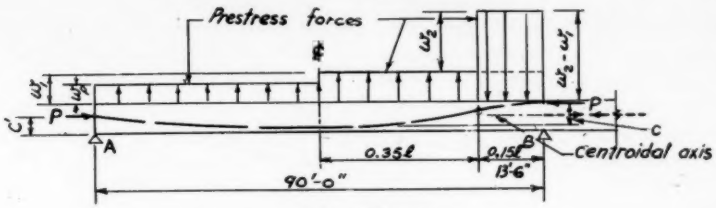

(a) end span

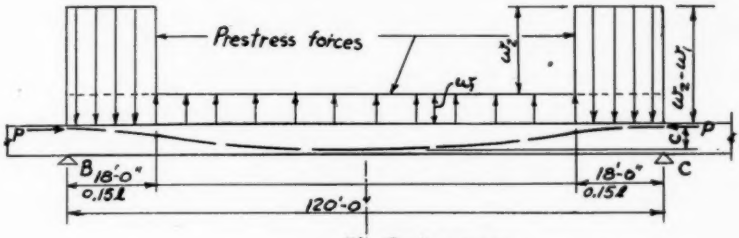

(b) Center span

Fig. 8—Loading for end span and center span of continuous prestressed bridge

$$M^F_{BC} = M^F_{CB} = \frac{4Pc}{12}\left(\frac{1}{a_1} + \frac{3a_2 - 2a_2^2}{a_1}\right) \quad \text{(10b)}$$

which can be reduced to

$$M^F_{BC} = M^F_{CB} = \frac{Pc\,(1 - a_2)}{1.5} \quad \text{(10c)}$$

Substituting numerical values, we have

$$M^F_{BC} = M^F_{CB} = \frac{937.5 \times 4 \times 0.85}{1.5} = 2125 \text{ ft-kips}$$

The fixed end moments due to the end thrust can be neglected since they are resisted by equal and opposite moments from the adjacent span. The unbalanced moment at B and C due to prestressing is 2407 − 2125 = 282

TABLE 2—DETERMINATION OF MOMENTS AT SUPPORTS DUE TO PRESTRESSING FORCE BY ONE CYCLE DISTRIBUTION METHOD

	A		B		C		D
Modified stiffness factor	3.40		3.00	2.63	2.63	3.00	3.40
Modified distribution factor	1.0		0.533	0.467	0.467	0.533	1.0
Modified carry-over factor	−0.233 →		← 0	−0.286 →	← −0.286	0 →	← −0.233
M^F for prestressing	0		+2407	+2125	+2125	+2407	0
Distributed moment	0		−150	+132	+132	−150	0
Carried over moment	0		−38	−38	−38	−38	0
Final moment	0		+2220	+2220	+2220	+2220	0

ft-kips as shown in Table 2. The procedure employed to obtain the final moment at B is based on one cycle of moment distribution, systemized in *Influence Lines Drawn as Deflection Curves.** The final moment after distribution at B and C is 2220 ft-kips as computed in Table 2. The moment produced by the prestress force at any other point can be obtained readily by subtracting the simple beam bending moments produced by loads w_1 and w_2 of the middle span, and loads w_p, w_1 and w_2 of the end spans from the ordinate of the negative moment diagram. A simpler method is to obtain the moment from the cable profile. The bending moment at any section can be shown equal to the algebraic sum of P times its eccentricity at the section plus the ordinate to the computed end moment curve minus the ordinate to the line connecting the moments of P times its end eccentricities. Thus in Fig. 7, the moment at any point in the end span is

$$M = Pe + M_{AB} + (M_{BA} - M_{AB})\frac{x'}{l} - P\left[e_A + (e_B - e_A)\frac{x'}{l}\right]$$

in which e_A and e_B are the eccentricities at A and B respectively and x' is measured from A. With $e_A = 0$; $e_B = 2.12$ ft; $P = 937.5$ kips; $M_{AB} = 0$; and $M_{BA} = 2220$ ft-kips, the moment at the third point with the eccentricty (e) at that section equal to -1.58 ft

$$M = -937.5 \times 1.58 + 2220 \times 0.3 - 937.5 \times 2.12 \times 0.3 = -1410 \text{ ft-kips}$$

The moment produced at tenth points by the prestress force is shown in row 7 of Table 1.

With moments produced by the prestress force and design loads determined, the final stresses are obtained by substituting numerical values in the expression $f_c = P/A + (My)/I$ as calculated in the first example. The stresses produced in the top fibers for conditions 1 and 2, page 51, are shown in Fig. 9 and in the bottom fibers for conditions 3 and 4 are shown in Fig. 10.

*Portland Cement Assn. publication.

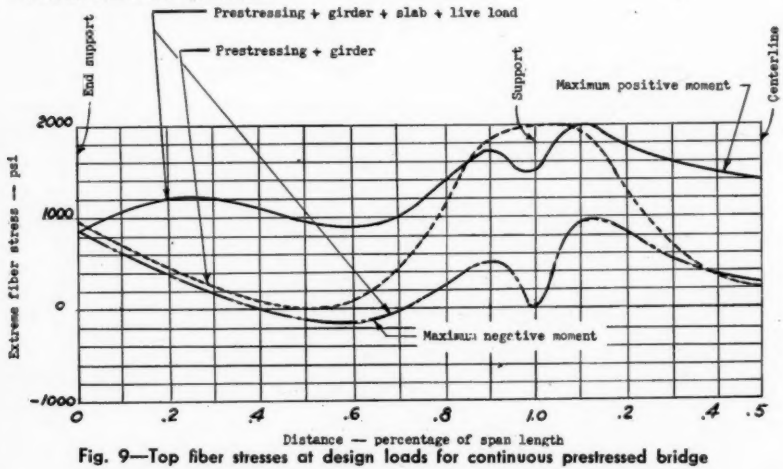

Fig. 9—Top fiber stresses at design loads for continuous prestressed bridge

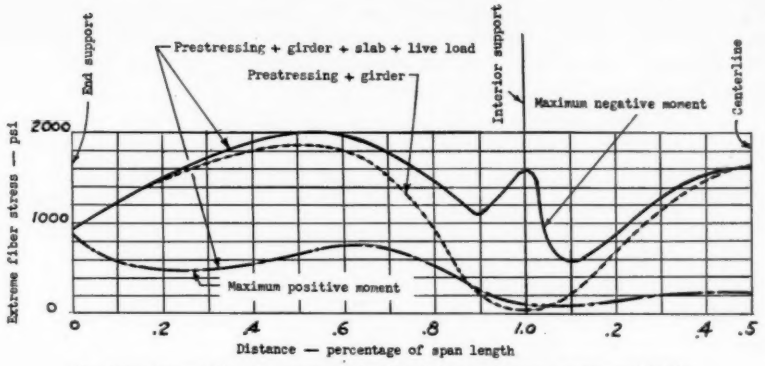

Fig. 10—Bottom fiber stresses at design loads for continuous prestressed bridge

Fig. 9 shows that small tensile stresses occur in the upper fibers. These stresses are negligible, and often are permitted in prestressed structures built abroad. However, this condition can be remedied by deepening the section and by applying greater prestress force. By these means the axial thrust and moment due to the prestress force is increased, while the flexural stresses produced by dead and live loads are reduced.

The reaction at B produced by the weight of girder and the prestress force will in all cases be upward. Consequently, there will be no tendency for the girder to lift off the pier during the prestressing operation.

CONCLUSION

In making the analysis, the effect of axial deformation has been neglected. This can be included as well as shrinkage and expansion. Since the investigation of these factors follows routine procedure of indeterminate analysis they are not included.

In tensioning curved cables, resistance is developed by friction between cables and concrete. Therefore, there is some loss in tension in the cables. Gustave Magnel, who has made tests on this question, states in the second edition of his book *Prestressed Concrete*, p. 80: "The writer has made some experiments on this (loss of tension due to friction) and finds that, with the type of cables used in Belgium, the loss due to friction does not exceed 5 percent, if there are not more than three spans and the stretching is applied simultaneously at both ends of the cable. For this reason it is recommended that there should not be more than three continuous spans." Moreover, this frictional loss can be minimized by applying an initial prestress force greater than that required and then reducing the force to the required tension before anchoring the wires.

Discussion has been limited to members with constant cross section; the design procedure can be applied to members of variable moment of inertia.

The coefficients for the fixed end moments, stiffness factors and carry-over factors can be obtained from tables for beams with variable moment of inertia. The moment created by the change in elevation of the centroidal axis can also be determined by an equivalent vertical loading.

The method of analysis developed is relatively simple and does not involve abstract integrations of complicated expressions. The problem of designing continuous prestressed structures is simplified to the extent that a physical relationship can be seen between the profile of the curved wires and the forces they exert on the structure. Because stresses produced by these forces can be readily determined, the method of analysis offers greater flexibility in the design of continuous prestressed structures.

Discussion of a paper by Alfred L. Parme and George H. Paris:

Designing for Continuity in Prestressed Concrete Structures*

By JUHAN RAUD and AUTHORS

By JUHAN RAUD†

The procedure used in this paper for calculating the effect of continuity in prestressed concrete structures is limited to a few problems, such as demonstrated in Fig. 6, 7, and 8, which were selected to show the usefulness of this method. The authors' assumption that curved cables exert a continuous upward force on the concrete along the entire length of the member is not quite correct. It can be readily demonstrated by simple means that it is not the normal pressure created by the cables, but the eccentricity of the cables that affects bending moments in continuous structures. To illustrate the point a few problems will be examined in light of a more general method.

USE OF ROTATION ANGLES

Problem 1

In any simply supported beam subjected to an eccentric prestress load, bending moments are produced from which deformation of the beam can be computed. In this connection we are mainly concerned about the angular rotation of the end tangents. Consider beam A-B prestressed as shown in Fig. A. The beam is subjected to a constant bending moment Pe that will deflect the beam upward. By using a simple and popular method such as conjugate beam, end rotation equals shear in the conjugate beam. Therefore, $\alpha_{AB} = PeL/2EI$; values E and I can be omitted. The fact that fixed-end mo-

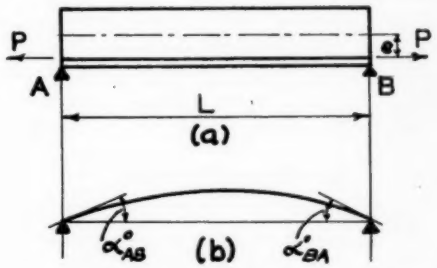

Fig. A—Problem 1. Simply supported beam

*ACI Journal, Sept. 1951, *Proc.* V. 48, p. 45. Disc. 48-5 is a part of copyrighted Journal of the American Concrete Institute, V. 24, No. 4, Dec. 1952, Part 2, *Proceedings* V. 48.

†Structural Project Engineer, Consulting Engineering Div., Hydro-Electric Power Commission of Ontario, Toronto, Ont., Canada.

ments can be determined in terms of angular rotations makes application of the method general and independent of the shape of prestressing cables. Referring to Fig. A, the fixed-end moments are

$$\left.\begin{aligned} M^{F'}_{AB} &= -2\frac{2\alpha_{AB} - \alpha_{BA}}{L} \\ M^{F'}_{BA} &= -2\frac{2\alpha_{BA} - \alpha_{AB}}{L} \end{aligned}\right\} \quad \ldots\ldots(1)$$

Where cables are placed symmetrically with respect to the center of the span $\alpha_{AB} = \alpha_{BA}$ and consequently

$$M^{F'}_{AB} = M^{F'}_{BA} = -\frac{2\alpha}{L} \quad \ldots\ldots(2)$$

If end A is free to rotate

$$M^{F'}_{BA} = -\frac{3\alpha_{BA}}{L} \quad \ldots\ldots(3)$$

Conversely, if end B is allowed to rotate

$$M^{F'}_{AB} = -\frac{3\alpha_{AB}}{L} \quad \ldots\ldots(4)$$

Analysis of rotation angles can be facilitated by using ϑ_{ik} tables, which are set up for different loading curvatures. To illustrate the significance of the effect of a straight cable to a restrained end, consider beam A-B, fixed at B, Fig. B. Since there is no angular change at B due to any loading, α_{BA} must be zero. To make $\alpha_{BA} = 0$ in Fig. A(b), a moment is required to act upon end B so as to rotate it back to its original position. Referring to Eq. 3, $M^{F'}_{BA} = 3Pe/2$. It should be pointed out that the $M^{F'}$ moments in Eq. 1 to 4 are additional moments that are to be added to the direct moments of Pe. It will be shown that for continuous beams the additional fixed-end moments only are to be used in moment distribution, while Pe is added when the final moments are calculated. The final or actual bending moment in Fig. B, is thus,

$$M^{F}_{BA} = -Pe + \frac{3Pe}{2} = +\frac{Pe}{2}$$

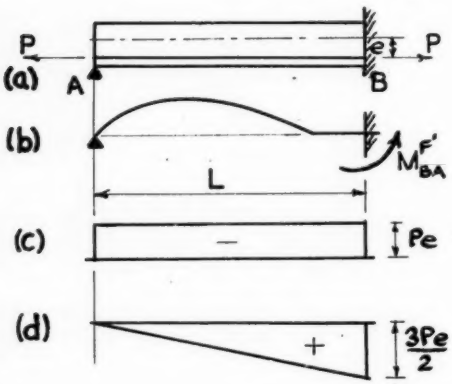

Fig. B—Problem 1. Beam fixed at one end

To avoid mistakes the following sign convention will be adopted. For prestressing members placed below the neutral axis of the structure deflecting the beam upward, a minus sign will be used for the rotation angles. Conversely, for prestressing members above the neutral axis deflecting the beam downward, a

plus sign will be used. By substituting the angles with their signs in Eq. 1 to 4, the correct answer is obtained automatically. In solving indeterminate structures it is useful to plot moment diagrams on the tension side. For further illustration consider the following problems, where prestressed members are placed in different ways.

Problem 2 (Fig. C)

In all practical cases it is possible to divide the profile of the cables into segments over various lengths of the members and compute the angular rotations. In this problem a rectangular and a parabolic segment is obtained with the centers of gravity determined from both ends. The angles are:

$$\alpha_{AB} = -\frac{1}{L}\left(\frac{PeL}{2} \times \frac{3L}{4} + \frac{PeL}{3} \times \frac{5L}{16}\right) = -\frac{23}{48} PeL$$

$$\alpha_{BA} = -\frac{1}{L}\left(\frac{PeL}{2} \times \frac{L}{4} + \frac{PeL}{3} \times \frac{11L}{16}\right) = -\frac{17}{48} PeL$$

Consider both ends fixed,

$$M'_{AB} = -2\left(-\frac{2 \times 23}{48} + \frac{17}{48}\right) Pe = +\frac{29}{24} Pe$$

$$M'_{BA} = -2\left(-\frac{2 \times 17}{48} + \frac{23}{48}\right) Pe = +\frac{11}{24} Pe$$

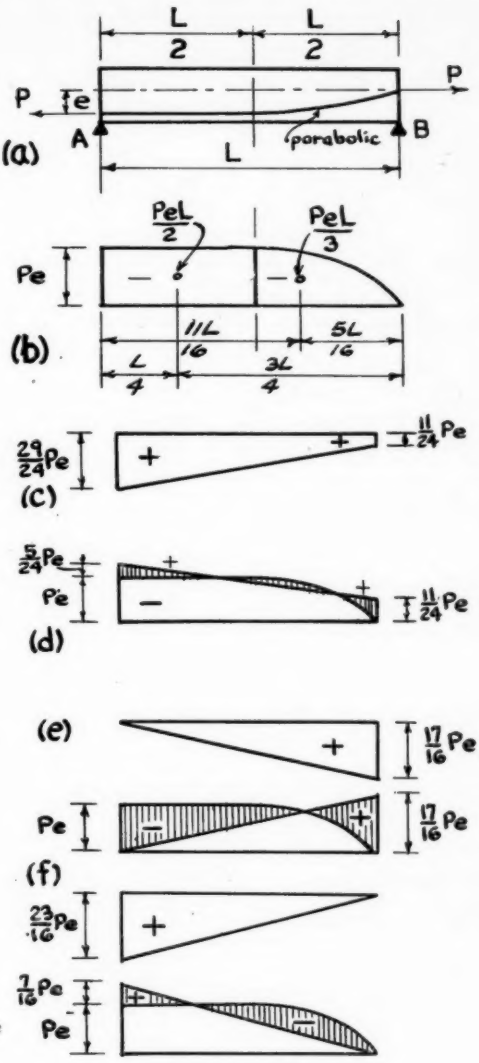

Fig. C—Problem 2

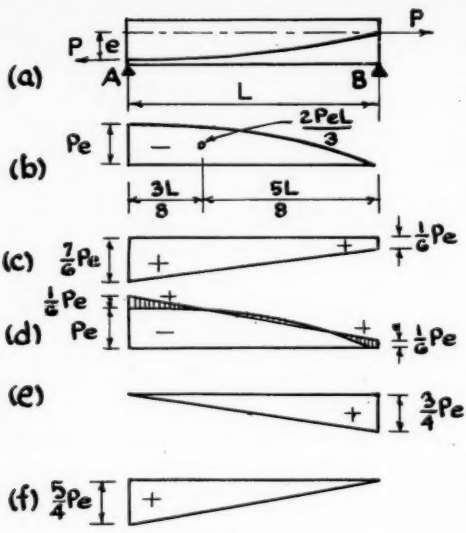

Fig. D—Problem 3

The final fixed-end moments are:

$$M^F_{AB} = -Pe + \frac{29}{24}Pe = +\frac{5}{24}Pe$$

$$M^F_{BA} = 0 + \frac{11}{24}Pe = +\frac{11}{24}Pe$$

If end A is free to rotate,

$$M^{F'}_{BA} = M^F_{BA} = 0 + \frac{3 \times 17}{48}Pe$$

$$= \frac{17}{16}Pe$$

If end B is free to rotate,

$$M^{F'}_{AB} = \frac{3 \times 23}{48}Pe = \frac{23}{16}Pe \text{ and}$$

$$M^F_{AB} = -Pe + \frac{23}{16}Pe = \frac{7}{16}Pe$$

Problem 3 (Fig. D)

A parabolic profile is used with the vertex at A.

$$\alpha_{AB} = -\frac{5}{12}PeL$$

$$\alpha_{BA} = -\frac{1}{4}PeL$$

Both ends fixed,

$$\left.\begin{aligned} M^{F'}_{AB} &= -2\left(-\frac{2 \times 5}{12} + \frac{1}{4}\right)Pe = +\frac{7}{6}Pe \\ M^{F'}_{BA} &= -2\left(-\frac{2 \times 1}{4} + \frac{5}{12}\right)Pe = +\frac{1}{6}Pe \end{aligned}\right\} \text{ Fig. D(c)}$$

$$M^F_{AB} = +\frac{1}{6}Pe;\ M^F_{BA} = +\frac{1}{6}Pe \quad \text{Fig. D(d)}$$

If end A is free,

$$M^{F'}_{BA} = M^F_{BA} = 0 + \frac{3}{4}Pe \quad \text{Fig. D(e)}$$

If end B is free,

$$\left.\begin{aligned} M^{F'}_{AB} &= +\frac{3 \times 5}{12}Pe = +\frac{5}{4}Pe \\ M^F_{AB} &= -Pe + \frac{5}{4}Pe = +\frac{1}{4}Pe \end{aligned}\right\} \text{ Fig. D(f)}$$

Problem 4 (Fig. E)

A parabolic cable is placed below the neutral axis for a length a.

$$\alpha_{AB} = -\frac{Pe}{3L}(2ab + a^2)$$

$$\alpha_{BA} = -\frac{Pea^2}{3L}$$

Both ends fixed,

$$M'_{AB} = \frac{2\,Pe}{3}(4ab + a^2)$$

$$M'_{BA} = \frac{2\,Pe}{3}(a^2 - 2ab)$$

If end A is free,

$$M'_{BA} = Pea^2$$

If end B is free

$$M'_{AB} = Pe\,(2ab + a^2)$$

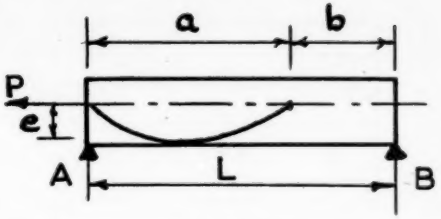

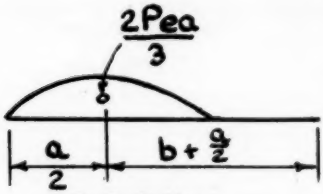

Fig. E—Problem 4

Problem 5 (Fig. F)

This case is identical to the problem analyzed in the paper, Fig. 6, except for cable P_1.

$$\alpha_{AB} = \alpha_{BA} = -\frac{P_2(e_1 + e_2)\,L}{3} + \frac{P_2 e_2\,L}{2} = \frac{P_2\,L}{6}(e_2 - 2e_1)$$

Both ends fixed,

$$M'_{AB} = M'_{BA} = \frac{P_2}{3}(2e_1 - e_2)$$

$$M^F_{AB} = M^F_{BA} = +\,P_2 e_2 + \frac{P_2}{3}(2e_1 - e_2) = +\frac{2P}{3}(e_1 + e_2)$$

If one end is free to rotate, the moment at the other end is,

$$M^{F'} = +\frac{P_2}{2}(2e_1 - e_2) \text{ and,}$$

$$M^F = +\,P_2\,e_2 + \frac{P_2}{2}(2e_1 - e_2) = \frac{P_2}{2}(2e_1 + e_2)$$

Problem 6

The arrangement of cables may vary widely to suit the purpose of the structure. In a good many bridges, straight cables have been used which are not in contact with the structure, with the exception of breaking points and ends (Fig. G(a), (b), (c)). In all these cases it is a

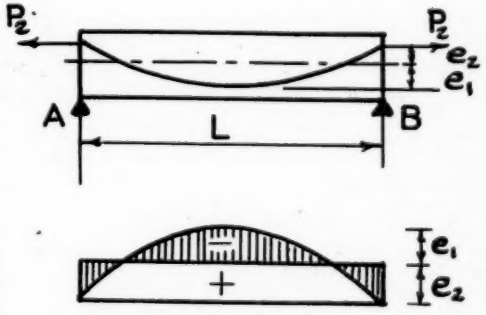

Fig. F—Problem 5

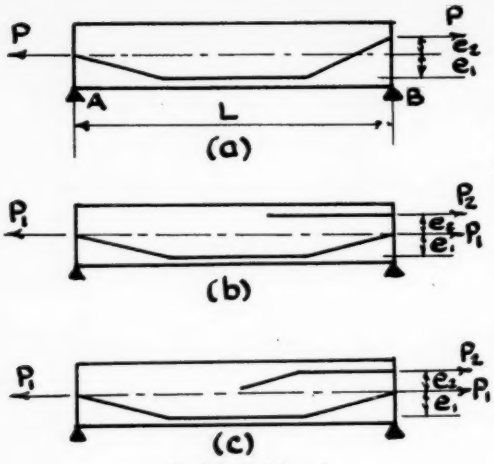

Fig. 6—Problem 6

simple matter to divide the moment areas into triangles and rectangles, find their center of gravity, and take moments about the supports. The procedure outlined in the paper is not applicable to these cases.

COMPARISON OF METHODS

Now consider the same problems using the method outlined in the paper. For comparison, the writer's figures are given in brackets. In problem 2 the curved portion of the cable will produce a constant upward load w, which is distributed on the right half of the beam. According to Eq. 2e

$$w = \frac{2\ Pb}{(aL)^2} = \frac{2\ Pe}{(L/2)^2} = \frac{8\ Pe}{L^2}$$

The fixed-end moments are

$$M^F_{AB} = \frac{5 \times 8\ Pe}{96 \times 2} = \frac{5}{24} Pe \qquad \left[\frac{5}{24} Pe\right]$$

$$M^F_{BA} = \frac{11 \times 8\ Pe}{96 \times 2} = \frac{11}{24} Pe \qquad \left[\frac{11}{24} Pe\right]$$

Allowing end A to rotate,

$$M^F_{BA} = \frac{9 \times 8\ Pe}{64 \times 2} = \frac{9}{16} Pe \qquad \left[\frac{17}{16} Pe\right]$$

conversely, if end B is free to rotate

$$M^F_{AB} = \frac{7 \times 8\ Pe}{64 \times 2} = \frac{7}{16} Pe \qquad \left[\frac{7}{16} Pe\right]$$

In problem 3 the cable exerts a constant pressure upward throughout the entire length, $w = 2Pe/L^2$, hence, the moments at the supports are,

$$M^F_{AB} = M^F_{BA} = \frac{2\ Pe}{12} = \frac{1}{6} Pe \qquad \left[\frac{1}{6} Pe\right]$$

End B fixed only,

$$M^F_{BA} = \frac{2\ Pe}{8} = \frac{1}{4} Pe \qquad \left[\frac{3}{4} Pe\right]$$

and end A fixed only,

$$M^F_{AB} = \frac{1}{4} Pe \qquad \left[\frac{1}{4} Pe\right]$$

In problem 4 the parabolic curvature creates a uniformly distributed load $w = 8Pe/a^2$ hence, the fixed-end moments are,

$$M^F_{AB} = \frac{2\,Pe}{3\,L^2}(6\,L^2 - 8aL + 3a^2)$$

$$M^F_{BA} = \frac{2\,Pe}{3\,L^2}(4\,La - 3a^2)$$

A more striking example of the effect of prestress is found in problem 5. The fixed-end moments for the case where both ends are fixed agree with those by the writer. But in cases where one end only is fixed, they deviate considerably.

Referring to the authors' statement on p. 60, "The joint at A is free to rotate. Consequently, if this joint is allowed to rotate, the moment produced at B by the vertical loads induced by prestressing is $M^F_{BA} = M^F_{BA} + 0.5\,M^F_{AB}$." Substituting the numerical values first in the writer's formula the moment at B will be

$$M^F_{BA} = \frac{P_2}{2}(2e_1 + e_2) = \frac{188{,}000}{2}(2 \times 6.22 + 7.58) = 1{,}920{,}000 \text{ in.-lb}$$

While according to the paper

$$M^F_{BA} = 1{,}820{,}000 + 0.5 \times 1{,}820{,}000 = 2{,}730{,}000 \text{ in.-lb}$$

In problems 2 to 6, as we have seen, the authors' Eq. 2e can be used to compute fixed-end moments with results equal in validity to those obtained by the writer, but in cases where one end only is fixed the procedure would lead to erroneous conclusions.

Application of the paper's equation to problem 5, resulted in a deviation of 70 percent. This example illustrates the significance of the two sets of moments, and it is absolutely necessary to distinguish between end moment Pe and the additional fixed-end moments. The practical meaning of the additional fixed-end moments in continuous beams was illustrated in these problems. In moment distribution only the additional fixed-end moments are to be used, and the balanced moments are combined with the straight values of Pe. To prove the point, analyze problems 2, 3, and 5.

Problem 2:

$$M^{F'}_{AB} = 0,\ M^{F'}_{BA} = +\frac{11}{24}Pe + \frac{29}{48}Pe = \frac{17}{16}Pe$$

$$M^{F'}_{BA} = 0,\ M^{F'}_{AB} = +\left(\frac{29}{24} + \frac{11}{48}\right)Pe = \frac{23}{16}Pe$$

Problem 3:

$$M^{F'}_{AB} = 0,\ M^{F'}_{BA} = \left(\frac{7}{12} + \frac{1}{6}\right)Pe = \frac{3}{4}Pe$$

$$M^{F'}_{BA} = 0,\ M^{F'}_{AB} = \left(\frac{7}{6} + \frac{1}{12}\right)Pe = \frac{5}{4}Pe$$

Problem 5:

$$M^{F'}_{AB} = 0,\ M^{F'}_{BA} = +\frac{Pe_2}{3}(2e_1 - e_2) + \frac{Pe_2}{6}(2e_1 - e_2) = +\frac{P_2}{2}(2e_1 - e_2)$$

The fundamental concept of the carry-over moment presumes that an equivalent moment, but of opposite sign, is applied to the end that is to be freed and, therefore, half of that moment can be added to the fixed end. In cases where cables are eccentric at the end of the member, the fixed-end moment consists of two sets of moments of which Pe is always there, regardless of whether the end is free to rotate or restrained. Therefore, it is felt that introduction of the additional moments computed from rotation angles will help considerably to evaluate the effect of prestress in statically indeterminate structures.

One more example (Fig. H) will be of interest. Parabolic cables are used in both cases illustrated, which would cause a direct uniformly distributed load for the extent of the cable length. The only difference is in sign, *i.e.*, in (a) the vertical load is acting upward, while in (b) it is acting downward. Therefore, the fixed-end moments are as follows:

$$w = \frac{8\,Pe}{L^2}$$

$$M^F_{AB} = \pm\frac{5}{24}Pe, \qquad M^F_{BA} = \pm\frac{11}{24}Pe$$

By applying the rotation angles the moments are:

$$\left.\begin{aligned} \alpha_{AB} &= -\frac{5}{48}PeL, \qquad \alpha_{BA} = -\frac{11}{48}PeL \\ M^F_{AB} &= 0 - 2\left(\frac{-2\times 5}{48} + \frac{11}{48}\right)Pe = -\frac{1}{24}Pe \\ M^F_{BA} &= 0 - 2\left(\frac{-2\times 11}{48} + \frac{5}{48}\right)Pe = +\frac{17}{24}Pe \end{aligned}\right\} \quad \text{Fig. H(a)}$$

$$\left.\begin{aligned} \alpha_{AB} &= +\frac{PeL}{16}, \qquad \alpha_{BA} = +\frac{13}{48}PeL \qquad M^F_{AB} = 0 - 2\left(\frac{2\times 1}{16} - \frac{13}{48}\right)Pe = +\frac{7}{24}Pe \\ M^F_{BA} &= Pe - 2\left(\frac{2\times 13}{48} - \frac{1}{16}\right)Pe = +\frac{1}{24}Pe \end{aligned}\right\} \quad \text{Fig. H(b)}$$

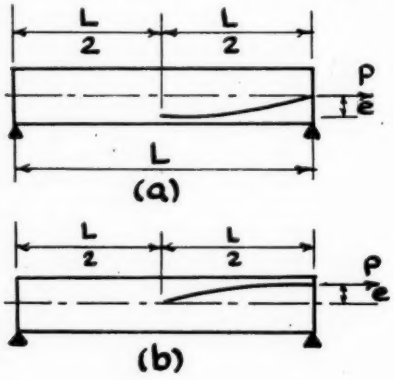

Fig. H—Parabolic cables extending through only half the beam

USE OF COLUMN ANALOGY

The column analogy method also can be used as a useful tool in analyzing fixed-end moments. In certain cases it may prove even more advantageous than rotation angles. For illustration consider a few cases from previous examples.

Problem 2 (Fig. C and I)

The properties that must be obtained for the column analogy are the areas of moments, location of their centroid, and the distance of the centroids in respect to the center of the member. The column formula gives

$$f = \frac{Q}{A} \pm \frac{m}{s}, \text{ where } \quad Q = Q_1 + Q_2 = \frac{5\,PeL}{6} \quad \text{and}$$

$$A = L,\ S = \frac{L^2}{6},\ m = \frac{Q_1 L}{4} - \frac{3\,Q_2 L}{16} = \frac{PeL^2}{16} \qquad M'^{F'}_{AB} = \frac{5\,Pe}{6} + \frac{Pe}{8} = \frac{29}{24}Pe$$

$$M'^{F'}_{BA} = \frac{11}{24}Pe$$

Problem 3 (Fig. D)

$$Q = \frac{2}{3}PeL$$

$$m = \frac{QL}{8} = \frac{PeL^2}{12}$$

$$M'^{F'}_{AB} = \frac{2\,Pe}{3} + \frac{Pe}{2} = \frac{7}{6}Pe$$

$$M'^{F'}_{BA} = \frac{2\,Pe}{3} - \frac{Pe}{2} = \frac{1}{6}Pe$$

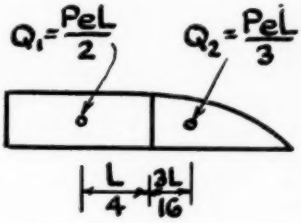

Fig. I—Column analogy example

CONTINUOUS BEAMS

Proceeding to the continuous beam analyzed in the paper, the angular rotations are computed as shown in Fig. J.

$$F_1 = -2/3 \times 45 \times 1.88 = -56.4 \qquad \alpha_{AB} = \frac{P}{L}$$

$$F_2 = -2/3 \times 31.5 \times 2.80 = -59.0$$

$$F_3 = +0.92 \times 31.5 = +29.0$$
$$F_4 = +0.92 \times 13.5 = +12.4$$
$$F_5 = +2/3 \times 1.20 \times 13.5 = +10.8$$

$$-56.4 \times 61.8 = -3490$$
$$-59.0 \times 33.2 = -1960$$
$$-5450$$

$$29.0 \times 29.25 = +850$$
$$12.4 \times 6.75 = +84$$
$$10.8 \times 5.10 = +55$$
$$+989$$
$$-4461$$

$$\alpha_{AB} = -\frac{4461}{90}P = -49.6\,P$$

Taking moments about support A, α_{BA} can be found,

$$\alpha_{BA} = -\frac{1242}{90}P = -13.8\,P$$

The fixed-end moments:

$$M'^{F'}_{AB} = -\frac{2}{90}(-2 \times 49.6 + 13.8)\,937.5 = +1775 \text{ ft-kips}$$

$$M'^{F'}_{BA} = -\frac{2}{90}(-2 \times 13.8 + 49.6)\,937.5 = -460 \text{ ft-kips}$$

$$M^{F}_{AB} = 0 + 1775 = 1775 \text{ ft-kips}$$
$$M^{F}_{BA} = -460 + 2.12 \times 937.5 = +1530 \text{ ft-kips}$$

As end A is simply supported the moment at B will become,

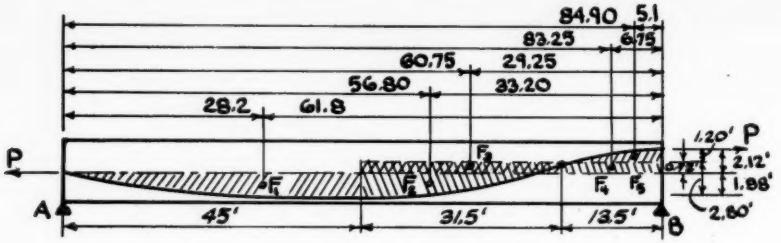

Fig. J—Continuous beam analysis

$$M_{BA}^{F'} = -460 + 0.5 \times 1775 = +887 \text{ ft-kips}$$

In the same manner the moments for the center span are computed, thus

$$\alpha_{BC} = \alpha_{CB} = -8.33\,P$$

$$M_{BC}^{F'} = M_{CB}^{F'} = -\frac{-2 \times 8.33}{120} 937.5 = +130 \text{ ft-kips}$$

After determining the additional fixed-end moments, moment distribution can be performed in the usual way. The one cycle moment distribution as used by the authors can be simplified further in this particular case, owing to the three symmetrical spans and symmetrical arrangement of cables in respect to the center span. Thus $\frac{3}{4} \times I/L$ is used for the end span, and $\frac{1}{2} \times I/L$ for the center span. To illustrate the short cut, use the numerical values of the above problem; for simplicity assume that $I = 360$.

$k = \frac{3 \times 360}{4 \times 90} = 3$ $\qquad$ B $\qquad$ $k = \frac{1 \times 360}{2 \times 120} = 1.5$

0.333

▲A $\qquad$ 427 ▲ 130

99

229

The total moment at B:

$$M_B = 229 + 1990 = 2219 \text{ ft-kips}$$

At the moment the writer is designing a bridge where straight cables are being employed throughout the three spans and are in contact with the bridge girders only at the ends (Fig. K). Hollow rectangular units will be used, forming a parabolic curve when assembled.

Moment areas and rotation angles are calculated as follows

$$F_1 = -\frac{2L\,(e_1 + e_2)}{3}; \qquad F_2 = Le_1$$

$$\alpha_{AB} = \alpha_{BA} = \frac{P}{L}(-F_1 + F_2)\frac{L}{2} = \frac{PL}{6}(e_1 - 2e_2)$$

Therefore,

$$M_{AB}^{F'} = M_{BA}^{F'} = -\frac{2\alpha}{L_1} = \frac{P}{3}(2e_2 - e_1) \quad \ldots\ldots (5)$$

Since A is simply supported,

$$M_{BA}^{F'} = -\frac{3\alpha}{L_1} = \frac{P}{2}(2e_2 - e_1) \quad \ldots\ldots (5a)$$

In problems where one or two unknowns are involved the method of virtual work could be used more advantageously than moment distribution. As a particular example of the application of this method, general equations of equilibrium for three unequal spans can be expressed thus,

$$\left.\begin{aligned} \vartheta_B + M'_B\,\vartheta_{BB} + M'_C\,\vartheta_{BC} &= 0 \\ \vartheta_C + M'_B\,\vartheta_{CB} + M'_C\,\vartheta_{CC} &= 0 \end{aligned}\right\} \quad \ldots\ldots (6)$$

Where

$$\left.\begin{aligned} &\vartheta_B = \alpha_{BA} + \alpha_{BC}\,;\ \vartheta_C = \alpha_{CB} + \alpha_{CD} \\ &\vartheta_{BB} = \frac{1}{3}(L_1 + L_2);\quad \vartheta_{CC} = \frac{1}{3}(L_2 + L_3);\qquad \vartheta_{BC} = \vartheta_{CB} = \frac{1}{6}L_2 \end{aligned}\right\} \quad \ldots\ldots (6a)$$

If $L_1 = L_2$, the moments at B and C will be equal, $M'_B = M'_C$, because $\vartheta_B = \vartheta_C$; $\vartheta_{BB} = \vartheta_{CC}$. Therefore,

$$\vartheta_B + M'_B\,(\vartheta_{BB} + \vartheta_{BC}) = 0$$

or $$M'_B = -\frac{\vartheta_B}{\vartheta_{BB} + \vartheta_{BC}} \quad \ldots\ldots (7)$$

Substituting Eq. 6a in Eq. 7

$$M'_B = -P\frac{(L_1 + L_2)\,(e_1 - 2e_2)}{2L_1 + 3L_2} \quad \ldots\ldots (7a)$$

For three equal spans Eq. 7a reduces to

$$M'_B = -\frac{2}{5}P\,(e_1 - 2e_2) \quad \ldots\ldots (8)$$

To sum up, the α values of Fig. A-D are characteristic of deformation when prestress forces are acting on the structure. The deformations occur whether the cables exert any direct pressure on the structure or not. For this reason Eq. 2e alone cannot reliably be used for estimating the effect of prestress on a continuous structure. Specific gaps and inadequacies in this method have been indicated, and the writer believes that by adhering to certain fundamentals in design procedure, any type of continuous prestressed structure can be analyzed so as to obtain satisfactory results.

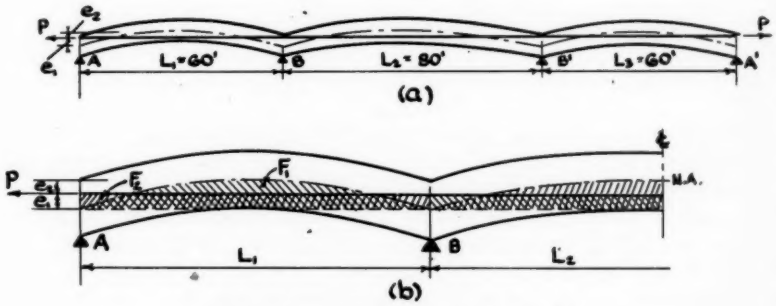

Fig. K—Three-span bridge with straight cables

AUTHORS' CLOSURE

The authors wish to thank Mr. Raud for confirming by the classical conjugate beam method the validity of the simplified procedure outlined in their paper for analyzing continuous prestressed members. Agreement between the authors' values and the values computed by Mr. Raud for the examples used as illustration is not accidental but must follow since the assumptions underlying the authors' procedure are fundamentally correct as will be demonstrated. As long as the correct vertical loading caused by curvature of the cables is used, the two methods will yield identical results irrespective of the proportions of the cable above the centroidal axis.

Mr. Raud's skepticism of the procedure apparently stems from the fact that in applying it he has neglected to include the effect of the horizontal components of the prestress force acting at the ends of the free bodies or beams. The paper did not elaborate on this point since the determination of the effects of the horizontal components can be readily evaluated. However, the importance and effect of horizontal forces acting at the ends is included in Eq. 3a, discussed on pages 46, 50, and 55, and shown in Fig. 1, 6, and 8. When the effect of horizontal forces is included in the examples computed by Mr. Raud, complete agreement between the two methods is obtained.

The article points out that the eccentricity of cables at the ends of fixed-end beams or at interior supports of a continuous beam has no effect on the moments in a prestress beam. But when the end of the beam is free to rotate, both fixed-end moments produced by vertical loads and the horizontal force must be distributed.

To illustrate the correct method of analysis, Mr. Raud's problems 2 to 5 will be computed.

Problem 2

From Eq. 2e the vertical load acting on half the beam (Fig. L) is

$$w_p = -\frac{2\,Pe}{0.5^2\,l^2} = -\frac{8\,Pe}{l^2}$$

For an upward load on one-half of the beam, the fixed-end moments are

$$M^F_{AB} = \frac{0.5^3\,(4 - 3 \times 0.5)\,8 \times Pe}{12} = +\frac{5\,Pe}{24}$$

$$M^F_{BA} = \frac{0.5^2\,(6 - 8 \times 0.5 + 3 \times 0.5^2)\,8 \times Pe}{12} = +\frac{11\,Pe}{24}$$

These fixed-end moments represent only the restraining moments for the vertical load. In addition, at A, there exists a moment equal to $-Pe$ due to the eccentricity of horizontal component P. In this connection, behavior of the prestress beam can be better visualized by imagining that the cable is cut at the ends of the beam. Tension in the cable is resisted by reactions on the concrete equal to P as shown in Fig. L. If beam AB were a simple span, this moment would produce rotation at A. To prevent this rotation, it is obvious that an equal though opposite moment must be applied. The

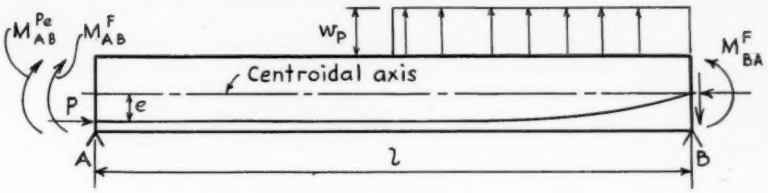

Fig. L—External loads created by prestress

total restraining moment at A required to prevent rotation of the beam at A by superposition is equal to

$$M^{F'}_{BA} = M^{F}_{BA} + M^{Pe}_{BA} = M^{F}_{BA} + Pe$$

in which M^{Pe}_{BA} is the restraining moment required to prevent rotation caused by the end moment $-Pe$, and $M^{F'}_{BA}$ is the moment in the restraining member. It should be noted that if the cable is eccentric at the end of the beam, the fixed-end moment in the beam differs from the restraining moment. With zero restraint at A, and full fixity at B, the moment at B by moment distribution is

$$M_{BA} = M^{F}_{BA} + \frac{1}{2}(M^{F}_{AB} + Pe)$$

Introducing numerical values, gives

$$M_{BA} = \left[\frac{11}{24} + \frac{1}{2}\left(\frac{5}{24} + 1\right)\right] Pe = \frac{17}{16} Pe$$

Since no restraining moments act at A, the moment there is naturally $M_{AB} = -Pe$. If end B is allowed to rotate, then because P acts along the centroidal axis, the moment at A is

$$M_{AB} = M^{F}_{AB} + \frac{1}{2}(M^{F}_{BA}) = \frac{5}{24} + \frac{1}{2} \times \frac{11}{24} = \frac{7}{16} Pe$$

and $M_{BA} = 0$.

Problem 3

Using the same procedure, end moments in problem 3 are:

$$w_p = \frac{2\,Pe}{l^2}$$

$$M^{F}_{AB} = M^{F}_{BA} = \frac{2\,Pe}{12} = \frac{Pe}{6} \quad \text{and} \quad M^{Pe}_{AB} = Pe \quad \text{and} \quad M^{Pe}_{BA} = 0$$

Therefore, if A is allowed to rotate

$$M_{BA} = Pe\left[\frac{1}{6} + \frac{1}{2}\left(\frac{1}{6} + 1\right)\right] = \frac{3\,Pe}{4}$$

$$M_{AB} = -Pe$$

And if B is allowed to rotate

$$M_{AB} = Pe\left[\frac{1}{6} + \frac{1}{2} \times \frac{1}{6}\right] = \frac{Pe}{4}$$

$$M_{BA} = 0$$

Problem 4

In problem 4, which represents a rather unorthodox prestress beam arrangement, besides the uniform load acting along the beam, there exists at the interior end of the cable a concentrated force induced by anchorage of the cable as shown in Fig. M by its two components. The vertical reaction P_v is necessarily equal to one-half of the total upward uniform load. With the uniform loading given by

$$w_p = \frac{2\,Pe}{(0.5\,a\,l)^2} = \frac{8\,Pe}{(a\,l)^2}$$

then $P_v = 4\,Pe/al$. The fixed-end moments for the uniform and concentrated loading are

$$M^F_{AB} = Pe\left[\frac{8}{12}(6 - 8a + 3a^2) - 4\,(1 - a)^2\right] = \frac{2\,Pea\,(4 - 3a)}{3} = \frac{2\,Pe\,(4ab + a^2)}{3}$$

$$M^F_{BA} = Pe\left[\frac{8a}{12}(4 - 3a) - 4a\,(1 - a)\right] = \frac{2\,Pea}{3}(3a - 2) = \frac{2\,Pe}{3}(a^2 - 2\,ab)$$

If A is free to rotate, then by moment distribution

$$M_{BA} = \frac{2\,Pea}{3}\left[3\,a - 2 + \frac{1}{2}(4 - 3a)\right] = Pea^2$$

$$M_{AB} = 0$$

and if B is free to rotate

$$M_{AB} = \frac{2\,Pea}{3}\left[4 - 3a + \frac{1}{2}(3a - 2)\right] = Pe\,(2\,ab + a^2)$$

$$M_{BA} = 0$$

Problem 5

In problem 5, the uniform vertical reaction produced by the prestress force is, from Eq. 2e

$$w_p = \frac{2\,P_2\,(e_1 + e_2)}{(0.5l)^2} = \frac{8\,P_2\,(e_1 + e_2)}{l^2}$$

Fixed-end moments due to the vertical prestress load are

$$M^F_{AB} = M^F_{BA} = \frac{8\,P_2(e_1 + e_2)}{12}$$

Restraining moments at A and B due to horizontal forces are

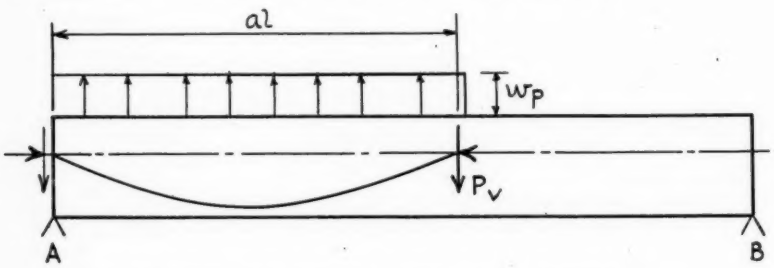

Fig. M—External loads created by prestress of a cable in portion of beam

$$M_{AB}^{Pe} = M_{BA}^{Pe} = -P_2 e_2$$

If end A is allowed to rotate, the end moment is

$$M_{AB} = P_2 \left\{ \frac{2(e_1 + e_2)}{3} - \frac{1}{2}\left[\frac{2(e_1 + e_2)}{3}\right] - e_2 \right\}$$

which reduces to

$$M_{AB} = \frac{P_2(2e_1 + e_2)}{2}$$

In addition to these problems, Mr. Raud presents two cases in Fig. H which warrant comment. In Fig. H(a) besides the uniform vertical load, there exists a horizontal force at midspan equal to P. The fixed end moments produced by this horizontal force can be shown to be respectively

$$M_{AB}^{F} = -\frac{1}{4}\frac{Pe}{4} \qquad \text{and} \qquad M_{BA}^{F} = \frac{Pe}{4}$$

The total fixed-end moments for horizontal and vertical loading will therefore be

$$M_{AB}^{F} = Pe\left(\frac{5}{24} - \frac{1}{4}\right) = -\frac{Pe}{24} \qquad \text{and} \qquad M_{BA}^{F} = Pe\left(\frac{11}{24} + \frac{1}{4}\right) = +\frac{17\,Pe}{24}$$

In Fig. H(b), at midspan there exists a concentrated reaction, whose horizontal component is P and whose vertical component (upward) is equal to $4Pe/l$. Fixed-end moments for this condition therefore are

$$M_{AB}^{F} = Pe\left(-\frac{5}{24} + \frac{4}{8}\right) = \frac{7\,Pe}{24} \qquad \text{and} \qquad M_{BA}^{F} = Pe\left(-\frac{11}{24} + \frac{4}{8}\right) = \frac{Pe}{24}$$

A comparison of the values obtained by the use of the vertical and horizontal forces exerted on the concrete by the cable and those obtained from the eccentricity of the cable shows that when the authors' procedure is correctly applied identical results are obtained. Validity of the method is thus clearly established for all conditions of end restraint and for any arrangement of parabolically draped cables in members of constant cross section. Moreover, the procedure has been extended in the paper "Analysis of Continuous Prestressed Concrete Structures" published in the Proceedings of the First United States Conference on Prestressed Concrete, held at MIT, to cover the case of beams with variable moments of inertia. Charts in this paper reduce the work of computing fixed-end moments to insignificant proportions.

Although the paper concerned itself mainly with prestressed beams with cables having a parabolic profile, the fundamental concept of analyzing a prestressed member by considering the forces which the cable exerts on the concrete is applicable to any profile. For example, it is evident that the prestressed cable shown in problem 6 will exert an upward concentrated force at the change in direction of the cable. For this particular case, the problem therefore reduces simply to an investigation of the effects of concentrated loads. The ease of analyzing for concentrated loads is readily apparent.

In his opening sentence Mr. Raud states that the procedure is limited to a few problems. No such limitation exists. Since the procedure actually expresses in a more realistic manner the action of prestressed cables on the con-

crete, the method is as universally applicable as any other classical method. Because of the evident relationship between the profile of the cable and the reaction it imparts to the concrete, the authors believe that a designer can better understand the action of a continuous prestressed member. For example, the total shear acting at any section can be more easily ascertained by the proposed procedure than by the conjugate beam method. Another important advantage is that the effect of frictional losses can be determined readily.

At the time of publication of the paper, little data was available on frictional losses in curved cables. Since then, however, an excellent series of tests on this subject has been discussed by Y. Guyon in his book *Beton Precontraint—Etude Theorique et Experimentale*, published by the Institut Technique du Batiment et Dès Travaux Publics, Paris, France. In this series of tests, it was found that the coefficient of friction of wires in metallic sheathing could be about 0.35, and about 0.19 for bituminous-coated wires in metallic sheathing. These values for the coefficient of friction give greater reduction in tension than those noted by Magnel.

Loss in tension due to friction can be determined by the method suggested in the article "Analysis of Continuous Prestressed Concrete Structures," from the MIT conference. Because the coefficient of friction cannot be determined with any degree of exactness, the loss in tension in curved cables may just as well be computed as the uniform vertical prestress reaction times the coefficient of friction. Thus in the example of the fixed-end beam, if we assume the cable tensioned at both ends, the loss in tension at the center on the basis that the coefficient of friction is 0.2 will be

$$\text{loss in tension} = P_2 \left(\frac{8 \times 14.5}{60 \times 2 \times 12} \right) 0.2 = 0.016\, P_2$$

For a coefficient of friction of 0.4, the tension at the center would be 97 percent of the tension at the end. In the continuous three-span example, the loss in tension at the center of the interior span can be obtained readily by taking advantage of the fact that the upward and downward prestress loads are equal. Hence, the tension at the center of an interior span in terms of the applied tension is, from the values for w_p and w, given on page 60, and for a coefficient of friction equal to 0.2

$$P_c = P \left[1 - 0.2 \left(\frac{8 \times 1.88 \times 0.5}{90} + \frac{2 \times 4 \times 4}{90} + \frac{2 \times 4 \times 4}{120} \right) \right]$$
$$= 0.86\, P$$

To minimize the effect of friction, the tension applied at both ends should first be $P/0.86$, and afterward reduced to P.

In conclusion, the authors wish to compliment Mr. Raud for his extensive analysis of prestressed members with various end conditions. The numerous foreign articles and conferences being held abroad on prestressed indeterminate structures indicate that in the near future continuous prestressed structures will play an important role.

Title No. 48-6

Pumice—Lightweight Aggregate*

By LESLIE I. NEHER†

SYNOPSIS

The growth of pumice production in the United States during recent years is worthy of note. Chemical and physical properties, mix design, presaturation of aggregates and the application of pumice aggregates in lightweight tilt-up and masonry construction are discussed.

INTRODUCTION

Pumice, used by the Romans before the time of Christ to reduce deadweight in the great domes of that age,‡ is likewise gaining favor with the modern architect and engineer.

Pumice is a rock of porous nature, emanating from an acid magma, and is formed by forceful ejection and subsequent expansion at extreme temperature from an active volcano. The magma is thrown high into the air and is broken into small pieces ideal for concrete aggregate. Occluded gases and water vapor at the elevated temperatures are suddenly released from their confining pressures and cause a volume increase of the molten magma, thus forming lightweight pumice aggregate.

The areas of production of pumice aggregates are limited and in the United States are found only in the western states where fairly recent volcanic action has occurred. California, New Mexico, Oregon and Idaho lead in its production.

Engineers have become acquainted with the structural possibilities of lightweight construction and considerable progress has been made in the field of pumice lightweight monolithic concrete.

PROPERTIES

Frequently the question arises as to whether a lightweight material is pumice or other volcanic rock of similar appearance. Pumice is a silica material with many thin-walled interstices invisible to the naked eye. Scoracious materials usually have continuous interstices or tubes that are visible without the use of magnification. There are many deposits of volcanic rock in western United States that, to the uninitiated, might appear to be pumice. Pumice

*Received by the Institute Feb. 28, 1951. †Title No. 48-6 is a part of copyrighted JOURNAL OF THE AMERICAN CONCRETE INSTITUTE, V. 23, No. 1, Sept. 1951, *Proceedings* V. 48. Separate prints are available at 50 cents each. **Discussion** (copies in **triplicate**) should reach the Institute not later than Jan. 1, 1952. Address 18263 W. McNichols Rd., Detroit 19, Mich.

†Member American Concrete Institute, Consulting Engineer, Marion, Ind.

‡*Information Circular* No. 7195, Jan. 1942, Bureau of Mines, U. S. Dept. of the Interior, p. 4.

is grey-white to white in color and will become brown to red when contaminated with organic materials. Seldom will scoracious materials be lighter in unit weight than pumice.

Chemical analysis

Pumice that has become colored through percolation, either downward or upward, of water through overburden or substratum should be analyzed for chemical composition to make certain that harmful materials have not damaged the aggregate for concrete purposes. Table 1 shows the chemical analyses of pumice from several sources currently being used for concrete aggregates. Pumice that has become contaminated will usually show large increases in the CaO, MgO, loss on ignition, solubility in water, solubility in 5 percent H_2SO_4, and a decrease in silica content.

Capillary action

For some time builders have known that pumice concrete has remarkable resistance to the passage of water from a bedding plane into the concrete by capillary action. In a recent test a sawed cube of 2500 psi pumice concrete was placed on a water-saturated material and the water gain into the concrete measured. The gain in weight of a room-dry sample was 0.0083 lb per sq in. of contact area after reaching stable conditions of maximum saturation by capillary action.

Sound absorption

Sound absorption of pumice concrete is high and buildings fabricated with

TABLE 1—CHEMICAL ANALYSIS OF SEVERAL SOURCES OF PUMICE AGGREGATE*

	Cochiti, N. M.	Guaje, N. M.	Typical Calif.	Santa Clara, N. M.	Southern Calif.	Deschutes, Ore.	Los Alamos, N. M.
SiO_2	70.28	74.32	71.04	71.67	68.66	73.49	73.77
Al_2O_3	13.54	11.28	14.22	12.64	14.94	16.39	12.67
TiO_2	0.26	0.02	0.34	Trace			0.05
Fe_2O_3	2.06	1.58	0.90	2.30	2.00	1.22	1.29
Mn_3O_4	0.30			Trace			0.28
CaO	1.96	0.10	1.87	0.60	4.26	1.08	1.19
MgO	0.88	0.29	0.61	0.70	2.91	0.01	0.10
K_2O	3.33	3.30	3.33	8.00		2.10	3.67
Na_2O	4.14	4.23				2.84	4.06
5% H_2SO_4 sol.							1.21
Water sol.					0.004		0.44
Ignition loss	3.73	4.73	1.81	4.46	3.50	2.23	3.38

*Sources of analysis:
Cochiti: Pittsburgh Testing Laboratory, No. 7812
Guaje: Pittsburgh Testing Laboratory, No. 403098
Typical California: California Division of Mines
Santa Clara: *Bulletin* 28, New Mexico Bureau of Mines & Mineral Resources
Southern California: Smith-Emery Co., No. P-159771
Deschutes: Northwest Testing Laboratories, No. 8116B
Los Alamos: *Publications in Engineering* No. 5, University of New Mexico

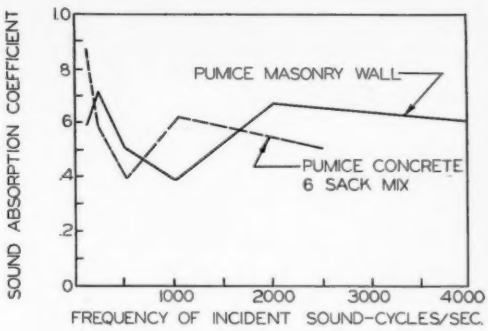

Fig. 1—Sound absorption for pumice concrete* and pumice masonry units†

*Pittsburgh Testing Laboratories, No. 372401.
†Riverbank Acoustical Laboratory, No. A-49-120.

pumice concrete or with pumice masonry units absorb more sound and are acoustically better than buildings constructed with conventional types of structural concrete aggregate. Data regarding the sound absorption of 8x8 x16 in., three core, pumice masonry units indicate that pumice units have a high coefficient of sound absorption. Sound absorption tests on a six-sack pumice concrete and pumice masonry units are plotted in Fig. 1.

The transmission loss of pumice masonry walls has also been determined (Table 2). The test wall consisted of 8 x 8 x 16 in. units laid up with tooled joints. The side of the wall exposed to the sound was unpainted and unplastered while the opposite side was plastered with 1 in. thick gypsum plaster. The wall weight was approximately 32.5 lb per sq ft of wall surface.

Fire resistance

In a fire test on 4 in. thick pumice concrete panels (ASTM Specification E 119-47, Fire Tests of Building Construction and Materials), the panels, 26½ x 45 in. and 26½ x 90 in., easily passed the fire endurance test and hose stream test for 4 hours. Maximum temperatures on the unexposed side of the test panels at the end of 4 hours was 142.5 F (Fig. 2) and the condition of acceptance permits a temperature rise of 250 F on the unexposed surface.

Masonry units made from pumice concrete will withstand more heat and fire for a stated time than other lightweight or sand and gravel load bearing masonry concrete units. An 8-in. masonry wall, interior or exterior, load bearing or nonload bearing, with noncombustible structural members, is

TABLE 2—TRANSMISSION LOSS OF MASONRY WALL*
8 x 8 x 16 in. pumice concrete units

Frequency range, cycles per sec.	Transmission loss, decibels
137 – 258 (7 frequencies)	37.7
290 – 517 (6 frequencies)	39.3
580 – 1034 (6 frequencies)	44.7
1161 – 2070 (6 frequencies)	50.2
Average (25 frequencies)	42.7

*Riverbank Acoustical Laboratory, No. TR 49-21.

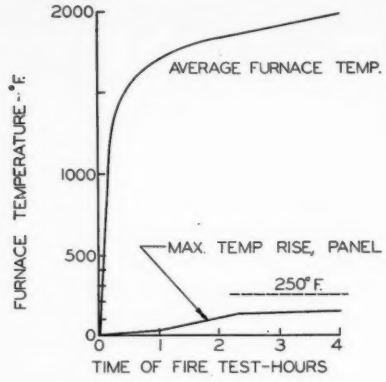

Fig. 2—Temperature data for fire tests on 4 in. thick, reinforced, pumice panel*

*Protexol Testing Laboratory, No. 192.

rated by the Underwriters Laboratories, Inc.,* as a Class B-4 retardant for a 4-hour fire rating. The average face shell thickness for this masonry unit must not be less than 1⅜ in. with a minimum thickness of 1¼ in.; the web thickness is specified at not less than 1 in.

Insulation

Test results on thermal insulation characteristics of pumice aggregates and pumice concrete have not always been in agreement as is usually the case in thermal conductivity determinations. Fig. 3 plots data from four sources and an "average" curve drawn from this data. It is suggested that the variation of thermal conductivity of pumice aggregate which weighs less than 45 lb per cu ft is caused by circulation of air from the two faces of the test material. A proper gradation, from coarse to fines, would undoubtedly preclude such thermal losses. Tests conducted at the University of New Mexico for the Atomic Energy Commission show that pumice aggregate in + 8 to − 4 gradation, weighing 31.0 lb per cu ft gives a thermal conductivity, k, of 0.438 BTU per sq ft per hour per degree F and will satisfactorily provide for space fill insulation such as in cores of masonry units.

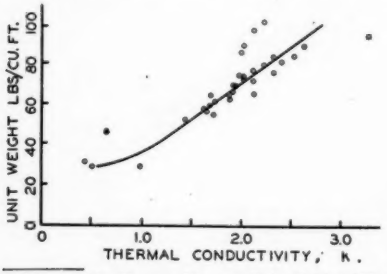

Fig. 3—Thermal conductivity of pumice aggregate and concrete

*Standard for Concrete Masonry Units, Subject 618, Third Edition, July 1949 (Pumice masonry wall tested by Retardant 2861).

Other physical properties

Pumice and pumice concrete have pyrometric cone equivalent values of cone 10 (2300 F—1260 C) for pumice aggregate and cone 5 (2156 F—1180 C) for a 1:4 mix by volume for Lumnite cement and pumice aggregate. The tests were made on an aggregate having a bulk density of 47.4 lb per cu ft and 11.25 gal. of water per sack of Lumnite cement were used. The cold strength at 24 hours was 2362 psi in compression and reduced to 817 psi and 225 psi for 4 days of firing at 1400 F and 1800 F respectively. The concrete bulk density after drying at 230 F was 77.1 lb per cu ft and became 70.9 and 69.2 after firing at 1400 F and 1800 F.

Further data on pumice aggregate and concrete is shown in Table 3.

TABLE 3—PHYSICAL PROPERTIES OF PUMICE*

Gradation	Wt. bone dry, lb per cu ft	Wt. saturated surface dry, lb per cu ft	Absorption, percent dry wt.	Specific gravity, saturated surface dry
Fine	38	46.5	21.5	1.38
Blend	33	44.0	33.4	1.35
Coarse	22	31.0	39.0	1.29

Strength								
Compressive, psi	1366	1805	1972	2038	2092	2170	2172	2492
Shear, psi	118	—	288	162	309	—	309	—
ACI allowable, 0.02 f_c, psi	27	—	40	39	42	—	43	—
Bond, psi	316	414	—	—	—	—	—	635
ACI allowable 0.05 f_c, psi	60	90	—	—	—	—	—	125
Tensile, psi	262	—	356	283	351	325	—	285

Compressive strength vs. modulus of rupture										
Compressive, psi	903	1270	1618	1768	1938	2066	2115	2230	2625	2718
Modulus of rupture, psi	216	290	276	344	370	382	350	433	377	502

*Data by William C. Wagner, Materials Engineer, University of New Mexico.

DESIGNING FOR STRENGTH

Pumice lightweight aggregates should be procured from reliable sources and from producers that can furnish design data for the particular gradations sold. There is considerable variation in strength-cement ratio and weight-strength ratio of the several aggregates now sold. Major producers will provide technical data and mix designs that should be carefully followed until experience indicates that local conditions will warrant a change. Typical design charts issued by producers are illustrated by Tables 4, 5 and 6. The engineer is usually interested in the strength that may be obtained for a given cement factor or in the strength of the concrete for a given concrete weight. Fig. 4 and 5 show these relations for three pumice aggregates. The information given in these curves is taken from published data by aggregate pro-

ducers. It will be noted that there is considerable variation in compressive strength-cement ratio of the several aggregates and perhaps much of the variation could be explained by different gradations furnished by the separate producers. Gradation will be a determining factor in the ultimate strengths obtained and must be held constant once a given mix is selected.

TABLE 4—DESIGN DATA ON PUMICE CONCRETE*

Compressive strength, psi	Wt., lb per cu ft		Steel	Structural design data					
	Wet	Dry		f_c	n	K	k	j	p
250	73.0	53.0		113	81.1	18	0.364	0.879	0.0013
500	74.5	54.5		125	54.1	42	0.432	0.856	0.0030
1000	77.5	57.5	$f_s = 16{,}000$	450	38.7	97	0.521	0.826	0.0073
1500	80.5	60.5		675	30.9	255	0.566	0.811	0.0119
2000	83.6	63.6	$a = 1.333j$	900	25.8	214	0.592	0.803	0.0167
2500	87.0	67.0		1125	22.1	273	0.608	0.797	0.0214
3000	92.0	72.0		1350	19.4	332	0.621	0.793	0.0262
1000	77.5	57.5		450	38.7	93	0.492	0.836	0.0062
1500	80.5	60.5		675	30.9	149	0.537	0.821	0.0101
2000	83.6	63.6	$f_s = 18{,}000$	900	25.8	206	0.563	0.812	0.0141
2500	87.0	67.0	$a = 1.500j$	1125	22.1	263	0.580	0.807	0.0181
3000	92.0	72.0		1350	19.4	321	0.593	0.802	0.0222
1000	77.5	57.5		450	38.7	88	0.465	0.845	0.0052
1500	80.5	60.5	$f_s = 20{,}000$	675	30.9	143	0.511	0.830	0.0086
2000	83.6	63.6	$a = 1.667j$	900	25.8	198	0.537	0.821	0.0121
2500	87.0	67.0		1125	22.1	254	0.554	0.815	0.0156
3000	92.0	72.0		1350	19.4	310	0.567	0.811	0.0191
1000	77.5	57.5		450	38.7	85	0.442	0.853	0.0045
1500	80.5	60.5	$f_s = 22{,}000$	675	30.9	138	0.487	0.838	0.0075
2000	83.6	63.6	$a = 1.833j$	900	25.8	192	0.514	0.829	0.0105
2500	87.0	67.0		1125	22.1	246	0.531	0.823	0.0136
3000	92.0	72.0		1350	19.4	300	0.543	0.819	0.0167
1000	77.5	57.5		450	38.7	81	0.421	0.860	0.0039
1500	80.5	60.5	$f_s = 24{,}000$	675	30.9	133	0.465	0.845	0.0065
2000	83.6	63.6	$a = 2.000j$	900	25.8	185	0.492	0.836	0.0092
2500	87.0	67.0		1125	22.1	238	0.509	0.830	0.0119
3000	92.0	72.0		1350	19.4	291	0.522	0.826	0.0147

Formulas used in computing above values:

$n = E_s/E_c = 30{,}000{,}000/E_c$. $\quad f = 0.45f_c$ $\quad k = \dfrac{1}{1 / (f_s/nf_c)}$

$j = 1 - (1/3)k \quad p\dagger = (f/2f_s)k \quad K = (f_c/2)kj$

$a = (f_s/12{,}000)$ (average j-value) for use in $A_s = M/ad$ or $A_s = NE/adj$

*Data by William C. Wagner, Materials Engineer, University of New Mexico.
†"Balanced steel ratio" applies to problems involving bending only.

TABLE 5—MIX DESIGN DATA FOR PUMICE CONCRETE*

Comp. strength, psi	Design weight, lb per cu ft	Pumice per cu yd yield						Cement		Water				Recommended slump, in.
		Fine, dry		Coarse, dry		Blend, dry		Sacks per cu yd	Lb per cu yd	to saturate		to mix		
		lb	cu ft	lb	cu ft	lb	cu ft			gal.	lb	gal.	lb	
150	40	0	0	792	36	0	0	4	376	36.1	300	—	—	0
250	46	914	24	264	12	1180	36	3	382	34.8	290	—	—	0
500	55	914	24	264	12	1180	36	4	376	34.8	290	—	—	0
1000	60	914	24	264	12	1180	36	5	470	34.8	290	50	417	½
1500	65	914	24	264	12	1180	36	6.5	611	34.8	290	52	433	½
2000	70	914	24	264	12	1180	36	7.5	705	34.8	290	53	442	1
2500	75	914	24	264	12	1180	36	8	752	34.8	290	48	400	2

*Data by William C. Wagner, Materials Engineer, University of New Mexico.

TABLE 6—TECHNICAL DATA AND MIX DESIGN*

Ingredients	Mix designation			
	A	B	C	D
Pumice, ⅛-in. to pan, lb	972	520	432	—
Pumice, ⅛ to ¼-in, lb	383	420	486	410
Pumice, ¼ to ⅜-in, lb	130	280	205	140
Columbia sand, F.M. 3.10, lb	0	600	745	1440
Portland cement, lb	634	660	726	720
Water, gal.	46	55	53	50
Physical properties				
Compressive strength: 7-day, psi	1240	1470	1770	2400
28-day, psi	1900	2220	2630	3170
Modulus of rupture, psi	330	325	400	440
Modulus of elasticity, 1×10^6, psi	1.135	1.414	2.021	1.984
Shear, psi	380	460	480	515
Bond, vert. steel area, sq. in.	385	425	500	585
Bond, horiz., steel area, sq in.	255	385	400	555
Weight per cu ft saturated, lb	84	93	100	108
Weight per cu ft dry, lb	75	82	88	96

All elements of this data are for 28-day strength concrete unless otherwise stated.

*Source: Deschutes, Ore. Data by Pittsburgh Testing Laboratories, 29385.2.

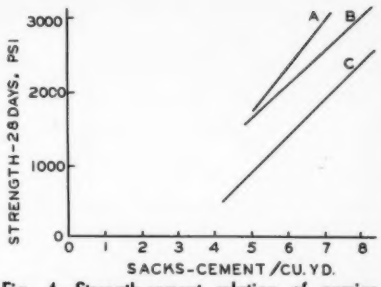

Fig. 4—Strength-cement relation of pumice concretes

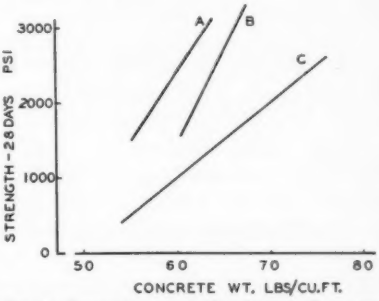

Fig. 5—Strength-unit weight relation of pumice concretes

PRESATURATION

Most aggregate producers recommend presaturation of aggregate before or during mixing and before the addition of cement. In an aggregate consisting of fine ($-\frac{1}{4}$) and coarse ($+\frac{3}{8}$) pumice the specific gravity of the particle sizes will vary over a considerable range as is shown in Fig. 6*, and it is quite likely that separation, floating of the larger sizes, may occur in wet mixes with slump in excess of 3 or 4 in. This separation will not appear in the dry mixes used in making concrete masonry products. Many ready-mixed plants produce a slurry of the total water and cement and then charge the mixer with pumice aggregates. A deficiency of water in the mix may produce balling but additional water and continued mixing will usually correct this undesirable condition. The determination and use of correct total water for the first batch will preclude balling in subsequent batches. Many times a batch will be correct at the plant and upon arrival at the job site will be found to have balled en route. This happens when the aggregates are relatively dry and too little water is used in the mix. The obvious remedy is addition of water to the mix to overcome a water deficiency caused by the absorbing action of the aggregate during transportation.

*Wagner, Walter K., *Rock Products*, Sept. 1948.

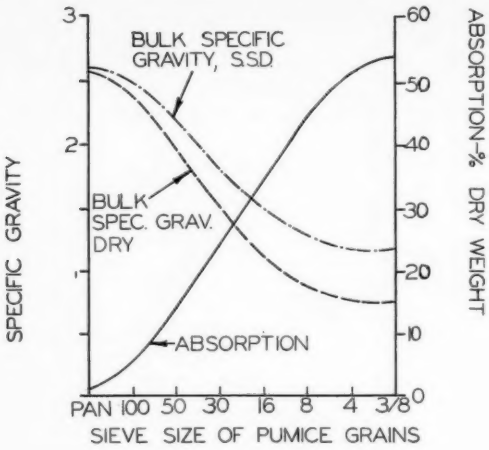

Fig. 6—Relation of the pumice grain size to specific gravity and absorption for a typical commercial grade

Some believe that concrete produced by charging the aggregates into the water-cement slurry will produce stronger concrete because the cement will occlude the minute interstices of the aggregate and permit the cement to be effective in producing higher strengths with a given cement factor. No reliable data are available to support or condemn this contention. Many plants, especially those producing concrete masonry products, have attempted to presaturate aggregates in storage bins or during unloading of railcars. These efforts to achieve uniform saturation have usually been ineffective because of the channeling of the water when played on the aggregate and in the end the aggregate absorption varied by strata from an "as-shipped" condition to 100 percent absorption.

APPLICATION TRENDS

Tilt-up construction

Pumice lightweight concrete is finding ready acceptance in tilt-up building construction. Low unit weight, ease of placing and low thermal conductivity are important factors to the architect and the engineer in the selection of concrete aggregate.

The low unit weight of pumice concrete, usually less than 70 lb per cu ft, permits fabrication of tilt-up panels at any point on the existing floor slab since they are readily lifted and moved to their wall location by a truck-mounted hoisting rig. External bracing during erection also is reduced by the low unit weight and additional savings are made by nailing the wood or steel bracing directly into the pumice concrete panels until the columns are placed and stripped. Pumice concrete walls need no additional insulation except in the north. Furring is thus eliminated with a resulting reduction of cost.

Precast homes

Factory precast panel construction for homes has received considerable attention for the past four or five years. Normac, Inc., has constructed hundreds of precast panel homes in California, Arizona, New Mexico and South America. Several hundred pumice concrete residences were built for the United States Navy during and since the last war. Within the past year, Normac, Inc., completed a housing project for the Atomic Energy Commission at Albuquerque, N. M., consisting of approximately 200 homes where New Mexico pumice was used for the concrete aggregate. An 800-unit military housing project at Biggs Air Force Base, El Paso, Texas, is now under construction and uses New Mexico pumice.

Twenty experimental homes have recently been completed by Wilson Homes, Inc., Wichita Falls, Texas. This company, now ready to enter the mass production field, has developed a factory-made home. The floor, roof and wall panels are transported from factory to erection site on semi-trailers. Pumice concrete is used in all parts of the home with the exception of the foundation. Pumice concrete applied with spray equipment provides grout between the wall sections as well as the interior and exterior finish. All panels are welded together before the spray finish is applied. These homes employ a production line floor slab and cottage type pumice concrete roof, which adds to the architectural design and gains favor where flat roof decks are not readily accepted. Additional insulation is not required because of the low thermal conductivity of the concrete. The coefficient of heat transmission, U, for the pumice concrete used in these homes is 0.25 BTU per hour per sq ft per degree F for a 6-in. wall section exclusive of internal or external finishes ($k = 1.86$ for 6-sack mix).

Masonry units

Pumice masonry units of commercially accepted quality have been manufactured on all types of block-making machines. However, as a general rule, the highest quality masonry units are produced on those machines that vibrate and compact the concrete. Tamping machines have been used with success but a highly skilled operator is necessary to produce a consistent product. The density of the masonry unit should be kept as high as possible to increase compressive strength with a given cement ratio and to decrease absorption of the block when exposed to the elements. Heavy mass production block-making machinery will produce a 3-core, 8 x 8 x 16 in. block that will weigh about 20 to 22 lb, yard dry, and it will have an absorption value within the ASTM specification. Many plants with small and light frame block-making machines add natural sand to the mix to obtain a heavier concrete that will properly fill the mold box.

Floor slabs

The fact that pumice concrete can be nailed and sawed is being used to

advantage in many places by nailing hardwood flooring directly to pumice concrete floor slabs. The slab is given the usual finish and an asphalt primer is then applied to the floor slab as a vapor seal. The hardwood floors are nailed directly into the floor slab. This eliminates the necessity of wood strips or sleepers and provides a flat even base for the wood flooring and tends to decrease the "creak" often found in wood floors.

The ever-increasing use of insulating materials under concrete floor slabs has caused engineers to search for a cheap, low weight, nondeteriorating material for under-the-slab insulation. Pumice aggregate is being used for this purpose. Aggregate, when hand consolidated for under-the-slab insulation, has a thermal conductivity of between 0.50 and 1.00 BTU per hour per sq ft per degree F. The aggregate may be lightly bound together on the upper surface with portland cement and fine pumice mix or slurry to provide a working base for the insulating slab. Pumice concrete should never be placed between radiant heating pipes and the space to be heated.

Other uses

The Far Eastern Branch, Office of International Trade, reports that pumice concrete from the Niijima region of Japan is used as linings for Glover and Gay-Lussac sulfuric acid manufacturing towers. The Japanese have used pumice concrete in the insulation of boilers, pipes, bathtubs, heat treatment rooms and cold storage rooms as well as for sound absorption in theaters, auditoriums, radio stations and for underground passageways.

Pumice concrete is ideally suited for use where high temperatures are involved and has been used to cover existing concrete walls in steel mill slag pits where the molten slags are poured against concrete retaining walls. Field reports indicate that the shell of pumice concrete on existing walls gives promise of much longer life than that of sand and gravel concretes which spall off easily. The pumice concrete was applied by the "Gunite" process and Lumnite cement was used to provide a rapid hardening of the concrete with no loss of plant operational time.

SUMMARY

Although pumice concrete has been used since ancient times, new uses are constantly being found in modern engineering. As architects, engineers and technicians become more familiar with the chemical and physical characteristics of pumice its use will be more wide-spread. Drying shrinkage of pumice concrete, and other lightweight aggregate concretes, is greater than that of heavy aggregates and still is a major problem. Progress is being made as the masonry industry learns more about manufacture of lightweight concrete products, but it may be some time before field tests of new methods and practical research will supply sufficient data for complete evaluation. Pumice concrete has advanced sufficiently for engineers to use it with confidence but more laboratory studies are necessary to exploit its full potentialities.

REFERENCES

1. Schmidt, F. Sommer, "Pumice as a Lightweight Aggregate," paper presented Oct. 20, 1947, at meeting of American Institute of Mining and Metallurgical Engineers, Los Angeles.

2. Wagner, Walter K., "Design and Control of Pumice Mixes," *Concrete Products*, V. 46, No. 9, Sept. 1948, pp. 125-7.

3. "The Story of Pumice," a series of articles in *Concrete:*
Part 1, "Mining, Processing, Grading," John W. Shaver, Aug. 1948, p. 3.
Part 2, "Precasting House Panels," A. V. Roemisch, Aug. 1948, p. 10.
Part 3, "Ready-Mixed Pumice," Walter K. Wagner, Sept. 1948, p. 22.
Part 4, "Monolithic Concrete Hospital at Altus, Okla.," Oct. 1948, p. 8.
Part 5, "Progress to Date on Structural Design," Jack Edwin Counts, Nov. 1948, p. 20.
Part 6, "Manufacture and Tests of Concrete Masonry Units," Dec. 1948, p. 3.

4. Niederhoff, A. E. "History of Pumice Concrete in California," *Proceedings*, ASCE, V. 75, June 1949, pp. 743-57.

5. Mathews, H. L. "Prefabricated Pumice Concrete Houses," ACI JOURNAL, May 1948, *Proc.* V. 44, p. 797.

6. Pierce, Jack, "Pumice—A New Mexico Industry," paper presented Oct. 26, 1948, at regional meeting, American Institute of Mining and Metallurgical Engineers, El Paso, Texas.

7. Niederhoff, A. E. "Machine-Built Desert Homes," *California Western Construction News*, Sept. 1947, p. 89.

Probable clues to why steam curing makes concrete products stronger

Hydration Products Formed in Cement Pastes at 25 to 175 C*

By GEORGE L. KALOUSEK† and MILTON ADAMS‡

SYNOPSIS

Research described indicates the chemical nature of a new potential hydration product of cements responsible for the high strength of steam cured cement products. Differential thermal analysis was used in studying hydration products of cement and related solids at temperatures between 25 and 175 C. Additions to the cement included gypsum and finely ground quartz. The trisulfate form of calcium sulfoaluminate and presumably the analogous sulfoferrate were found as the initial R_2O_3-bearing hydrates at temperatures between 25 and 100 C, but these transformed to the related solid solution of the SO_3-bearing solids. The latter then converted to phase X. At 100 C these consecutive reactions appeared to be complete in 3 to 4 hours, and increasingly longer time was required for completion as the temperature was lowered. The solid solution formed in greater abundance at about 70 to 100 C than at lower temperatures.

The hydrogarnets were not found in any sample of cement hydrated at temperatures between 25 and 175 C. Samples of pure $4CaO \cdot Al_2O_3 \cdot Fe_2O_3$ converted initially to hydrogarnets in the presence of water, but with periodic regrinding of the solids it was found that in the interval between about 3 and 6 months the initial product was transformed completely into $4CaO \cdot Al_2O_3 \cdot 13H_2O$, which probably contained some integrally bound Fe_2O_3, and a gel.

Experimentation on the synthesis of phase X indicated that this solid may be a gel consisting of all the oxide constituents of cement. Lime, silica and ferric oxide are required constituents for the formation of this phase.

Ground silica added to the cement in an amount of about 8 to 10 percent appeared to combine with all the hydrolytic $Ca(OH)_2$ at 175 C, the reaction product being the crystalline dicalcium silicate hydrate discovered by Thorvaldson and Shelton. The total amount of this phase was estimated to be about one-third to one-half of the reaction products. Further additions of silica reacted in turn with this compound and at about 40 to 45 percent addition the new product of reaction approached in composition a $CaO:SiO_2$ molar ratio of about 1.0 and is characterized in thermal analysis by a pronounced exothermic peak at 840 ± 5 C.

INTRODUCTION

Results obtained recently by differential thermal analysis[1] suggested that

*Received by the Institute Feb. 5, 1951, Title No. 48-7 is a part of copyrighted JOURNAL OF THE AMERICAN CONCRETE INSTITUTE, V. 23, No. 1, Sept. 1951, *Proceedings* V. 48. Separate prints are available at 50 cents each. **Discussion** (copies in **triplicate**) should reach the Institute not later than Jan. 1, 1952. Address 18263 W. McNichols Rd., Detroit 19, Mich.

†Member American Concrete Institute, Lecturer in Chemistry, Dept. of Chemistry, Univ. of Toledo, Toledo, Ohio.
‡Fellow in Silicate Chemistry, Dept. of Chemistry, Univ. of Toledo, Toledo, Ohio.

hydrated cements contain a previously unidentified solid (designated phase X). Results of attempts to synthesize phase X at room temperature indicated that prolonged processing would be required. To accelerate the reactions involved, various mixtures pertaining to this and other phases were processed at 25 to 175 C, in saturated water vapor, and examined for the hydrous solids that formed.

Attention was directed primarily towards elucidating the manner in which Al_2O_3 and Fe_2O_3 combine in hydrating cements. Although it has generally been believed that the R_2O_3-bearing products are crystalline, more recently Powers and Brownyard[2] presented several observations in studies of surface characteristics of hardened cement pastes indicating that these products may occur as gels. Results of thermal analyses[1] have shown that the $3CaO \cdot Al_2O_3 \cdot 6H_2O$, one of the potential products of cement and water, did not form in hydrating cements. That study also indicated that calcium sulfoaluminates and probably the analogous sulfoferrates may appear only as metastable phases in hardening cement pastes, the transformation product being phase X.

Lafuma and Brocard[3] reported that $3CaO \cdot Al_2O_3 \cdot 3CaSO_4 \cdot 31H_2O$ transformed to $3CaO \cdot Al_2O_3 \cdot CaSO_4 \cdot 12H_2O$ and gypsum at about 60 to 70 C, and to $3CaO \cdot Al_2O_3 \cdot 6H_2O$ and gypsum in an autoclave at 140 C. Most of the published reports on the Al_2O_3-bearing hydrates state that $3CaO \cdot Al_2O_3 \cdot 6H_2O$ is stabilized at elevated temperatures. The solid solution of the hydrogarnets of which $3CaO \cdot Al_2O_3 \cdot 6H_2O$ is an end member, was synthesized by Flint, McMurdie and Wells[4] and suggested as stable hydrates in steam cured concrete.[5] These solids were prepared and their potential occurrence in cements hydrated at different temperatures was studied.

High pressure steam curing enhances certain properties, especially strength, of cement products, but only if ground silica is present. Menzel[6] has demonstrated that improvements were most marked for products made of definite composition of cement and finely ground silica. Possible correlations between the kinds of reaction products and amounts of added silica were accordingly studied by the present method.

MATERIALS AND METHODS

A Type I portland cement* in a water to cement, or water to cement plus additions, ratio (w/s) of 0.7 by weight was used in the preparation of all cement pastes. The mixtures for test at room temperature were stored in tightly stoppered glass vials, one of which was broken at each period of test and the lumps, free of adhering glass, prepared for test. The samples processed at 40 to 175 C were contained in small stainless steel autoclaves previously described[3] and heated at any desired temperature ($\pm$ 1 C) in a laboratory oven.

The cement and silica (ground quartz passing a No. 200 sieve and containing 99.7 percent silica) mixtures were prepared by replacing cement by the silica in small increments over the range of 2 to 60 percent replacement. The dry materials were thoroughly mixed first and then with water and the pastes were autoclaved at 175 C.

The samples of cement with additions of gypsum were prepared in the manner described. The conditions of processing will be given along with the results.

*This cement is No. 15 described by Lerch and Ford.[7] It was selected for its low MgO and relatively high Al_2O_3 to avoid interference from $Mg(OH)_2$ in thermal analysis, and so that the Al_2O_3-bearing products of this constituent would be present in relatively greater abundance and therefore more easily detected in thermal analysis curves.

The hydrogarnets were prepared by slowly adding dilute solutions of mixtures of $AlCl_3$ and $FeCl_3$ having the alumina and iron in Al_2O_3 to Fe_2O_3 molar ratios of 3:0, 3:1, 2:1, 1:1, 1:2, 1:3, and 0:3 to a boiling solution of $Ca(OH)_2$ in a glass flask according to the method described by Flint, McMurdie and Wells.[4] These samples were not analyzed chemically but considering the range of Al_2O_3/Fe_2O_3 ratios and variations in the refractive index [5] it is believed that they represented a wide difference of compositions in the series. Other related products were obtained at room temperature from mixtures of $4CaO \cdot Al_2O_3 \cdot Fe_2O_3$ with or without added gypsum in a water to solids ratio of 0.7, at 7, 28, 60, 90 and 180 days. To accelerate reactions, the entire sample was crushed thoroughly at 7 days and then washed and dried by the procedure to be described. A portion of this dried sample was withdrawn for the required tests and the remainder was again mixed with water and set aside to react. The same procedure of crushing and drying the sample was repeated at the other ages of test.

The calcium sulfoaluminates, the trisulfate form ($3CaO \cdot Al_2O_3 \cdot 3CaSO_4 \cdot 31H_2O$) and the solid solution ($3CaO \cdot Al_2O_3 \cdot CaSO_4 \cdot 12H_2O$—$3CaO \cdot Al_2O_3 \cdot Ca(OH)_2 \cdot 12H_2O$) were prepared according to the procedure described previously.[1] Details of the method of preparing pure $3CaO \cdot Fe_2O_3 \cdot CaSO_4 \cdot 12H_2O$ by slowly adding iron alum to a solution of $Ca(OH)_2$ were reported by Adams.[9]

Attempts to prepare phase X included the processing at room temperature of mixture of $Ca(OH)_2$, silicic acid, $4CaO \cdot Al_2O_3 \cdot Fe_2O_3$, with and without added gypsum. The mixtures to be discussed had molar ratios of 1.75 CaO/SiO_2, 0.25 $(4CaO \cdot Al_2O_3 \cdot Fe_2O_3)/CaO + SiO_2$, and 0.5 or 0.0 SO_3/R_2O_3. These products were also reground at each age of test.

All solids after processing were ground finely in a mortar, placed on a sintered glass filter funnel connected to a water pump and washed three to four times with acetone and then three to four times with ethyl ether. After the final washing, the sample was placed in a receptable connected to a vacuum pump and maintained at a pressure of 0.1 mm or less for 1 hour, the pump operating continuously.

As required, the samples were analyzed chemically, following standard procedures. The analysis included the determination of the insoluble residue (quartz) in the cement-silica sample.

Differential thermal analysis [1] served as the primary means of identifying the solids. All samples were analyzed thermally and many were also examined with a petrographic microscope.

The thermal curves of the pure samples of known identity were compared to those of the cements and other products of interest. The curves consist of bulges and peaks at definite temperatures that characterize different phases and attention will be directed to these as they served to identify the phases in the mixtures.

RESULTS

Sulfur trioxide-bearing products

Study of the temperature stability of SO_3-bearing products was largely concerned with the transformations of calcium sulfoaluminates as they occurred in cement pastes hydrated at 25, 50, 60, 70, 80, 90, 100 and 105 C. The pure $3CaO \cdot Al_2O_3 \cdot 3CaSO_4 \cdot 31H_2O$, placed in water in a closed system, did not decompose in 3-day tests at temperatures below 100 C. Between 100 and 105 C this compound broke down into $3CaO \cdot Al_2O_3 \cdot CaSO_4 \cdot 12H_2O$ and gypsum, and between 130 and 140 C into $3CaO \cdot Al_2O_3 \cdot 6H_2O$ and gypsum. Addition of lime and silicic acid in parallel experiments caused transformations at lower temperature and probably also formation of products other than those just mentioned. It appeared possible that the temperature stability of sulfoaluminates in hydrating cements would be similarly effected

as noted for those in the mixtures and for this reason detailed study on the pure salts was not pursued further.

The thermal analysis curves illustrating most closely the presence of the phases of interest for cement pastes hydrated at 25, 50, 80 and 100 C are presented in Fig. 1. A series of curves showing more comprehensively the transformations at one temperature (25 C) have been reported previously (Fig. 7, of reference 1), and the present results were similar to them. At 25 C the trisulfate was present in largest amount at 14 hours as shown by the extent of the endothermic bulge at 150 C in Fig. 1. This bulge is characteristic of the trisulfate form of the calcium sulfoaluminate and probably also of the analogous Fe_2O_3-bearing product.[9] The 24-hour sample gave a thermal curve containing a relatively small bulge at 150 C and a large bulge at 130-140 C which is associated with phase X. At 28 days the product showed a still larger bulge at 130-140 C and a small bulge at 220. This latter thermal change characterizes the solid solution of the sulfoaluminates ($3CaO \cdot Al_2O_3 \cdot CaSO_4 \cdot 12H_2O$ — $3CaO \cdot Al_2O_3 \cdot Ca(OH)_2 \cdot 12H_2O$) and of the analogous Fe_2O_3-bearing products.[9]

Increasing the temperature to 50 C caused formation of the maximum amount of the trisulfate between about 3 and 4 hours, the 4-hour curve is included in Fig. 1. Comparison of curves obtained on cements hydrated at 25 and 50 C indicates that amounts of the trisulfate were roughly the same in the 14-hour and 3.5- to 4-hour samples, respectively, at the stated temperatures. This suggests that the hydration reaction is about four times faster at 50 C than at 25 C. Also the amount of solid solution formed in 14 hours was about the same as that obtained in a corresponding sample hydrated at 25 C for three days. Prolonging the induration to 24 hours at 50 C resulted in complete transformation of the solid solution to phase X.

Processing at 80 C produced a further marked increase in rate of reaction. The curve for the 2-hour sample showed comparatively large amounts of both forms of the sulfoaluminates, and at 16 hours, or somewhat less, the transformation of the solid solution to phase X was complete. The bulge at 130-140 C representing phase X was smaller than at the lower temperatures for a comparable degree of transformation of the solid solution to phase X.

At 100 C, the trisulfate was found in relatively small amount in the half-hour sample. As shown by the large bulge at 220 C in Fig. 1, the 2-hour product contained a comparatively large amount of the solid solution, larger than observed for any other sample of hydrated cement at any temperature. However, the solid solution transformed rapidly at this temperature, its presence being undetected in a 4-hour sample. The transformation product, presumably phase X, did not generally show as large a bulge at 100 C as at 80 C.

The decrease in the extent of the 130-140 C bulge at higher temperatures does not necessarily mean that phase X was not formed. If phase X is a gel, and on the basis of findings by Powers and Brownyard[2] it may be assumed to

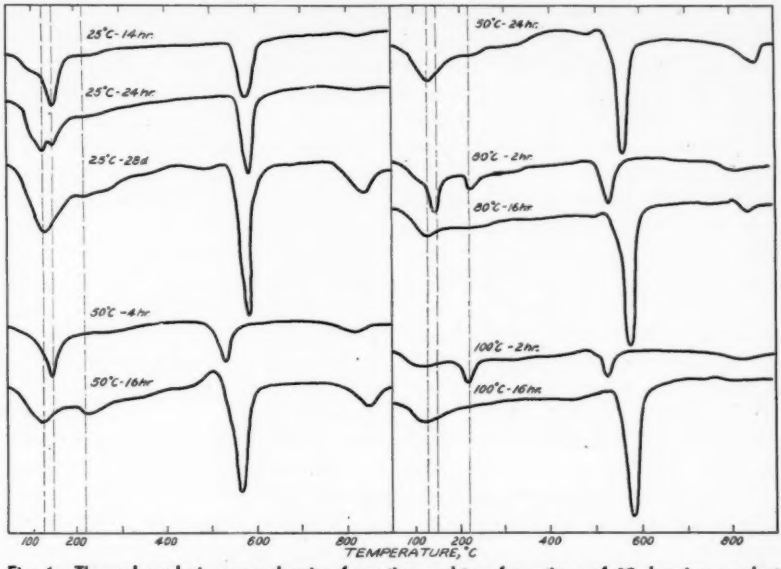

Fig. 1—Thermal analysis curves showing formation and transformations of SO_3-bearing products in hydrating cements at different temperatures

be such a solid, the decrease in the extent of the bulge would not be inconsistent with the known behavior of the gel phase in hydrated cements. This solid when formed at room temperature has a large internal porosity for retaining water, and drying of the water from the minute capillaries would be accompanied by absorption of heat at a temperature higher than required for evaporating water from a plane surface. Increasing the processing temperature may be the cause of a marked increase in the pore size and this could account for the decrease in the extent of the endothermic bulge at 130-140 C. However, in view of this marked alteration in the thermal characteristics it follows that increasing the temperature of the reactions was not helpful in the study on the isolation of phase *X*. Also there is the possibility, of course, that phase *X* is altered chemically at higher temperatures.

The preceding results indicate that the solid solution appears in greater abundance than the trisulfate at temperatures of about 70 to 100 C during the earlier periods of hydration. This observation substantiates that of Lafuma and Brocard.[3] The present results, however, indicate that the solid solution does not appear as a transformation product of the trisulfate at some fixed temperature, but is formed at all temperatures used in these tests. Increasing the temperature increases the rate of the reactions involving the SO_3-bearing products. In general, in all tests, except those with additions of excess gypsum, the sulfoaluminates and presumably the sulfoferrates form and transform in the following sequence,

trisulfate ⟶ solid solution ⟶ phase X.

The interesting formation and transformation of the sulfoaluminates appeared to merit further consideration particularly with respect to the effect the higher amounts of gypsum might have on the reactions. It has been reported[1] that excess gypsum stabilized the trisulfate in hydrating cements at room temperature and it seemed worthwhile to extend these studies to higher temperatures. The range 70 to 100 C, as suggested by the results discussed, is of interest to concrete block technologists and tests were accordingly made over this range. The cement was treated with 2.75, 5.5, 11.0 and 16.5 percent SO_3 as gypsum, these amounts corresponding to SO_3:R_2O_3 molar ratios of 0.5, 1.0, 2.0 and 3.0. Induration was at 175 C for 24 hours. The thermal analyses curves on samples processed at 70 and 100 C are presented in Fig. 2, the broken-line curve representing the sample cured at 100 C. The curves for the 80 and 90 C samples are not given as the bulges of these were intermediate in extent between those at 70 and 100 C. The thermal curves for samples with the 1.9 and 2.75 percent addition showed phase X at 70 C, the transformations having proceeded through the trisulfate and solid solution states at this temperature in 24 hours. With the 5.5 percent SO_3 addition, the samples contained both the trisulfate and solid solution but in decreasing amounts with increasing temperatures. At 100 C as shown by the curve in Fig. 2 the extent of the bulge for phase X was markedly reduced. The sample with 11 percent addition and cured at 70 C gave a curve similar to that with the 5.5 percent addition except that the trisulfate bulge was larger and the shape of the curve suggested that a small amount of gypsum* may have been present. The companion samples processed at 80 and 90 C also contained trisulfate and phase X, but at 100 C the trisulfate was no longer detected and the extent of the bulge for phase X was markedly decreased. The samples with the 16.5 percent addition gave results similar to those with the 11 percent addition except that the product obtained at 100 C contained a phase showing an endothermic bulge at 240-250 C, a temperature somewhat higher than that for the solid solution. The results in Fig. 2 and related results at 80 and 90 C indicate that the trisulfate is stabilized at the higher temperatures by additions of the higher amounts of gypsum, but not at 100 C.

Hydrogarnets

The series of hydrogarnets were prepared so that thermal curves of these solids would be available for comparison with those of hydrated cements. Results of representative samples are presented in Fig. 3. The Fe_2O_3-free sample had the largest endothermic bulge and also the one occurring at the highest temperature, about 380 C, in the series. As the amount of Fe_2O_3

*Relatively small amounts of gypsum in cements hydrated at room temperature show two dehydration bulges, at 150-160 C and 195-205 C. The first bulge appears at the same temperature as that for the trisulfate and hence does not necessarily indicate the presence of gypsum in samples that may contain the trisulfate. The second bulge appears at a slightly lower temperature than that for the solid solution and may indicate the presence of gypsum. However, the presence of small amounts of gypsum cannot be detected with assurance because of the coincidence or near coincidence of the other bulges with those of gypsum and also because of the possibility that gypsum in the presence of cement may undergo dehydration at the stated temperature during processing.

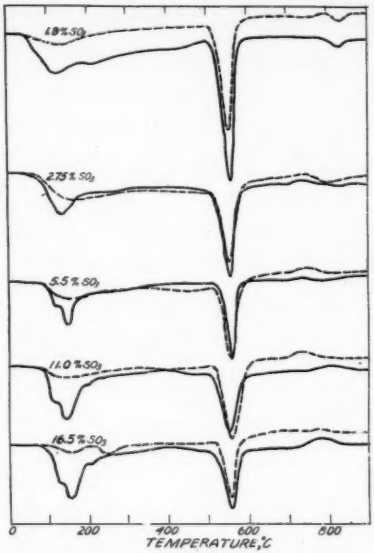

Fig. 2—Thermal analysis curves of cement treated with different amounts of gypsum and processed at 70 C (solid line) and 100 C (dash line)

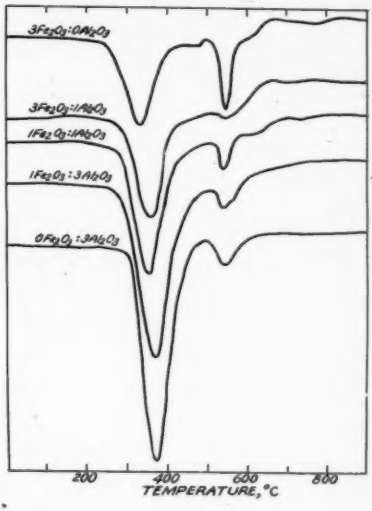

Fig. 3—Thermal analysis curves of hydrogarnets containing Fe_2O_3 and Al_2O_3 in the indicated ratios

was increased, the extent, and also the temperature, of this characteristic bulge was found to decrease and was found at about 330-340 C for the Al_2O_3-free product. Small amounts of these products when present together with hydrated cement or ignited Al_2O_3 show[1] the thermal bulge at a temperature about 20 to 40 C lower than indicated in Fig. 3.

Examination of curves in Fig. 7 (to be discussed in connection with other tests) and many others for cements hydrated at 25 to 175 C failed to show the thermal bulge characteristic of the hydrogarnets. It seems unlikely therefore that the hydrogarnets form in hydrating cements for the stated conditions. It seemed desirable in view of this development and other considerations to ascertain if the products resulting from the prolonged hydration of $4CaO \cdot Al_2O_3 \cdot Fe_2O_3$ at room temperatures would be the hydrogarnets or the related hexagonal crystalline compound. Thermal curves for hydrates of $4CaO \cdot Al_2O_3 \cdot Fe_2O_3$ with and without gypsum (0.7 w/s by weight) obtained at 7, 28, 60, 90 and 180 days are presented in Fig. 4. The 7-day sample without gypsum showed the presence of the hydrogarnets and a small amount of the hexagonal plates of presumably, $4CaO \cdot Al_2O_3 \cdot 13H_2O$. Microscopic examination confirmed the presence of both these solids and also revealed the persistence of cores of unreacted anhydrous solid. With increasing age the hydrogarnets decreased, and the $4CaO \cdot Al_2O_3 \cdot 13H_2O$ or related phase, in-

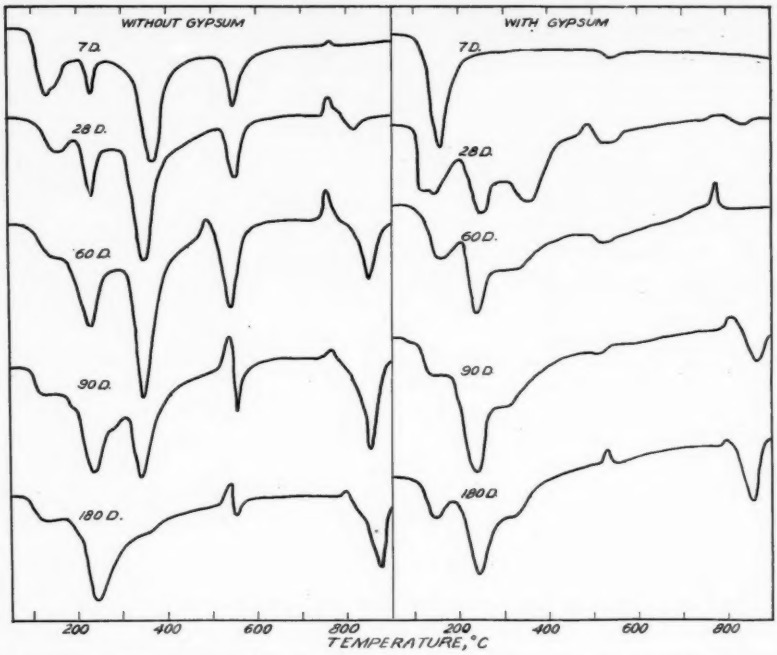

Fig. 4—Thermal analysis curves of $4CaO \cdot Al_2O_3 \cdot Fe_2O_3$ without and with added gypsum ($0.5SO_3/R_2O_3$) processed at 25 C

creased in amount. At 180 days the hydrogarnet was completely transformed to the phase occurring as hexagonal platy crystals which were faintly pleochroic and may have contained some Fe_2O_3, and an isotropic phase presumably a gel containing a substantial portion of Fe_2O_3.

Thermal curves of the corresponding series of gypsum treated samples are also presented in Fig. 4. Comparison of the curves of the two series shows that gypsum altered markedly the course of early reactions. The 7-day product was essentially the trisulfate form of the sulfoaluminate and sulfoferrate of calcium. By 28 days this solid had transformed in part to the solid solutions of the Al_2O_3- and presumably the Fe_2O_3-bearing variety. No member of the hydrogarnet series was detected microscopically although the relatively large bulge at 330 C would suggest its presence. It is possible that this bulge developed to greater extent in the present samples of directly hydrated $4CaO \cdot Al_2O_3 \cdot Fe_2O_3$ than observed previously[1] for products precipitated from aqueous solutions. The sample also contained cores of unreacted $4CaO \cdot Al_2O_3 \cdot Fe_2O_3$, and some Fe_2O_3-bearing gel. The reaction in this series of tests compared to that without added gypsum proceeded much more rapidly. At 90 days the product was essentially a mixture or solid solution of $3CaO \cdot Al_2O_3$

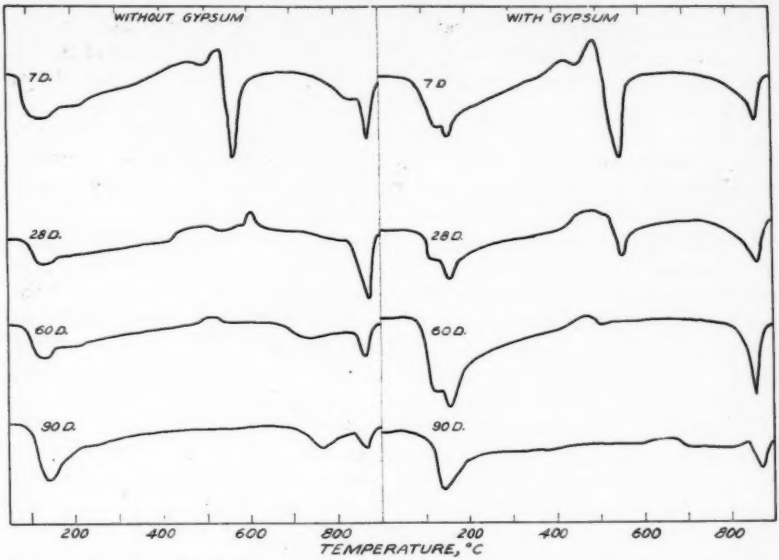

Fig. 5—Thermal analysis curves showing formation of phase X at 25 C from mixtures of CaO, SiO_2 (C/S = 1.75), $4CaO \cdot Al_2O_3 \cdot Fe_2O_3$ ($0.25C_4AF/C+S$) without and with added gypsum ($0.5SO_3/R_2O_3$)

$\cdot CaSO_4 \cdot 12H_2O$—$3CaO \cdot Al_2O_3 \cdot Ca(OH)_2 \cdot 12H_2O$ and presumably $3CaO \cdot Fe_2O_3 \cdot CaSO_4 \cdot 12H_2O$—$3CaO \cdot Fe_2O_3 \cdot Ca(OH)_2 \cdot 12H_2O$. Some slight transformation occurred between 90 and 180 days and a moderate amount of isotropic solid presumably a gel was detected microscopically in the 180-day sample. Attention is directed to the similiarity of the curves for the 180-day samples with and without added gypsum. These two products are probably members of a solid solution.

The preceding results indicate that the hydrogarnets formed from $4CaO \cdot Al_2O_3 \cdot Fe_2O_3$ at room temperature are metastable products. The stable product appears to be the $3CaO \cdot Al_2O_3 \cdot Ca(OH)_2 \cdot 12H_2O$ or a related phase which probably contains Fe_2O_3 in the same manner as the given compound contains Al_2O_3. The hydrogarnets transform slowly to the stable product. A sample hydrated for 180 days but not reground periodically as are the samples represented in Fig. 4 gave a curve similar to the 28-day curve in Fig. 4. This slow transformation appears to be the reason why previously the hydrogarnets were believed to be equilibrium phases for the stated conditions. In the presence of gypsum the hydration of the $4CaO \cdot Al_2O_3 \cdot Fe_2O_3$ proceeded more rapidly and the hydrogarnets did not form.

Phase X

Thermal analysis results indicate that none of the known crystalline R_2O_3-

bearing products persist in hydrating cement notwithstanding the fact that some of these are equilibrium compounds in the systems consisting of related pure oxide constituents. The possibility that SiO_2 effects the stability of calcium sulfoaliminates was clearly indicated by results of the study on the temperature stability of these compounds. Accordingly, series of samples of lime, silicic acid, $4CaO \cdot Al_2O_3 \cdot Fe_2O_3$ with and without added gypsum were prepared, processed and tested in a manner similar to that followed in the tests of the $4CaO \cdot Al_2O_3 \cdot Fe_2O_3$.

Thermal analysis curves of these products are shown in Fig. 5. The added gypsum resulted in the formation of the trisulfate which was still present in the 60-day sample, but not in the 90-day product. With the exception of the bulges characterizing the trisulfate and phase X the two series, with and without added gypsum, gave similar thermal curves at each age of test. The 90-day curves showed nearly identical bulges at about 140 C characteristic of phase X. The results on the products without added gypsum show that the crystalline hydration compounds of $4CaO \cdot Al_2O_3 \cdot Fe_2O_3$ did not form in the presence of SiO_2 (Compare Fig. 4 and 5). This observation suggests that the SiO_2 is a major factor in the formation of phase X, and it follows that the major constituents of phase X are CaO, SiO_2, Fe_2O_3, Al_2O_3 and H_2O. In the absence of Fe_2O_3, phase X did not form.

Previous studies[10] have shown that the lime-silica-water gels absorb or combine with Na_2O forming quaternary gels of variable compositions. Also the possibility that Al_2O_3 might be an integral constituent of a quaternary lime-silica-alumina-water gel was indirectly suggested in earlier tests.[1] These considerations and others already mentioned suggest that phase X may be a multicomponent gel in which sulfate may be included without significant alteration of the thermal curve of the related product without sulfate. More experimentation is required, however, before the composition and nature of this phase are adequately defined.

Products of reaction of cement, silica and water at 175 C

The relation reported by Menzel[6] showing the effect of added silica on the strength of cement-silica-water products obtained at 177 C (350 C) is reproduced in Fig. 6. Cements with replacements of 2 to 60 percent of ground quartz were hydrated at 175 C for 24 hours in this study duplicating closely the conditions used by Menzel in the cited test. The products were analyzed thermally and the thermal curves for many of the samples illustrating various solids that formed are presented in Fig. 7. The endothermic bulge at about 560 C in these curves identifies $Ca(OH)_2$. The extent of this bulge decreased with small additions of silica. An 8 to 10 percent addition resulted in the complete elimination of $Ca(OH)_2$ as a reaction product. The $Ca(OH)_2$ probably reacted with the finely ground silica.

The endothermic bulge at 470-480 C characterizes the plate-like crystalline dicalcium silicate hydrate discovered microscopically in high-pressure steam cured cement by Thorvaldson and Shelton[11] and subsequently isolated in

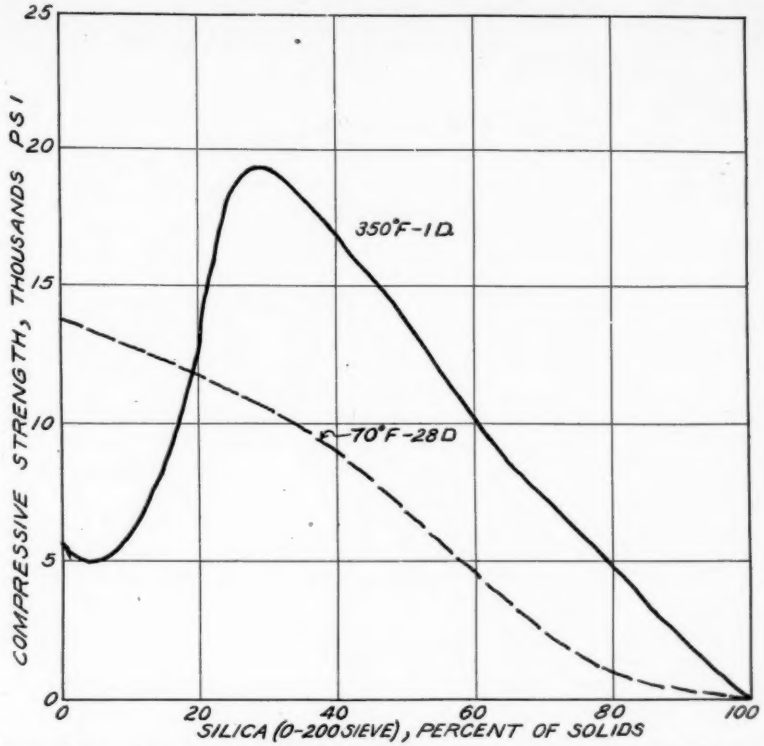

Fig. 6—Relation between compressive strength and amount of ground quartz by weight of cement and quartz, reproduced from report by Menzel[6]

pure form by Vigfusson, Bates and Thorvaldson.[12] This solid was present in relatively large amount in the cement sample with no added silica, and increased in amount with the additions of silica up to about 8 to 10 percent. At this point the processed mixtures would probably show minimum strength as suggested by Menzel's results and since this addition is associated with the maximum amount of the platy dicalcium silicate hydrate it is assumed that the crystalline compound did not contribute much to the strength. Observations based on sizes of the bulges of the thermal curves of pure compound and mixtures of it in different amounts with hydrated cement pastes indicate that approximately one-third to one-half of the paste with the 8 to 10 percent addition converted to this compound.

In the range of silica additions of about 9 to 20 percent the amount of the platy dicalcium silicate hydrate decreased, and thermal curves simultaneously showed another change beside the decrease in the bulge at 470 C. There appeared first an exothermic bulge at about 800-820 C which in turn was

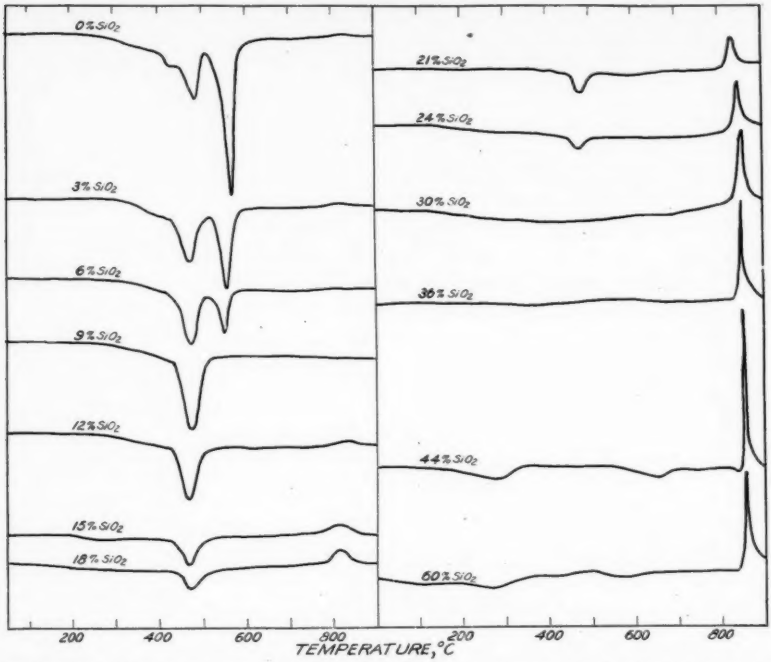

Fig. 7—Thermal analysis curves of cement-silica mixtures processed at 175 C for 24 hours, the percentages representing replacement of cement by silica in the dry mix

replaced by an exothermic peak at 840 C. With further additions of silica above 20 percent, this peak increased in extent and showed a maximum size with silica additions of 40 to 45 percent. As indicated in Fig. 6, approximately this amount of silica resulted in the highest strength which was about three times as great as that of the cement without added silica. This coincidence permits ascribing tentatively the high strengths to the phase characterized by the peak at $840 \pm 5°$ C.

It appeared desirable to estimate the composition of the reaction products in terms of $CaO{:}SiO_2$ molar ratio to interpret the changes occurring in thermal analysis curves among different samples. It may be assumed, in view of the vigorous processing conditions, that the cement had hydrated completely. Accordingly in samples not containing $Ca(OH)_2$, which included all those containing additions of silica in excess of 8 percent, the $CaO{:}SiO_2$ ratio would express the composition of the reaction product or products provided that free silica was not present. To allow for this constituent, if present, the free silica was determined following standard procedure for insoluble residue. The amount of silica in the original mix was corrected for that remaining in the free state and the $CaO{:}SiO_2$ ratio of the product was com-

TABLE 1—AMOUNTS OF UNREACTED SILICA IN CEMENT-SILICA PASTES AFTER INDURATION AT 175 C FOR 24 HOURS AND THE CaO:SiO_2 MOLAR RATIOS CORRECTED FOR THE UNREACTED SILICA

Amount of added SiO_2 in dry mix, percent	Ignition loss of product, percent	Unreacted SiO_2, ignited basis, percent	$CaO : SiO_2$ ratio (corrected)
3	13.2	0.26	3.06*
6	12.8	0.15	2.68*
9	11.2	0.14	2.35
12	11.3	0.61	2.14
21	10.8	0.64	1.55
24	10.5	1.2	1.41
30	10.2	4.2	1.25
33	9.8	6.5	1.19
36	9.8	8.4	1.12
45	9.7	15.0	.95
50	9.3	21.4	.92

*Crystalline $Ca(OH)_2$ present.

puted (Table 1). The ignition loss obtained on samples dried at 100 C is also included in this table.

The amounts of free SiO_2 in the products remained at less than 1.2 percent up to an addition of 24 percent SiO_2. This suggests that the reaction between SiO_2 and the cement had proceeded nearly to completion in those samples. Mixtures containing the higher percentages of added SiO_2 showed increasing amounts of free SiO_2. The corrected CaO:SiO_2 molar ratios of the reaction product were found to decrease to values approaching unity. This tendency towards constancy of the ratio notwithstanding the fact that abundance of free SiO_2 was present in the mixes of the higher silica contents suggests that the composition of the product responsible for high strength approaches that of a hydrous mono-calcium silicate.

SUMMARY

1. Thermal analysis results indicate that the R_2O_3- and SO_3- bearing products form and transform in hydrating cements at temperatures of 25 to 100 C in the following sequence, $3CaO \cdot Al_2O_3 \cdot 3CaSO_4 \cdot 31H_2O$ and presumably the analogous sulfoferrates appear first but convert to the related solid solutions of these products which in turn are converted to phase X. At 70 to 100 C the solid solution was found in greater abundance than the trisulfate product but transformed rapidly to phase X.

2. At processing temperatures of 80 to 100 C the products showed a marked decrease in the endothermic bulge at 130-140 C characterizing phase X. This could indicate a change in porosity of that solid or alteration of its chemical composition.

3. The hydrogarnets in pure condition show pronounced dehydration bulges. The hydrogarnet forming initially from $4CaO \cdot Al_2O_3 \cdot Fe_2O_3$ transforms slowly to the related compound or compounds occurring in the hexagonal crystalline form, and a gel.

4. The hydrogarnets were not detected in cement pastes hydrated at temperatures between 25 and 175 C.

5. Phase X may be a gel consisting of all oxide constituents of cement. This phase could not be prepared from raw mixtures not containing CaO, Fe_2O_3 or SiO_2.

6. Finely ground silica (quartz) reacts with cement at 175 C to form the orthorhombic dicalcium silicate hydrate of Thorvaldson and Shelton. The reaction product of cement and an addition of about 8 to 10 percent of silica consisted of approximately one-third to one-

half of this dicalcium silicate hydrate, the remainder being the still unindentified product or products responsible for the strength of the hydrated cement. This mixture gave the product of potentially the lowest strength. The product from a mixture containing 40 to 45 percent finely ground silica is indicated to possess the highest strength. The composition of the cementitious phase at these amounts of silica additions appears to approach a $CaO:SiO_2$ molar ratio of unity. This phase showed an extensive exothermic peak at 840 ± 5 C.

REFERENCES

1. Kalousek, G. L., Davis, C. W., Jr., and Schmertz, W. E., "An Investigation of Hydrating Cements and Related Hydrous Solids by Differential Thermal Analysis," ACI JOURNAL, June 1949, *Proc.* V. 45, p. 693.

2. Powers, T. C. and Brownyard, T. L., "Studies of the Physical Properties of Hardened Portland Cement Paste," ACI JOURNAL, Oct. 1947-April 1947, *Proc.* V. 43, pp. 101-249, 469, 549, 669, 845, 933. PCA *Bulletin* 22, 1948.

3. LaFuma, H. and Brocard, J., "Recherches sur la Stabilite du Sel de Candlot," *Technical Publications* No. 15, Centre d'Etudes et de Recherches de l'Industries des Liants Hydrauliques (Paris), 1950.

4. Flint, E. P., Mc Murdie, H. F., and Wells, L. S., *Journal of Research*, NBS, V. 26, 1941, p. 13, RP. 1355.

5. Flint, E. P. and Wells, L. S., *Journal of Research*, NBS, V. 27, 1941, p. 171, R. P. 1411.

6. Menzel, C. A., "Strength and Volume Change of Steam-Cured Portland Cement Mortar," ACI JOURNAL, Nov.-Dec. 1934, *Proc.* V. 31, pp. 125-148.

7. Lerch, W. and Ford, C. L., "Long-Time Study of Cement Performance in Concrete, Chapter 3—Chemical and Physical Tests of the Cements," ACI JOURNAL, May 1948, *Proc.* V. 44, p. 743. PCA *Bulletin* 26.

8. Morey, G. W., and Ingerson, E., *Am Mineral*, V. 22, 1937, p. 1121.

9. Adams, M., "A Study of Iron-bearing phases in Hydrating Cements," Dissertation, University of Toledo, 1949.

10. Kalousek, G. L., *Journal of Research*, NBS, V. 32, 1944, p. 285, RP 1590.

11. Thorvaldson, T. and Shelton, G. R., *Canadian Journal of Research*, V. 20, 1936, p. 20.

12. Vigfusson, V. A., Bates, G. N. and Thorvaldson, T., *Canadian Journal of Research*, V. 11, 1934, p. 520.

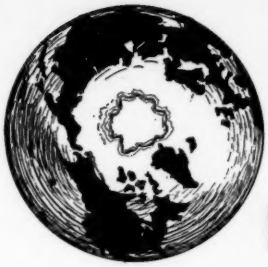

Letters from Readers*

BY WAY OF SYNOPSIS

CHARLES MACKLIN describes a method of setting small column bases on concrete.

E. L. HOWARD comments on factors influencing concrete strength.

ROBERT B. COLEMAN, JR., discusses the use of portland-slag cement to correct alkali-aggregate expansion.

I. E. MORRIS emphasizes that rational use of the Building Code makes possible the design of economical structures.

B. KELLAM describes investigations on the water-solubility of alkalies in portland cement.

RAYMOND C. REESE answers a reader's question on spacing of beam stirrups.

E. L. HOWARD believes that metal molds are superior to paper for test cylinders.

HOMER M. HADLEY concludes discussion on the merits of the plastic theory of design.

W. P. HIRSCHBERG questions omitting hooked ends on reinforcing bars.

Leveling Screws Simplify Setting Column Bases (LR 48-1)

In setting small steel columns, with base plates attached in the shop, the usual details call for two anchor bolts and the column is adjusted to elevation by steel shims. With only two anchor bolts it is also necessary to guy the column in an upright position. The accurate setting of anchor bolts is of vital importance and shimming is at best a trial and error operation.

To simplify this operation a double nut and long thread on the anchor bolts have been used with success. By using at least three bolts guying can be eliminated except on small footings where it may be necessary to prevent overturning of isolated footings.

Details of the column base assembly are shown in Fig. 1. The double nut is helpful in setting the bolts since the nuts may be tightened on a rigid template, thus keeping the bolts at right angles. It is recommended that the bolt pattern be kept square when four bolts are used to allow for turning the column 90° in case of shop errors or plan changes. Bolts should have a ¾-in. minimum diameter and nuts should have a free fit. The holes in the base plate should be at least ¼ in. larger than the bolt. Where variations in the setting of bolts are expected, the holes should be larger and special washers used to span the larger opening.

The sequence of setting the column is shown in Fig. 2: (1) set the top of the nut or

*A part of copyrighted JOURNAL OF THE AMERICAN CONCRETE INSTITUTE, V. 23, No. 1, Sept. 1951, *Proceedings* V. 48. Separate prints of the entire Letters from Readers Section are available at 35 cents each. Address 18263 W. McNichols Rd., Detroit 19, Mich.

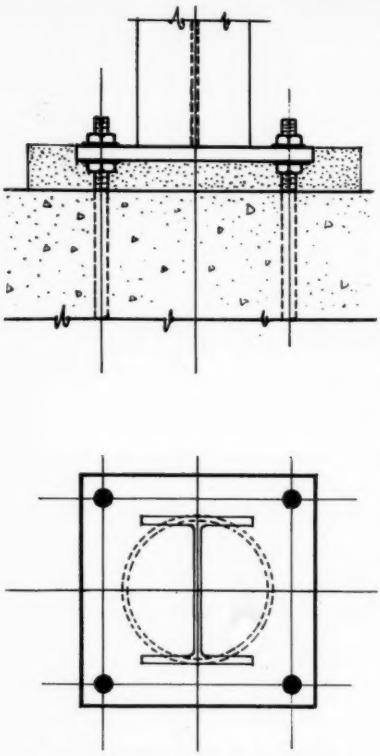

Fig. 1—Details of column base assembly

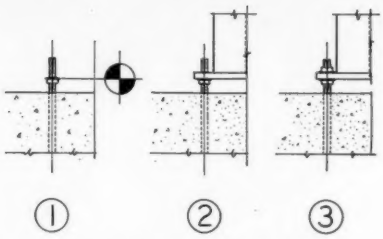

Fig. 2—Sequence of operation

washer to the theoretical elevation of the bottom of the base plate; (2) land the column and (3) tighten the upper nut.

If for any reason the top of the column needs to be drifted or the elevation changed or adjusted, the operation is relatively simple. The space between base plate and concrete should be grouted as soon as the steel has been checked for alignment and elevation.

The use of the double nut anchor jack is not new; its first large use was on some cell blocks for the State of Illinois in 1946. Nor are the use of these bolts limited to steel columns. Amirikian's "Precast Concrete Offers Protection Against Atomic Blast," in the March 1951 JOURNAL illustrated their use in precast construction (Section 1-1, Fig. 7, p. 509).

CHARLES MACKLIN, architect and structural engineer, Springfield, Ill.

Factors Influencing Concrete Strength (LR 48-2)

We have noted the differences in strength yields of the several brands of cement we work with. To aid in the design of concrete mixes we made an extensive study of Type I cement from several producers (Fig. 1). It will be noted that the cements were as divergent in strength yield as those shown in Fig. 3 of Price's paper in the February 1951 JOURNAL.*

Price says, "For approximately the same compressive strength the difference in cement content for concrete containing aggregate up to ¾ maximum, and one containing aggregate graded up to 1½ maximum, is about ⅔ sacks per cu yd of concrete."

Job test data does not always agree with this premise. Ready-mixed concrete customers who buy "sack mixes," *i.e.*, specifying only maximum size aggregate and cement content per yard, have found it easier to handle a ¾ maximum mix than a 1½ maximum mix. Better concrete results with the use of smaller material. We have found that a job foreman can handle drier concrete

*Price, Walter H., "Factors Influencing Concrete Strength," ACI JOURNAL, Feb. 1951, *Proc.* V. 47, pp. 417-432.

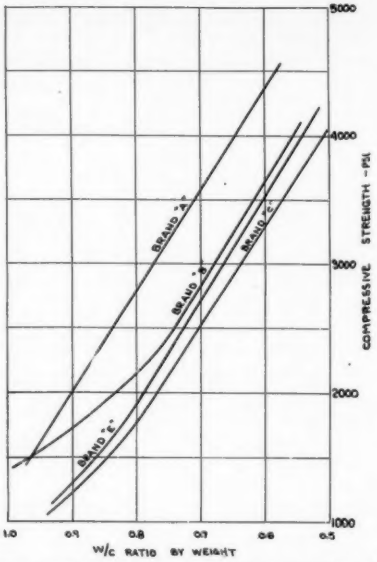

Fig. 1—Comparative compressive strengths of concrete made using each of four brands of cement

better using ¾ maximum aggregate than when 1½ maximum aggregate is specified. The ¾ maximum mixes have the better strength record (Table 1); this table is representative of tests taken from several jobs using regular 6-sack mixes.

TABLE 1—28-DAY COMPRESSIVE TEST DATA

Number sacks per cu yd concrete	6	6
Maximum size aggregate, in.	¾	1½
Number cylinders	220	140
Highest psi	4950	4630
Lowest psi	2580	2900
Average psi	3860	3780

Of course, it is true that in concrete having substantially the same consistency and identical cement contents, the mix with the larger aggregate should yield the greater compressive strength. But as noted above, the men on the job use drier concrete when smaller aggregate is used.

We are in complete accord with Price in the matter of molds used to cast concrete specimens. Our experience has been that concrete cast in paraffined paper molds yields 4 percent less compressive strength than concrete cast in metal molds. This difference is greatly increased when curing conditions are not good as is often the case with job-made cylinders.

On a recent job we had occasion to take seven cores. In each case they were higher in compressive strength than test cylinders cast when the pours were made. The cylinders averaged 85 percent of the cores in compression tests.

E. L. Howard, testing engineer, Pacific Coast Aggregates, Inc., San Francisco, Calif.

Alkali-Aggregate Expansion Corrected with Portland-Slag Cement (LR 48-3)

The paper by Federico Barona De La O in the March 1951 Journal* tends to substantiate work done by the writer and others† where a slag was used which was in itself high in alkali content, 1.39 percent. We were surprised to find that slags of such low alkali content as were reported by Barona are available. It should be pointed out that slag does not have to be of low alkali content in itself as was indicated in the paper. Published data indicate that addition of alkali in the mix as was done by Barona does not always correlate with expansions obtained when the alkali is an integral part of the portland cement. Where high alkali cement is unobtainable, such a clinker can be produced in the laboratory by grinding clinker with sodium or potassium oxide, fusing the mix in a high temperature furnace and regrinding the material with the required

*"Alkali-Aggregate Expansion Corrected with Portland-Slag Cement," ACI Journal, Mar. 1951, *Proc.* V. 47 pp. 545-552.

†Cox, Herbert P., Coleman, Robert B., Jr. and White, Locke, Jr., "Effect of Blast Furnace Slag Cement on Alkali-Aggregate Reaction in Concrete," *Pit and Quarry*, Nov. 1950.

gypsum. An excess amount of alkali has to be used to take care of evaporation or sublimation loss.

Our work also indicated that as little as 25 to 33.3 percent slag is beneficial when used as replacement for portland cement. It should be re-emphasized that a 50 to 60 percent replacement can be made without sacrificing strength. Another advantage of slag is that it may be interground with the portland without sacrificing workability or ease of placement. It is generally recommended that fly ash not be interground for this reason.

The fineness reported for the portland-slag cement is probably meaningless since the 15 percent hydrated lime content would account for the higher surface areas obtained. We made some mixes keeping the slag-portland ratio constant and varying the lime content from 20 to 40 percent. The surface area obtained on the Blaine apparatus varied from 5100 to 8400 sq cm per g.

The ASTM specification for granulated blast furnace slag for use in portland-slag cement requires that the ratio

$$\frac{CaO + MgO + \frac{1}{3} Al_2O_3}{SiO_2 + \frac{2}{3} Al_2O_3}$$ be not less than 1.

To our knowledge all slags being used for cement will meet that specification.

Our studies indicate that acid slags actually foam better than do the more basic slags; they also seem to make better glass or a more stable glass. Robert C. Lied, graduate student at the University of Alabama, is doing some research on the effect of the glassy phase constituent in blast furnace slag on its pozzolanic properties; the results of his study should shed more light on the desirability of the present ASTM specification.

ROBERT B. COLEMAN, JR., research engineer, Southern Cement Co., Birmingham, Ala.

Rational Use of ACI Building Code for Economical Structures (LR 48-4)

In structural design the goal is maximum economy with the requisite degree of safety. Economy involves formwork as well as concrete and steel. The design of continuous T-beams requires the careful consideration of moment, shear, bond, and compression in the stem at interior supports. It is rare indeed that material at all critical points of a T-beam can be stressed to the maximum allowable. It is the job of the designer to strike a logical balance of all conditions; that is, over-all economy may in some instances dictate maximum stresses in reinforcing steel with relatively low shear stresses. In other instances, it may necessitate the use of high shear stresses. No code could possibly set up allowable stresses which could be utilized to the maximum at all critical points of a member for all design conditions. It is necessary that the designer display ingenuity in using allowable stresses to the greatest advantage.

For instance, if a beam design is governed by maximum moments, the designer may get an acceptable beam, with actual bond and shear stresses considerably below those allowed with new deformed bars in the 1951 Building Code. Many times the designer could make the beam only 2 in. deeper with a saving of both moment and shear reinforcement, and with further reduction of shearing stress. This would, of course, increase slightly the concrete and formwork cost. But here is where a knowledge of costs and a "feel" for correct proportions come into play.

It has been proved conclusively in recent years that the slab band or flat beam type of construction produces the greatest over-all economy, with the possible exception of the flat plate floor. In these flat beams, with an average width of about 36 in. and an effective depth of about 12 in., shear is an important consideration. The shallow depth normally requires a close spacing of stirrups. If the use of maximum shearing stresses were attempted, the number of stirrups would be so great as to make the design uneconomical. But by keeping the shearing stresses low, which in turn lowers bond stresses, the construction as a whole is economical.

There are many special conditions, however, in which the higher shear and bond stresses allowed in the new ACI Code enable the designer to solve problems much more economically than he could with the old stresses. Increased bond stresses, for instance, frequently obviate the necessity for

hooks at noncontinuous ends of members. With two or more heavy beams ending on one column, the old method of hooking the ends of all bars frequently created an almost impossible situation. It is these situations particularly which the new bond stresses alleviate.

The main purpose of the Code is to set limits beyond which, in the opinion of writers of the Code, the designer should not go. The idea is to produce within those limits a combination of stresses which will lead to maximum economy.

Some designers claim that there is nothing new in the 1951 Code as far as T-beam design is concerned that could not have been handled by the 1947 Code by using special anchorage. Essentially this is true, *but* special anchorage involves the use of additional steel, either as hooks or additional extensions into adjoining spans. We cannot provide special anchorage of old-type bars without doing something special; with the new bars we automatically have special anchorage. Moreover, the increased shear values are particularly helpful where the cross section of a member is limited by architectural requirements. To provide for compression in the stem of T-beams at interior supports, it is sometimes necessary to extend compression steel into the adjoining span. With new-style bars, the extension required is less than with old-style bars.

It is a bit illogical to say that higher stresses are not advantageous. If that were true, we should now be using the stresses which were in use in 1918.

I. E. Morris, consulting engineer, Atlanta, Ga.

Water Solubility of Alkalies in Portland Cement (LR 48-5)

Work reported by Gilliland and Bartley on water-solubility of alkalies in the October 1950 Journal* brings to mind some work by the Hydro-Electric Power Commission of Ontario. In 1930 the Commission was working on a rapid method for determination of cement content of concrete, where the Na_2O content of the cement was known. The latter was determined by six successive leachings with boiling distilled water which removed all Na_2O and this was determined with zinc uranyl acetate reagent. The determination of Na_2O from similar leachings of the ground concrete enabled the determination of its cement content with accuracy. Canadian cements seem to contain a higher $Na_2O + K_2O$ content than American cements, but no difficulty was experienced in obtaining excellent check on Na_2O content by the leaching method.

In an investigation of the effect of percolating water through 6 in. diameter, 2 in. thick, moist-air-cured mortar cylinders, all the effluent was analyzed. The first gallon of water that came through contained 95-98 percent of the total Na_2O content, the remainder in the next gallon.

In another series, 2 x 4-in. mortar cylinders were used in percolating tests. Since it was necessary to have a complete accounting of all constituents, when these were cured in water the curing water was analyzed. It was found that practically all the Na_2O of the cement in the cylinders was dissolved in the curing water. This explains the need for moist-air curing of mortar bars made for expansion tests, instead of water curing. The latter process will extract sodium compounds and give erratic results, the extraction being facilitated by the small cross-sectional area of the bars.

The writer believes that placing of concrete tends to reduce alkali content to varying degrees due to loss of the water-soluble sodium and potassium compounds carried off by water lost through forms, etc. For example, laitance water which rose to the top of concrete conveyed about one-half mile in a wheeled bucket contained 1580 ppm Na_2O and 4057 ppm K_2O.

It is also believed that from the analytical viewpoint, a technique could be evolved to remove all Na_2O in a cement by leaching alone. So far as K_2O is concerned, this may be more difficult and time consuming.

B. Kellam, chemical engineer, Research Division, Hydro-Electric Power Commission of Ontario, Toronto, Ont., Canada

*Gilliland, J. L. and Bartley, T. R., "Water-Solubility of Alkalies in Portland Cement," ACI Journal, Oct. 1950, *Proc.* V. 47, pp. 153-160.

Spacing Beam Stirrups (LR 48-6)

The question of spacing the first stirrup from the face of the support in a beam seems to have two answers. One method is to keep a constant 2 in. from support to initial stirrup and then to follow design spacing as presented in the schedule. The other method is to make the distance between support and stirrup one-half the spacing nearest the support. Which is correct?

READER

The writer has always used about 2 in. from the face of the support; frequently this comes out half a stirrup space, sometimes less.

The technically-minded person could probably present a fair case for a half space. Current theory is to apply a flat amount of shear to the concrete and carry the balance of shear prism on the reinforcing steel, spacing the stirrup at the centroid of equal volumes of this excess shear prism. Using that theory, the first stirrup would be at the center of gravity of the first stirrup trapezoid, which is likely to be a couple inches off the face of the support.

This whole theory is open to challenge. Moretto's tests at the University of Illinois* coupled with Clark's at the Bureau of Standards† have shed considerable light on the problem of diagonal tension. (The word "shear" is used loosely; shear reinforcement is really reinforcing concrete against diagonal tension failures.)

It has been found that the dowelling action of longitudinal steel is of considerable assistance in knitting the beam together.*

It has also been found that the position of the load on the beam is a factor. Two concentrated loads near the center of a beam will produce the same end shear as those two loads moved closer to each end. But the variation in diagonal tension reinforcement is considerable and a proper formula must include a term locating the applied load.

Since the philosophy of diagonal tension is changing, it is not of too vital importance just where the first stirrup starts. It should be kept within 2 or 3 in. of the face of the support as a precautionary measure and then spaced out, not exceeding the d/2 recommended in the Building Code.

RAYMOND C. REESE, consulting engineer, Toledo, Ohio

Metal Versus Paper Molds for Test Cylinders (LR 48-7)

Burmeister's study in the September 1950 JOURNAL‡ of paper molds used in making concrete specimens should create considerable interest and further study by testing agencies.

The test cylinder molds we have used in the hot dry valley areas of California have never given full satisfaction. Many jobs during summer months look good, but compression tests of job-made specimens have more often than not yielded low strengths.

It is general practice on construction jobs to make three cylinders at a time, two of which are broken in 28 days. To compare the effect of different type molds in hot weather, on a job in Fresno, Calif., one of these 28-day cylinders was cast in a standard paraffine dipped paper mold with a paper bottom, one cylinder was cast in a "tin" mold. The metal molds conformed to specifications of the California State Highway Commission.

The cylinders were cast on the job and picked up the following day, stored in the local laboratory office for two or three days, and then delivered to San Francisco to be stripped and stored moist at 70 F until

*Moretto, Oreste, "An Investigation of the Strength of Welded Stirrups in Reinforced Concrete Beams," ACI JOURNAL, Nov. 1945, *Proc.* V. 42, pp. 141-164.

†Clark, Arthur P., "Diagonal Tension in Reinforced Concrete Beams," unpublished manuscript.

‡Burmeister, Robert A., "Tests of Paper Molds for Concrete Cylinders," ACI JOURNAL, Sept. 1950, *Proc.* V. 47, pp. 17-24.

TABLE 1—28-DAY STRENGTHS OF JOB SAMPLED CONCRETE CYLINDERS*

Slump, in.	Compressive strength, psi		Date
	Metal mold	Paper mold	
4¾	2670	2580	3 July
4	2970	2770	5 July
3½	2650	2370	7 July
4	2610	2410	11 July
4½	2690	2100	12 July
4½	2770	2230	14 July
5	2130	1830	17 July
4½	2590	2180	18 July
5	2560	2260	21 July
4	2360	1930	26 July
4¼	2230	1830	28 July

*Mix used was: cement, 517 lb; moist sand, 1220 lb; ½ to ¼-in. gravel, 180 lb; ¾ to ½-in. gravel, 820 lb; 1½ to ¾-in. gravel, 1000 lb.

broken. This treatment is similar to general practice in this area.

The data shown in Table 1 are evidence that the metal mold forms the best cylinder. We believe that the differences between the two molds are due to the rapid drying of concrete cast in paper molds. (The data show a steady decrease in strength as the job progressed. This decrease has been tied directly to the cements used, but that might make another letter.)

E. L. Howard, testing engineer, Pacific Coast Aggregates, Inc., San Francisco, Calif.

Skepticism Regarding the Plastic Theory of Design (LR 48-8)

(Concludes discussion of LR 47-66)†

The most interesting feature of discussions published in defense of various "plastic theories" of design is their bland assertion that any compressive or flexural deviation from the straight-line stress-strain pattern observed in the past 50 or 60 years is evidence "which substantiates these theories." Talbot, Turneaure and other great names of concrete's past are by this reasoning champions of plastic theories and automatically their defenders against anyone who questions or denies their validity. Actually neither Talbot, Turneaure nor any of their contemporaries had any thought of our modern plastic theories. These theories by Saliger, Whitney and Jensen are distinctly identified by the fact that all of them not only employ the stress-strain curve of cylinders up to the point of maximum stress, as their predecessors had done, but they go further and make chief use of the curve's farthest extension into the "plastic range" as the physical basis of their proposed stress-patterns. Because this descending branch of the compression stress-strain curve is the distinguishing feature of plastic theories, the writer denies the relevance of earlier data and theories to them. Nobody thought of employing the descending branch of the stress-strain curve before these theories were propounded.

What corroborative evidence is offered by their authors or by others? The support and corroboration falls into three categories: cylinder tests, beam tests and "authorities."

Cylinder tests

Consider first the cylinder tests. In the synopsis of his paper Whitney[1] states:

> The writer proposes the adoption of the plastic theory which recognizes the true characteristics of the material determined by research since the standard "straight-line theory" was adopted about a generation ago. The plastic theory takes into account the plasticity of the material and is itself sufficiently "plastic" to be adjusted empirically to actual conditions.

Under the section titled "Stress-Strain Characteristics of Concrete" and regarding the curves of his Fig. 1, Whitney states:

> Fig. 1 shows some typical stress-strain curves for concrete cylinders . . . . It will be noted that the maximum stress occurs at a strain of approximately 0.002 in. per in., and that the failure does not occur suddenly but that the stress is reduced gradually as the strain continues to increase.
>
> . . . . The effect of time on the stress-strain relation is believed to be similar to that in the case of tests on beams. It is probable, therefore, that these curves indicate the form of compressive stress distribution in a beam at ultimate load in the concrete in the zone where the unit strain exceeds about 0.002 in. per in.

The continuity of these curves and absence of any qualifying notes left the reader no other possible interpretation than that they pre-

†See also ACI Journal, Nov. 1950, *Proc.* V. 47, p. 257; Jan. 1951, *Proc.* V. 47, p. 398; Feb. 1951, *Proc.* V. 47, p. 485; Mar. 1951, *Proc.* V. 47, p. 570; and May 1951, *Proc.* V. 47, p. 748.

sented the record of the cylinders' behavior and that the concrete was as sound and unbroken at the end of the tests as it was at the outset. Does anyone question the correctness of this interpretation of these curves, particularly when Whitney previously declared in his paper, "Even short-time measurements are affected by plasticity"?

Anderson and Cohen[2] feel there is no cause for the writer to be surprised when cylinders are found to be shattered and worthless at the extreme end of the descending branch of the stress-strain curve. The surprise arose, not from the shattered condition of the concrete but from the fact that such was evidence of short-time plasticity. He was further surprised to discover in tests of cylinders that a sudden, slight increment of load applied at any point past the maximum, even when no cracks were visible, caused the cylinders to break into fragments and fall completely apart. This seemed strange evidence of plasticity.

Jensen[3] presented specific physical data for only the minor part of his stress pattern; for the major part he presented no physical data whatsoever — merely Saliger's conjecture. What he did submit in his Fig. 1, "Typical Stress-Strain Curves for Concrete Made with Gravel Aggregates," were curves for concrete of varying strengths attaining presumably maximum values at unit strains of 0.0015 and there terminating. A note specifically designates them as cylinder tests. These are the basis of the minor part of his stress-pattern. For the major part he furnished the Saliger curve in Fig. 2, "Possible Stress-Strain Diagram for Concrete at Strains Approaching Rupture—Saliger." These two curves Jensen combined into his Fig. 3, "Idealized Stress-Strain Curves for Concrete of Different Strengths," which idealized curves he then subjected to further treatment called "Approximation." Thus shaped and fashioned, the curves conformed with his subsequent mathematics. Nevertheless as the basis of a serious engineering paper this foundation is surprising.

Concerning Saliger, Gilkey's[4] discussion of the Jensen paper contains the following paragraph:

> Much of Saliger's backlog of evidence, such as it is, seems to date back to relatively early tests when techniques for controlling rate of loading and for securing good observations on strains were in an elemental state. Even today it would require some of the best of modern testing and observational equipment and carefully planned, skillfully executed tests to secure significant evidence on the post-ultimate [post-maximum]* compressive behavior of concrete. It is not surprising, therefore, that Saliger should have worked backward from the beam-test strength results to evolve an imaginary compressive stress-strain diagram which would account for the observed excess beam strengths.

This then is the cylinder evidence submitted: smooth, continuous curves; no qualifying notes; talk about "plastic range" and "short-time plasticity." The writer's cylinders fail to substantiate these claims.

Returning to the Whitney curves, unit deformations of 0.008 in. per in. recorded give a total deformation in a 12-in. cylinder of 0.096 in. The testing machine head moved 0.060 in. per min.

$$\frac{0.096 \text{ in.}}{0.060 \text{ in.}} \text{ per min.} = 1.6 \text{ min.}$$

How is that for abrupt, almost instantaneous plasticity? Who can really believe that concrete, brittle and structured as it is known to be, can be loaded, tightened and compressed to its extreme limit and that then it will plasticize and conform with the Saliger or Whitney or Jensen curve? Probably nobody believes it but we have had such a wonderful time in the past 20 years talking about plastic flow, time yield, creep and whatnot that the plastic theories just had to originate.

The cold facts are that concrete does not plasticize but, under extreme short-time pressure, it simply loosens, comes apart and disintegrates. Not only will this happen after maximum load has been reached but given more time, it will do so before maximum load has been attained. Shank[5] presents data of cylinders loaded to 90 percent of maximum and holding intact for 6 hours but completely failing in about 1 minute when loaded to 93 percent or more of maximum. The paper states:

> The percentage representing the "true" ultimate strength may be expected to fluctuate both above and below the 90 percent point. The third batch made for the thesis work showed 85 percent as the location of the "true" ultimate strength.

Undoubtedly it is this data which forms the basis of the Anderson and Cohen state-

*Added by the writer

meant that "loads from 85 to 90 percent of ultimate strength can be maintained permanently despite extremely large strains." As stated above the reported data covers a period of 6 hours only—not perpetuity. Attention should be directed to the fact that Price[6] states:

> Fig. 14 shows that if a specimen is loaded slowly it will break at a much lower load than when it is loaded at the standard rate and that concrete can be expected to withstand indefinitely only 70 percent of its ultimate load, as determined by the standard rate of loading.
>
> Concrete will sustain an indefinite number of repeated applications of stress where the maximum stress is maintained at a value of 50 percent below the ultimate [maximum]* strength of the concrete. The 50 percent figure was found to hold for both flexural and compressive stresses.

Beam tests

As for the corroboration afforded by beam tests, this is its nature: One assumes a maximum fiber stress, usually f'_c. Then one assumes whatever general shape of stress-pattern—rectangular, "idealized" rectangular, parabolic—that may please his fancy. Then he fits these to the beam tests. To quote again from the Whitney paper "leaving certain empiricial constants to be determined by actual tests on beams." Or as Jensen stated in the closure of his paper "For the sake of the record it may be stated that the form of Eq. (2) was originally determined by trial and error using the test results obtained by Slater and Lyse as an experimental basis."

In short, make the *assumed* maximum fiber stress and the *assumed* stress pattern fit the beam tests by empirical constants and then the beam tests will prove that all the assumptions have been correct. It is truly an extraordinarily simple method of proof and a most convenient one! But as Sawyer[6a] says, "Obviously, any shape [of stress-pattern]* can be made to satisfy these requirements such as triangular, rectangular, trapezoidal, parabolic or hyperbolic." The writer has no objection to fitting assumed stresses and assumed stress patterns to beam data but on the other hand he dislikes marveling at arbitrarily created agreement.

With the straight-line pattern of stress distribution as the established basis of design, with everyone agreeing it is suitable for use with ordinary working stresses and with stress-strain curves being practically straight up to 60 or 70 percent of maximum stress value, it seems pointless to do otherwise than use it for determining the load of beams at concrete compression failure. A useful theory is wanted and when practically every designer in the country now uses the straight-line theory why abandon it for plastic theories based and founded as here described? It may be of some value to know what ultimate strengths are, but it is vastly more important to know reasonably closely what the strength is that will withstand sustained loading and repetitive loadings. As for maximum loads, if the Slater-Lyse constants are applied to cylinder strengths the result will be quite as reliable as with any of the plastic theories. Close precision is not attainable when concrete is crushing and breaking up.

As for the application of the straight-line theory to beams heavily reinforced and failing by compression in the concrete, many engineers seem to think that since beams do not fail until the computed stress is 40 or 50 percent greater than cylinder strength it indicates a fatal weakness in the theory. For example, Hajnal-Konyi[7] states:

> The "classic method" [straight-line]* *does not give any possibility of explaining the excess resisting moment and therefore cannot be in accordance with the real conditions at failure.*† For this reason many engineers have tried to find a better method of calculating reinforced concrete in bending.

Of course this apparent discrepancy can be eliminated completely by changing one's assumptions: cease to believe that flexural strength should be identical with compressive stress as measured in a 6x12-in. cylinder and instead believe that flexural strength is 50 percent greater. When concrete strength varies with every change of dimension and shape of test specimen, why regard the 6x12-in. cylinder strength as something that must at any cost be developed when beams fail in flexure, even if the price be the abandonment of the generally used theory?

R. H. Evans[8] presented beam test data clearly, definitely and dispassionately. Of outstanding interest is his determination of the position of the neutral axis during various stages of loading. With normal percentages of reinforcement the neutral axis position determined by straight-line theory applied well up to failure due to steel passing the yield point; then it rose. With the heavy

*Added by the writer

†Italics added by the writer

percentages of reinforcement required to cause compressive failure in concrete, it agreed with straight-line theory up to a certain point; then it fell. Anderson and Cohen apparently feel that this drop in the neutral axis is evidence of plasticity but a more reasonable interpretation is that it is simply the result of internal weaknesses, minute slippages, fissurings and bucklings that precede complete collapse and disintegration. Naturally these have their initial development in the outermost fibers where stress is a maximum up to the point of local failure. This is the converse of the steel failure.

Various references have been made to economies to be effected by adoption of plastic theories of design without any specific procedure being outlined as to how they may be realized. Evans makes use of these words in his paper . . . "but in an economically designed beam, with equal concrete and steel strengths . . . " Of course on this point he is quite mistaken. Economy depends on the relative prices of concrete, forms, reinforcement, on span lengths and on other variables —not on equality between concrete and steel strengths in a beam. Concrete would have to be extremely costly and reinforcement extremely cheap to satisfy Evans' criterion. Hognestad's[9] closing words "whether or not the construction industry is ready to use an ultimate design procedure to an advantage in dollars and cents" indicates that he knows how the economies are to be realized. It is to be hoped he will enlighten the construction industry.

Authorities

The third support of plastic theories are the "authorities." Authorities are human beings who presumably are possessed of wisdom and understanding in the field or fields of knowledge in which they specialize. From broad experience and study they have acquired such insight into the operations and ways of natural law that they know its workings and can anticipate its actions. Their words are usually straightforward and simple and have an undertone of basic gumption and common sense. In consequence their opinions command respect and in a busy world where multitudinous demands are made on everyone's attention, many less experienced persons, aware of their own limited knowledge, defer to them and come to accept their views unquestioningly. This is all very well so long as the authorities, figuratively speaking, "stay on the track" but should they get off of it, the derailment, as on a railroad, involves not only the prime power but also those that trail along behind. Hence it is well for their followers to occasionally make a quick but critical appraisal of their authorities and see what it is they are telling them and if they are telling them something that they find extremely difficult to believe; then the solution is simple: don't believe them.

The general tenor of Hognestad's comments on the writer's earlier letter can only be adjudged to be adverse, which is of course to be regretted. He says its conclusion is based on such arguments that he finds it difficult to meet them in detail. As an example he cites the writer's statement, "The column formulas which are used resulted from the long-time column tests at Lehigh University and the University of Illinois and are in accordance with those tests" and says that the statement is not in accordance with the tests reported and conclusions reached in Bulletin 267 of the University of Illinois. The tests to which the writer referred were initiated by the American Concrete Institute in 1929, were made in duplicate at Lehigh University and University of Illinois, and are known as the American Concrete Institute Column Investigation. Today's generally used column formulas are those of the 1940 Joint Committee Report. That report, Section 851(a) states "The following recommendations are based largely on the results of the extensive American Concrete Institute Column Investigation." Hognestad's paragraph ends "This type of argument can therefore not be met with normal logic." The writer would agree with him.

Being unable to read his foreign technical reference, the writer would express the hope that if therein be any tangible physical *proof* of concrete short-time plasticity—not mere opinion and assumption, heavily coated with mathematics, curves and cross references—Hognestad will translate and report it. His few references in English provide no more than assumptions.

The writer's views on several points raised in Professor Cowan's courteous letter have

been previously stated here. However, his statement, "He (Hadley) takes no account of the absence of satisfactory evidence to support the elastic working stress theory," bears further discussion. The writer does not believe there is any such absence or lack of physical basis for the straight line theory. On the contrary, he thinks there is ample support for it, or for all but the uppermost reaches of it and there it does not depart widely from reality. Consider the three critical points on the stress-strain curve: the origin; the point of maximum stress, $E = 0.0015$ to 0.0020; and the point of ultimate stress, $E < 0.0080$. Between origin and maximum point everyone agrees that concrete may be regarded as a reliable structural material. Between maximum point and ultimate point, it should be regarded as structurally worthless. The straight-line theory is based only on that portion of the curve between origin and maximum point. The plastic theories of Saliger, Whitney and Jensen find the basis for the major portion of their stress patterns in the structurally worthless part of the curve between maximum point and ultimate point. For this reason the writer believes the straight-line theory has a vastly sounder basis than the plastic theories.

A friend recently directed the writer's attention to a French paper, "Stress Measurements in a Cross Section of a Deflected Reinforced Concrete Beam," by L. P. Brice of Paris.* In this small beam the concrete was completely eliminated for a short distance at midspan and a series of separated steel measuring devices replaced it from the top of the beam down to the reinforcing bars. Two loads, symmetrically placed with respect to notch and center line, were applied. Successive loads and reading were taken, the last of which came at 80 percent of the load at which the beam failed. In its English summary of results found, the second is "The stresses of the concrete are linear; the neutral axis of the concrete has been determined accurately."

It is possible to compare mathematically the straight-line stress pattern with those of the plastic theories on the basis of least work. Using the Slater-Lyse value of $1.50f_c'$ with the straight line pattern and $1.00f_c'$ or $0.85f_c'$ with any of the plastic theories, it will be found that the plastic theories entail a greater amount of work.

In this broad land are many research laboratories. Some are small and impecunious; some, like Rachel of old, are goodly and well-favored. And there are many researchers, some of whom have championed plastic theories. It would be a momentous occasion should some such source provide the conclusive proof that what appears to be nothing but structural worthlessness—nothing but loosening, coming apart, disintegration—is "really truly" plasticity! That is what is lacking and that is what is needed: proof of short-time plasticity—plain physical proof. Who among its advocates will be the first man to produce it?

Allons, enfants de la plastique! Allons!

For the alternative is this: either furnish convincing evidence of concrete's short-time plasticity or accept the fact that the plastic theories have no physical basis and warrant. And be it recognized by everyone that an engineering theory found lacking physical basis and warrant is not unlike a punctured balloon, flat, wrinkled and bereft of its former brave rotundity.

HOMER M. HADLEY, consulting engineer, Seattle, Wash.

References

1. Whitney, Charles S., "Plastic Theory of Reinforced Concrete Design," *Transactions*, ASCE, V. 107, 1942, p. 251.

2. Anderson, Boyd G. and Cohen, Edward, "Skepticism Regarding the Plastic Theory of Design," ACI JOURNAL, Feb. 1951, *Proc.* V. 47, p. 485.

3. Jensen, V. P., "The Plasticity Ratio of Concrete and Its Effect on the Ultimate Strength of Beams," ACI JOURNAL, June 1943, *Proc.* V. 39, p. 565.

4. Gilkey, H. J., Discussion of reference 3, ACI JOURNAL, Nov. Suppl. 1943, *Proc.* V. 39, p. 584-6.

5. Shank, J. R., "Plastic Flow of Concretes at High Overload," ACI JOURNAL, Feb. 1949, *Proc.* V. 45, p. 493.

6. Price, Walter H., "Factors Influencing Concrete Strength," ACI JOURNAL, Feb. 1951, *Proc.* V. 47, p. 417.

6a. Sawyer, Herbert A., Jr., "Skepticism Regarding the Plastic Theory of Design," ACI JOURNAL, Mar. 1951, *Proc.* V. 47, p. 570.

7. Hajnal-Konyi, K., "The Modular Ratio—A New Method of Design Omitting *m*," *Concrete and Constructional Engineering*, Jan.-Mar. 1937, V. 32.

8. Evans, R. H., "The Plastic Theories for the Ultimate Strength of Concrete Beams," *Journal*, Institution of Civil Engineers, Dec. 1943.

9. Hognestad, Eivind, "Skepticism Regarding the Plastic Theory of Design," ACI JOURNAL, Jan. 1951, *Proc.* V. 47, p. 398.

**Publications*, International Assn. For Bridge and Structural Engineering, 1950.

Hooked Ends on Reinforcing Bars Still Desirable? (LR 48-9)

Provisions in the 1951 ACI Building Code for the omission of hooked ends on reinforcing bars raise some doubts of building safety under severe overload. From observations of several wrecked reinforced concrete buildings, the question arises whether or not there are other considerations than bond resistance for design loads when detailing reinforcement. In a concrete structure where the reinforcement ties it together one is prompted to ask whether, in the interests of safe construction, it is advisable to omit hooked ends.

In one overloaded building, where bar ends were not hooked there was considerable loss of life, the collapse occurring with insufficient warning for occupants of the first floor to escape. In another building where a dust explosion occurred, loss of life might have been minimized had adequate attention been paid in the design to other considerations than economy.

This matter is not only important in this atomic age but seems important in any age. Engineers interested in design have a responsibility that reaches further than economy, however important that may be in serving one's client.

W. P. Hirschberg, architectural engineer, Milwaukee, Wis.

Current Reviews*

of Significant Contributions in Foreign and Domestic Publications

Rigid frames computed without equations (I telai piani semplicemente cenessi calcolati senza equazioni)

BRUNO DALL'AGLIO, *Giornale Del Genio Civile* (Rome), V. 88, No. 4, Apr. 1950, pp. 225-231
Reviewed by GENNARO MIANULLI

In this installment formulas for hinged frames are given. Application of the method is illustrated by numerical examples. It is limited to one condition of loading.

Prestressed concrete warehouse of Edinburgh

Concrete and Constructional Engineering (London), V. 46, No. 3, Mar. 1951, pp. 92-93
Reviewed by GLENN MURPHY

The completion of the three-story warehouse for H. M. Stationery Office, Edinburgh, is noteworthy because it is said to be the first multistory prestressed concrete building in Europe. The design was described in *Concrete and Constructional Engineering*, Nov. 1949.

Secondary stresses investigation at the bottom of an Intze-type reinforced concrete tank cylindrical wall (Sforzi secondari al piede della parete cilindrica di un serbatoio typo Intze in cemento armato)

LORENZO CONTRI, *Giornale Del Genio Civile* (Rome), V. 88, No. 4, Apr. 1950, pp. 218-224
Reviewed by GENNARO MIANULLI

Approximate formulas are derived for the determination of secondary stresses for Intze-type tanks. The two conditions considered are for a tank whose walls are stressed internally by the entire volume of the liquid and when the liquid is totally removed. A numerical example illustrates the procedure proposed.

Grinding, sieving and storage of hydraulic products (Broyage, tamisage, silotage des produits hydrauliques)

JOSEPH DEFORGE, *Revue des Materiaux* (Paris), No. 424, Jan. 1951, pp. 26-30
Reviewed by PHILLIP L. MELVILLE

A review of French practices on grinding of cement clinker and hydraulic lime. Advantages are claimed for finer grinding up to a certain point. The need to store cement and allow it to age is declared of importance especially if free lime is present.

Roof in prestressed concrete

Civil Engineering and Public Works Review (London), V. 46, No. 539, May 1951, p. 342
Reviewed by CHARLES W. DOHN

The roof of the Fairway Cafe building of the Festival of Britain is of precast concrete units in a square grid, post-tensioned with Freyssinet cables. Weighting of intersections according to a detailed schedule was necessary to prevent vertical bowing as tensioning of individual beams progressed. A plan of the roof and a photo after completion of tensioning are included.

Moments at fixed ends of circular beams (in Portugese)

CUNHA AMARAL, *Revista da Ordem dos Engenheiros* (Lisbon), V. 8, No. 79, July 1950, pp. 299-311
Reviewed by J. J. POLIVKA

In this addition to his previous paper the author develops the formulas for fixed-end moment of circular beams under torsional loadings: (1) uniformly distributed load, (2) two symmetrical concentrated loads, (3)

*A part of copyrighted JOURNAL OF THE AMERICAN CONCRETE INSTITUTE, V. 23, No. 1, Sept. 1951, *Proceedings* V. 48. Address 18263 W. McNichols Rd., Detroit 19, Mich. Copies of articles or books reviewed are **not** available through ACI. In most cases they can be obtained direct from the original publishers. Address, when available, will be furnished by ACI on request.

concentrated load at the mid-point of the circular span, (4) asymmetric concentrated load and (5) load uniformly distributed over a section of the circular beam.

A new building of the Peruvian Telephone Co. in Lima (Nuevo edificio para la Compania Peruana de Telefonos Ltda. en Lima)

Informes y Memorias de la Sociedad de Ingenieros de Peru (Lima), V. 50, No. 4, Apr. 1949, pp. 116-118

Reviewed by FRANCISCO J. CORDOVA

This article describes the new headquarters building of the Peruvian Telephone Co., Ltd., in Lima, Peru. It consists of a basement, main floor, mezzanine and seven additional floors. It will be an air-conditioned, reinforced concrete structure. Due to frequent earthquakes in the immediate vicinity the design was in accordance with the building code of the City of San Francisco.

Resistance of concrete to triaxial stresses (Resistance du beton aux contraintes triaxiales)

R. CHAMBAUD, *Annales de L'Institut Technique du Batiment et des Travaux Publics* (Paris), *Manuel du Beton Arme*, No. 20, No. 173, New Series, Feb. 1951

Reviewed by C. P. SIESS

Discussion and interpretation of the triaxial compression tests reported in Structural Research Laboratory Report No. SP-23, U. S. Bureau of Reclamation. The author's interpretation of the tests differs from that given in the original report. Reference is made to previous tests in France by Brice (1934) and to their interpretation by Caquot.

New theory of reinforced concrete in the plastic range (Die neue Theory des Stahlbetons auf Grund der Bildsamkeit vor dam Bruch)

R. SALIGER, F. Deuticke Verlag (Vienna), 1950, 135 pp. 106

Reviewed by RUDOLPH FISCHL

This book, first published in 1945, is basically unchanged in its revised and enlarged third edition. The conditions of plastic flow in concrete and steel are discussed and the influence of reinforcement considered. Results of numerous tests have been evaluated to support the theory of plastic behavior. The presentation of this difficult subject is clear and comprehensive. Ninety-two figures aid in understanding this interesting book.

New prestressed reinforced concrete bridge over Salmoggia River (Ricostruzione del nuovo ponte del Salmoggia in cemento armato precompresso)

GIUSEPPE RINALDI, *Giornale Del Genio Civile* (Rome), V. 88, No. 4, Apr. 1950, pp. 210-212

Reviewed by GENNARO MIANULLI

Construction of a prestressed girder bridge over the Salmoggia River in Italy is described. The single span bridge will carry highway traffic between Bologna and Verona. Magnel's type anchorage and prestressing method was used. Comparison of cost with another type of bridge, suitable to the site condition is also given, with data on the saving in concrete, reinforcement and forms.

Principal development of a multi-hinged girder with tie rods (Grundsaetzliche Entwicklung eines Mehrgelenktraegers mit Zugband)

R. T. BECKER, *Beton- u. Stahlbetonbau* (Berlin), V. 45, No. 7, pp. 161-165

Reviewed by RUDOLPH FISCHL

The author developed a system of trussed girders with several hinges in the deck, which serves as upper chord. It is possible to place the tie rods so that shear forces in the hinges and moments for dead load in the upper chord are eliminated. The use of the deck as upper chord saves weight and concrete.

Examples of trussed girders with two to four hinges are given, and the stresses and influence lines are developed.

Lateral forces of earthquake and wind

Separate No. 66, *Proceedings*, ASCE, V. 7, 1951, 38 pp. $0.50

From AUTHORS' SUMMARY

A lateral force provision drafted by a Joint Committee of the San Francisco section, ASCE and the Structural Engineers Assn. of Northern California as a reasonable requirement for building codes. Although prepared specifically for California conditions, the code is generally applicable, possibly with some qualitative modifications to suit different local conditions. The report includes the development of a more rational criterion for design seismic forces than has been attempted heretofore in lateral force codes.

Aerated concrete—Part 2

Digest No. 29, Building Research Station, Garston, Watford, Herts., England, Apr. 1951, 4 pp.

This is a continuation of *Digest* No. 28 which described the manufacture and prop-

erties of aerated concrete (See ACI JOURNAL, June 1951, p. 850). In this part some of the uses of aerated concrete are considered and information is also given on various matters that should be taken into account when using it.

Aerated concrete may be used as precast blocks or in larger composite units, or it may be cast in place. Limited British experience is supplemented by observations of practice in other countries, particularly Sweden.

Construction with moving forms

L. E. HUNTER, Concrete Publications, Ltd., London, 1951, 56 pp. $1.75

Following a discussion of factors affecting the success of moving formwork, the construction of wood and steel forms for this purpose are treated in detail. Preliminary site preparations are described as are the layout and operation of the concreting plant and the provisions for supplying and placing reinforcement. Many practical suggestions are given for avoiding dragging of forms and other difficulties inherent in the method.

A short chapter deals with horizontally traveling forms used for sewers, culverts, sea-walls and similar structures.

Reconstruction of a concrete road in Leicestershire

Concrete and Constructional Engineering (London), V. 46, No. 3, Mar. 1951, pp. 95-97

Reviewed by GLENN MURPHY

The reconstruction described consists in correcting drainage defects and superimposing a new surface of 1:2.6:3.9 (by weight) concrete with a water-cement ratio of 0.55. Mechanized methods, including spreading and compacting machines, are being used. The average cost to date is 16s. ($2.24) per sq yd, and is expected to average less for the completed project. The Road Research Laboratory and the Cement and Concrete Assn. are cooperating on research on placement, compaction, forms and riding quality of the finished surface.

Flexible mould stop for long line prestressed concrete

N. W. B. CLARKE, *Civil Engineering and Public Works Review* (London), V. 46, No. 539, May 1951, pp. 351-352

Reviewed by CHARLES W. DOHN

In the bonded method of prestressing, long lines of beam may be cast in one piece and separate units cut off after the concrete has hardened. The labor and inconvenience of making many saw cuts by carborundum or diamond impregnated saws can be avoided by use of the simple stop described in this article. The flexible stop of rubber or plastic requires no threading or anchoring and is easily removed. Spaces are left between units for cutting of wires after release. The manufacture and use of the stop are illustrated.

Review of 75 years history of Wayss & Freytag AG (Rueckblick auf 75 Jahre Firmengeschichte)

Beton- u. Stahlbetonbau (Berlin), V. 45, No. 6, pp. 125-148

Reviewed by RUDOLPH FISCHL

This issue is completely dedicated to the 75th anniversary of Wayss & Freytag AG., one of the leading construction companies in Germany.

A historical review, which links the company's activities with the development of reinforced concrete in Germany, is given, and it is emphasized how Morsch's association with the company proved to be especially valuable. His scientific work, supported by the company, was verified for practical use, thus giving new creative power to the building industry.

Articles by different authors discuss the most important construction methods developed by the company, which still is pioneering in the newest development of reinforced concrete.

A generalization of the Hardy Cross method—application to continuous circular beams (in Portugese)

CUNHA AMARAL, *Revista da Ordem dos Engenheiros* (Lisbon), V. 8, No. 75, Mar. 1950, pp. 120-142

Reviewed by J. J. POLIVKA

The author refers to the only known application of the Hardy Cross method to structures in torsion as developed by Correia de Araujo for structures consisting of straight members connected under right angles and presents his own application to continuous circular beams. Bending moments are distributed to the adjacent spans by using both flexural and torsional rigidity factors K_f and K_t derived from the principle of least work. Two examples with two and three spans, respectively, demonstrate the method.

New ways in building concrete roads (Neue Wege im Betonstrassenbau)

Forschungsgesellschaft für das Strassenwesen e.V. (Köln-Deutz), 1950, 100 pp.

Reviewed by RUDOLPH FISCHL

This booklet contains 12 reports given Oct. 29, 1949, in Stuttgart under the presidium of Prof. Otto Graf.

Included are articles on a test section, poured 10 years ago with a concrete of fluid consistency (H. Ippach and K. Eberle), the improvement of cements by air entrainment (E. von Gronow and F. Keil), selection of cement in highway building (O. Graf), cement road slab and subgrade (L. Schaible), influence of the reinforcement of concrete road slabs (W. Schütte), the use of prestressed reinforced concrete in road building (F. Leonhardt), and others.

Construction of new buildings of the Belgian National Bank at Brussels (Construction des nouveaux batiments de la Banque Nationale de Belgique a Bruxelles)

M. VAN GOETHEM, *Annales de L'Institut Technique du Batiment et des Travaux Publics* (Paris), *Architecture et Urbanisme* No. 7, No. 184, New Series, Mar.-Apr. 1951

Reviewed by C. P. SIESS

The new buildings were constructed adjacent to and partly over a railroad tunnel, and the foundations rested partly on the tunnel and partly on footings on the ground. Of special interest is the use of hinges between the structure and foundation to avoid damage from unequal settlements. Stone columns 70 ft long were prestressed by wires passing through holes drilled in the centers of the individual blocks. Many other architectural and construction details are described.

Who invented prestressed concrete (Chi ha inventate il precompreso?)

GIORGIO NEUMANN, *L'Industria Italiana del Cemento*, Mar. 1951

Reviewed by J. J. POLIVKA

Dr. Neumann, a leading engineer in Italy connected with prestressing since early practical applications, reviews developments since 1886 when P. H. Jackson originated this idea, followed by Mandl (1896), Rabut (1904), Koenen (1907), Vianini (1914), Wettstein (1919), Emperger (1922), Ruml (1929), and then by a number of well-known specialists (Freyssinet, Dischinger, Magnel, Finsterwalder). Special reference is made to the paper "Patents and Codes Relating to Prestressed Concrete" by Curzon Dobell in ACI JOURNAL, May 1950 and to Discussion, ACI JOURNAL, Part 2, Dec. 1950.

Review of current research

Engineering College Research Council, American Society for Engineering Education, Cambridge, Mass., 1951, 250 pp. $2.25

The new edition of this book, which outlines policies and activities of engineering research in 91 colleges and universities holding membership in ECRC, is said to be the only complete guide to current research contributions of engineering schools.

In addition to complete research project titles, the volume shows for each school the names of responsible research administrative officers, a brief digest of policies which govern research projects and contracts at each institution, number of personnel engaged in research activities, annual expenditures, and special conferences and short courses of interest to research workers.

The research projects listed represent the work of more than 11,500 faculty, graduate students and research engineers.

NF-VP control of cements at the mills within the framework of the French Standards (Le controle NF-VP des cements en usine dans le cadre de la normalisation Francaise)

H. LAFUMA, *Annales de L'Institute Technique du Batiment et des Travaux Publics* (Paris), New Series, No. 185, Mar.-Apr. 1951

Reviewed by PHILLIP L. MELVILLE

A rather complete review of the establishment of the AFNOR (French Standard Assn.) and of cement specifications. Several conflicts between requirements of AFNOR (Government sponsored) and previously established standards of the City of Paris resulted in the writing of an omnibus set of specifications designated as NF-VP, and products meeting the compromise requirements (as verified by engineers in the laboratory of the City of Paris) are thus marked. Finally, some problems are brought up concerning the quality of cements and research in progress for standardization of some properties of hydraulic binders.

Analysis of straight beams by means of Mohr's corollary (Sulle applicazioni del corollario di Mohr allo studio delle travi ad asso rettilineo)

ANGELO BERIO, *Il Cemento* (Milan), V. 47, No. 7, July 1950, pp. 117-120

Reviewed by GENNARO MIANULLI

Mohr's corollary is based on two differential equations, one expressing the relation of

bending moment to a uniformly distributed unit load (by assumption, always normal to the axis of the beam), the other the relation of deflection to bending moment, whenever the fundamental hypotheses, of the theory of elasticity are fulfilled and within necessary conditions for the validity of St. Venant's postulate. The two differential equations being of the same type, Mohr enunciated his corollary, stating that the elastic curve in a beam coincides with the bending moment diagram in a conventional beam fictitiously loaded.

This corollary has been applied to beams with various conditions of loading and restraint and to slabs on elastic soil, to obtain deflections and reactions.

Volume changes in sand-gravel concrete

F. H. JACKSON and A. G. TIMMS, *Public Roads*, V. 26, No. 8, June 1951, pp. 162-172

AUTHORS' SUMMARY

Abnormal expansion, as evidenced in map-cracking, has been observed in concrete pavements built with sand-gravel aggregate in some midwestern states. Tests with this and two other aggregates of widely different mineral composition, combined with different types of cement and subjected to various weathering conditions, produced effects in the laboratory which correlated with those observed in the field.

Expansion of concrete specimens made with sand-gravel was much greater than that of similar specimens containing the other aggregates, and appeared to be due to some characteristic related to the mineral composition of the sand-gravel. The magnitude of the expansion was markedly influenced by the properties of the cements used.

The addition of crushed limestone to the sand-gravel, producing a normally graded coarse aggregate which contained about 50 percent calcareous material, eliminated the abnormal expansion entirely.

The Glen Affric hydro-electric works—II

Concrete and Constructional Engineering (London), V. 46, No. 3, Mar. 1951, pp. 81-85

Reviewed by GLENN MURPHY

In this installment the tunnels and the Fasnakyle power station are described. The Mullardoch-Benevean tunnel has a fall of 3 ft in a length of 5738 yd. The horseshoe cross section has an equivalent diameter of 15.75 ft and is to operate under a maximum pressure of 32 psi. No lining is required except for the invert. The Benevean-Fasnakyle tunnel, which is in three sections, has a total length of 5788 yd. Over 70 percent of the length consists of a horseshoe section with an equivalent diameter of 14.5 ft and is to operate under a pressure of 62 psi. The high-pressure section, which is 1408 yd long, is 14.5 ft in diameter and is to operate at a maximum pressure of 260 psi. Both of these sections are concrete lined. The remaining 267 yd consists of three parallel concrete-backed steel pipes 8.3 ft in diameter. Details of construction, including placement of the concrete lining, are described. The features of the power house, which contains 9000 cu yd of concrete, are described briefly. Several photographs are included.

New methods for treatment of concrete (Nouveaux procedes de traitment du beton)

R. L'HERMITE, *Annales de L'Institut Technique Du Batiment et des Travaux Publics* (Paris), New Series No. 180, Mar.-Apr. 1951

Reviewed by PHILLIP L. MELVILLE

Tests were performed on vacuum concrete, air-entraining concrete and grouting of the "Prepakt" type. It was found that in concrete under vacuum a depression wave moves at constant speed. The concrete ahead of the wave acts as a perfect filter (no depression). A theoretical ratio between the coefficients of permeability at a given point before and after passage of the vacuum is named packing coefficient and is between 2.5 and 1.1 (wave speed $\frac{3}{8}$ to $\frac{3}{4}$ in. per minute). Cohesion as well as internal friction increases and according to Mohr's circle, the strength of fresh concrete after treatment would be 15 psi. The gains in strength and modulus of elasticity are also appreciable.

Air-entraining concrete is discussed with recommendations to users for design of mixes, mixing and vibration. A theoretical study explains the observed advantages of air entrainment in durability and workability. It is stated that the losses in strengths will average 3 percent per 1 percent entrained air.

As far as injection of mortar is concerned there is little understanding of its action. Much caution is advised especially in the composition of the mortar.

Design of bridge floors with multiple beams and their torsional resistance

Ch. Massonet, *Memories*, International Assn. for Bridge and Structural Engineering (Zurich), V. 2, 1950, pp. 147-182

Reviewed by J. J. Polivka

The author refers to his previous paper on design of this type of bridge floors without considering torsional resistance, and generalizes Guyon's method (*Annales Ponts et Chaussees*, France, 1947) based on assumption of a continuous grid of longitudinal and transverse beams, for the special case of torsional resistance of structural members. Numerical values of transverse distribution coefficients of the loads for all bracing parameters and for various values of torsional stiffness of beams are tabulated, which makes it possible to calculate characteristic coefficients of bending moments in transverse beams.

Practically, the method may be adopted like that of Guyon, if it is restricted to the first term of Fourier's series; it thereby becomes possible to take the torsional resistance of the bridge into consideration without additional calculations. If necessary, it also allows exact determination of the influence of any load by developing into a Fourier series. The method is not only more accurate than the classic methods in case of typical one-span bridges, but can also be modified and used for bridges with continuous beams prestressed transversely, and for bridges in reinforced and prestressed concrete of greater economy.

In the theoretical part, reference is made to Timoshenko's *Theory of Plates and Shells*, to research of University of Illinois Engineering Experiment Station, and to papers by Richart, Newmark, Siess and Leonhardt.

Prestressed concrete railroad ties (Traverses pour voies ferrees en beton precontraint)

La Technique Moderne-Construction (Paris), V. 6, No. 5, May 1951, pp. 194-196

Reviewed by Alexander M. Turitzin

A detailed description of shop fabrication of prestressed concrete railroad ties by the patented Valette-Weinberg system. In this system compression is transmitted to the concrete by high-strength wires tensioned by pulleys before concrete is placed in the forms. Anchorages are placed at the ends of these wires and compression is transmitted to the concrete by internal anchorages as well as by bond. Bent steel pins served as internal anchorages.

Longitudinal tension wires and anchoring pins were made of hard steel 5 mm in diameter with an elastic limit of 105 kg per sq mm and an ultimate limit of 140 kg per sq mm. Hoop or diagonal reinforcing bars were made of soft steel with an elastic limit of 1.3 kg per sq mm.

Aggregates for concrete were carefully graded and forms were vibrated with high frequency vibrators. After 5 hours of curing at 60 C, the tension in the wires was released. At this point concrete had an average strength of 150 kg per sq cm. After an additional five hours curing the railroad ties were ready for use. At eight days the strength of concrete was 400 kg and at 90 days 550 kg per sq cm.

Old street car tracks revived for traffic use in novel way (Rails in dienst van het verkeer)

G. S. Bos, *Cement* (Amsterdam), No. 3-4, 1951, pp. 59-61

Reviewed by J. W. T. Van Erp

An ingenious example of "making the best of it" was presented in the reconstruction of a war-demolished highway bridge. The bridge, of conventional rib construction, was completely destroyed except for one of its abutments. For street traffic the 55-ft span had to be reconstructed on short notice, but no reinforcing bars were available and little timber for formwork. The new bridge also had to accommodate heavier traffic load specifications. The designing engineers, however, went to work and overcame all obstacles, developing an arched slab construction, reducing the amount of formwork to a minimum.

Old street car rails were available in abundance, due to the change-over from street cars to busses in many localities, and the design was adapted for their use. It was found that the double purpose of obtaining the desired cross-sectional areas and at the same time introducing the desired degree of curvature to suit the arch could be accomplished by flame cutting rail sections lengthwise, the flamecut side always being convex. The lengths of rail proved ample to develop sufficient bond even for the largest cross sections. For temperature steel and tie-bars the cut-out web sections were used.

Bond of steel bars in concrete (Adherence des barres d'acier dans le beton)

L. P. Brice, *Annales de L'Institut Technique du Batiment et des Travaux Publics* (Paris), *Essais et Mesures* No. 9, No. 179, New Series, Mar.-Apr. 1951
Reviewed by C. P. Siess

The author assumes that bond resistance is due entirely to friction and is of constant value and independent of slip. The frictional resistance is reversible, but the slip is not. This hypothesis is stated by the author to be based on tests by A. Bichara. However, in a note appended to the paper, Bichara presents some of his test results and demonstrates that Brice's assumption is valid only for smooth (polished) plain bars, is approximately true for ordinary plain bars at high slips, but is not correct for deformed bars. Nevertheless, the simplicity of Brice's assumptions permits both qualitative and quantitative study of slip, concrete cracking, stress in bar, etc., in both pull-out specimens and beams. His discussions of these factors, though probably not quantitatively correct except for plain bars, are thought provoking and provide reasonable explanations for many of the phenomena of bond.

Bichara's tests are also reported in part in this paper. Pull-out tests with the concrete in tension were made on plain bars. Each specimen consisted of two bars embedded end-to-end in a single cylinder of concrete. Steel stress distribution along the bars was measured by SR-4 wire resistance strain gages attached inside the bar. This was accomplished by cutting the bar along a diameter, grooving each half, attaching gages at 7-10 cm spacing in the grooves, and joining together the two halves of the bar. Apparently more tests were made by Bichara than are reported in this paper.

New mixture for cement—sulpho-aluminous-pozzolanic cement (un nuovo cemento di miscela—il solfa-alumino-pozzolanico)

Carlo Goria and Mario Appiani, *Il Cemento* (Milan), V. 47, No. 7, July 1950, pp. 112-116
Reviewed by Gennaro Mianulli

In the first installment (*Il Cemento*, pp. 34-37, pp. 54-57, 1949) a study was made on the behavior of the new sulfo-aluminous-pozzolanic cement and its expansive effect. Three mixtures were selected to determine which had maximum expansive action. Comparison of its physical properties and a mixture of normal cement was made. A series of tests in which other properties were observed followed. In this second installment, tests on the sulfo-aluminous-pozzolanic cement are reported. The experiments were based on the control of the expansive action by changing quantities of tricalcium aluminate and silicate in the portland cement mixture. It was possible to obtain an average expansion, an improvement in workability and mechanical resistance. For greater expansion the analogy was between the sulfo-aluminous-pozzolanic cement and a cement containing blast-furnace slag, substituting slag in this case for pozzolan.

Experiments on expansion and contraction and determination of its physical properties followed. Calorimetric and chemical measures of hydration, using the two cementing agents, were also observed.

Comments on "imaginative" cement and concrete chemistry

Nathan C. Rockwood, *Rock Products*, V. 54, No. 4, May 1951, pp. 83-85 and 94-100
Reviewed by Donald M. Agrimson

The author presents theories on cement and concrete—some his own and some which have been contributed by readers of *Rock Products*. A friend of the author described previous articles in that magazine pertaining to concrete and cement research as "highly imaginative" hence the use of the word "imaginative" in the title.

Rockwood says there is a serious need for better or more durable portland cement, especially for pavement construction. What is needed is a portland cement that can be used with the aggregates readily available. In other words, cements must be adapted to the aggregates to be used, and not an attempt to adapt aggregates to the cement. This conclusion is logical since portland cement is the only manufactured product in concrete and therefore its qualities or characteristics are the only ones that can be changed.

Factors believed to affect cement and concrete favorably or unfavorably are (1) some portland cements contain more lime than desirable for best results, (2) excess of calcium hydroxide in hardened cement paste is responsible for much poor quality concrete. This can be overcome by intergrinding and

blending pulverized granulated blast-furnace slag, (3) calcite crystals incorporated in cement produce a concrete more resistant to sea water erosion, (4) an additive—altered anorthosite is claimed by a consultant in Los Angeles to be a solution to the problem of alkali-aggregate reaction and (5) water retained in hardened concrete is undesirable. In pavement construction a base course of granular material is essential in draining out of the setting concrete some of the excess mixing water.

Contemporary structure in architecture

LEONARD MICHAELS, Reinhold Publishing Corp., New York, 234 pp. $10.00

A well-presented survey, illustrated with 259 photographs and 75 drawings, of structural methods and their relation in architecture. Every major structural system is carefully analyzed and compared with other systems.

The first half of the book considers the skeleton frame. The various methods used to join framing members is discussed, then the relation of these jointing methods to single and multistory frames. Methods for providing the horizontal infilling for the collection of loads on a horizontal plane is discussed and the structural slab and shell are analyzed.

Precasting and prestressing are illustrated and discussed in relation to framing. The author notes that precast concrete elements used as forms, to become an integral part of the structure, offer many possibilities. He also notes that reinforced concrete has greatly increased the range of forms that can be used in single-story spans, and emphasizes the contribution prestressing has made in increasing the economic spans of reinforced concrete beams. Arch and shell-dome construction are also discussed.

Structure in architectural design is discussed at great length in the second section of the book. The author relates structure to plan, section and massing, and points out the importance of considering structure in building design.

An appendix discusses the positive structural influences of steel, aluminum alloys, reinforced concrete and timber.

The book presents an excellent pictorial coverage of structural systems, and although discussion of each type of construction is necessarily brief, should assist both engineer and architect in co-ordinating structural and architectural design.

Contribution to design of bridge floors with multiple beams (in French)

CH. MASSONET, *Annales des Travaux Public de Belgique* (Brussels), June, Oct. and Dec. 1950

Reviewed by J. J. POLIVKA

Presentation and discussion of a practical method of analyzing bridge floors consisting of a concrete roadway slab continuous over stringers. Previous methods of analysis examined and discussed are (a) Slab-and-stringer method, (1) exact methods (Emperger, Ostenfeld, Bleich, Melan, Schindler, Hardy Cross, Hondermarcq, Southwell, Jannsonius, Genntner, Hilal) and (2) approximation methods (Engesser, Courbon, Mallet, Leonhardt); and (b) Method using the principle of anisotropic slabs, (1) exact method (Guyon) and (2) approximation method (Leonhardt).

In the second part of the paper the author presents his own approximate method based on the assumption that the distribution of concentrated loads in longitudinal direction (parallel with the axis of the bridge floor) follows a sinusoidal law, and in transverse direction is proportional to a deflection factor. Tables simplify determination of transverse distribution. Obtained deformations are compared with deflections of a continuous beam on elastic foundations and with those resulting from methods developed by Faltus and Leonhardt. Bridge floors with small and large number of beams are investigated, and the author's method is extended to bridge floors with continuous beams. Test results of the University of Illinois and British Research Station are discussed and conditions for composite beams (concrete slab combined with steel beams) are investigated.

Practical application of the author's method is demonstrated by two examples: a prestressed concrete bridge, 137-ft span, with five beams 7 ft high, 8 ft on centers, designed by Henrion and a two-span bridge, each span 60 ft, with concrete roadway slab continuous over steel stringers 3 ft 3 in. on centers recently erected over the Sambre River in Charleroi. Bibliography lists 36 publications.